AD-A081 246 WASHINGTON UNIV SEATTLE DEPT OF OCEANOGRAPHY F/G 17/1
WORKSHOP ON DEEP-TOWED, LOW FREQUENCY ACOUSTIC SOURCES AND RECE--ETC(U)
MAY 79 N00014-75-C-0502
UNCLASSIFIED NL

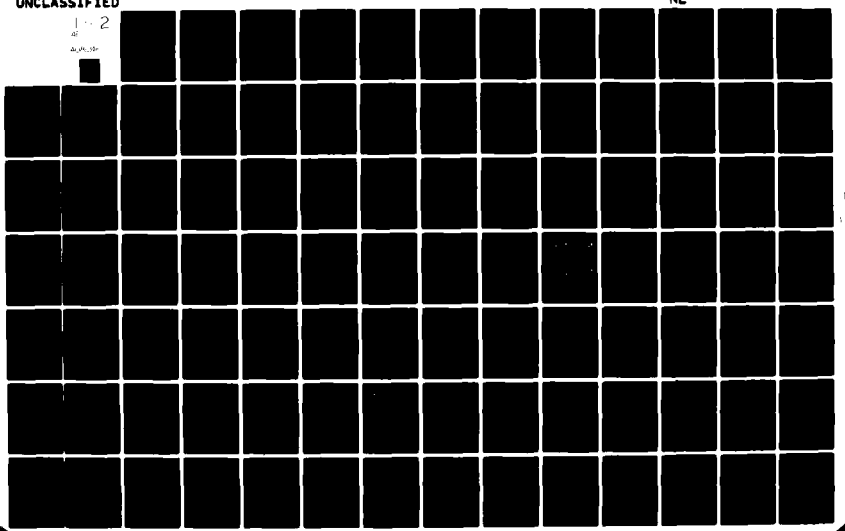

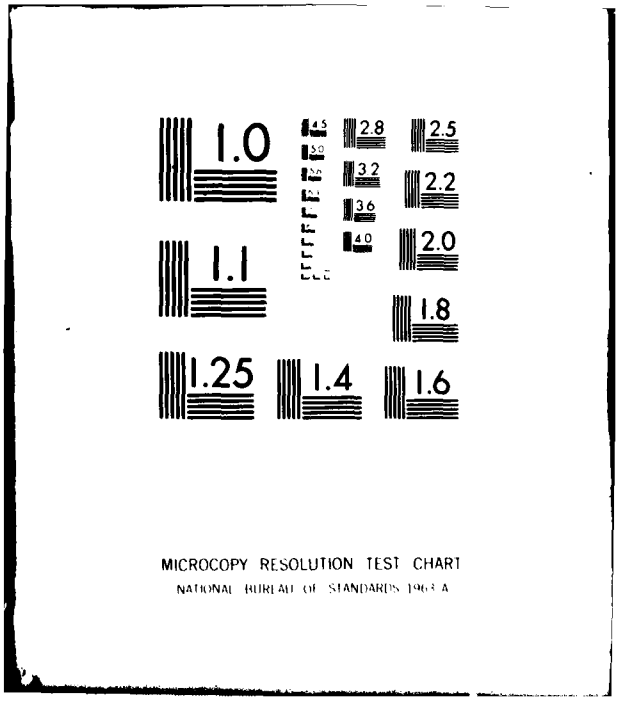
1.0
1.1
1.25
1.4
1.6
1.8
2.0
2.2
2.5
2.8
3.2
3.6
4.0
MICROCOPY RESOLUTION TEST CHART
NATIONAL BUREAU OF STANDARDS 1963 A

LEVEL II

12

WORKSHOP ON DEEP-TOWED, LOW FREQUENCY ACOUSTIC SOURCES AND RECEIVERS

Sponsored by the Office of Naval Research
Held at Bay St. Louis, Mississippi
May 25 and 26, 1978

Chaired by Brian T. R. Lewis
Dept. of Oceanography
University of Washington, Seattle

Distributed May 25, 1979

Contract # N00014-75-C-0502 1

(6)

WORKSHOP

ON

DEEP-TOWED, LOW FREQUENCY ACOUSTIC SOURCES AND RECEIVERS

Sponsored by the Office of Naval Research
Held at Bay St. Louis, Mississippi
May 25 and 26, 1978.

(11) 25 May 79

(15) N0001 4-75-C-0502

(12) 143

Chaired by

Brian T. R. Lewis
Associate Professor
Dept. of Oceanography
University of Washington
Seattle, Washington 98195
206/543-6043

Distributed May 25, 1979

370 280

1 B

TABLE OF CONTENTS

1. WORKSHOP OBJECTIVES

The two principal objectives of this workshop were:

1. To clarify what useful acoustic and geologic information can be obtained by deep-towed sources and receivers that cannot be obtained by conventional methods.

2. To review the state of the art in deep-towed sources and receivers and to pinpoint those areas of technology that need development in order to achieve those objectives.

II. INTRODUCTION

This workshop was sponsored by the Office of Naval Research through its Marine Geology and Geophysics and Acoustics programs. The meeting was held at the NORDA facility at Bay St. Louis, Mississippi on May 25 and 26, 1978, and was attended by an average of 23 people who represented a mixture of acousticians and marine geophysicists and geologists from the Navy, from industry, and from academic institutions. The agenda for the two-day meeting was arranged so that the early discussions concerned those specific problems that required deep-towed sources and receivers and the later discussions centered on present systems and technology.

The motivation for the workshop was multifold although the dominant theme was improved resolution. Some of the specific objectives of deep-towed acoustic equipment are:

1. Better resolution and definition of basement topography when overlain by sediments and identification of layering within basement. In most deep ocean situations the basement topography is sufficiently rough that back-scattering and reflections off objects to the side arrive at the same time as reflections from directly beneath the observation point. This gives rise to a very blurred record of the subbottom. By having either the source or the receiver and ideally both near the bottom side reflections will arrive at a time later than the events of interest and with a relatively reduced amplitude. In addition to the topographic resolution problem drilling results in basement often show interlayered sediments and basalts. With present surface observations, this interlayering has not been resolved and probably can only be resolved by increased signal bandwidth and observations close to the seafloor. Identification of these features is of great importance to understanding the mechanisms of crustal formation and the factors controlling acoustic wave propagation.

2. Lateral variability of velocity and attenuation in the oceanic basement. It has been shown by Houtz and Ewing that there is an overall pattern of increasing velocity with age in the topmost part of the crust. Superimposed on this there is however a high degree of local variability which could conceivably be related to such features as hydrothermal circulation, fractured pillow sequences versus massive lava flows, interbedded sediments in basalts, etc. In addition to this velocity variability, there may also be a large variation in the effective attenuation or energy loss in the bottom. It has been found that refracted converted shear waves are observed in some areas but not in others, possibly related to sediment cover or attenuation by extensive fracturing. Ocean bottom seismometer refraction experiments can be executed to determine average velocities over distances of tens of kilometers but are not altogether suitable for relating small scale variations in velocity and attenuation to geologic conditions. These measurements could be made by long deep-towed hydrophone arrays.

These types of measurements and geologic conditions also have important implications for what marine acousticians call "bottom loss". Urick (1974) defines bottom or reflection loss as "the ratio, in decibels, between the known amount of acoustic energy of an explosive shot at a short unit distance, to that received at a longer distance, after reflection

from the deep seabed at a known angle, when the transmission loss in the water (using ray trace calculations and an assumption as to the attenuation coefficient) has been accounted for". For frequencies above several kilocycles the attenuation in the seafloor is so high that only water paths are important and the bottom can be neglected. At the lower frequencies (1 - 100's Hz) refracted and reflected paths can have amplitudes comparable to or even larger than the water paths. The amplitude of these bottom paths is going to depend on many factors, such as the velocity gradient in the upper crust, the amount of energy converted to shear waves and the attenuation of P and S waves. These are seismological and geological problems which clearly bear on "bottom loss". In a series of workshops held under the auspices of ONR during 1977-78 the state of knowledge of wave propagation in the 1 to 50 Hz range was reviewed. It seems clear that a detailed understanding of "bottom loss" will benefit greatly from acoustic studies near the seafloor.

3. Another area where deep-towed sources and receivers are likely to be important and where considerable technological advances have already been made is in the exploration industry. The world's hunger for energy and mineral resources is causing increasing interest in the potential for mining the deep ocean seafloor. These interests range from oil and gas to manganese nodules. The discovery and mapping of these resources is going to depend very heavily on various types of high resolution near bottom observations of which acoustic methods will be very important. Two examples of new technology developments in industry were presented at this workshop; one by INCO involving a deep-towed side scan system with a parametric source for subbottom profiling; another by Huntec of Canada involving a deep-towed subbottom profiling system for characterizing and mapping sediment types.

III. PRINCIPAL CONCLUSIONS

An understanding of acoustic wave propagation in the ocean and oceanic lithosphere in the frequency range of 1 Hz to several hundred Hz is closely linked to an understanding of the geologic structure of the oceanic lithosphere. The more closely we study the oceanic crust, the more laterally variable it appears to be and we have reached the limit of resolution using our standard acoustic tools. Higher resolution, and thereby a more detailed understanding of the physics and geology of the problem, can be achieved with observations closer to the seafloor.

Technologically the problem at present appears to resolve into two frequency ranges. Between about 100 Hz and 1 kHz, it appears entirely feasible to construct and deploy deep-towed sources and receiving arrays. These systems would principally allow investigations of the sedimentary part of the geologic record and possibly the upper 100 meters of the oceanic basement (igneous and metamorphic rocks).

The resolution of fine-scale variations in the propagation of acoustic waves in the 1 Hz to 100 Hz range is technically feasible in terms of deep-towed arrays and surface sources, but deep sources still need some basic design breakthroughs. The principal difficulties here will be the generation or transmission of sufficient power to drive a repetitive sound source towed at depths of several kilometers.

IV. DEEP SOURCES

A. NORDA STUDY OF DEEP SOURCES
(Groves *et al.*, USRD)

B. A 3 kHz PARAMETRIC SOURCE
(J. Kosalos, INCO)

C. COMPUTER SIMULATION MODEL OF A TRANSIENTLY EXCITED UNDERWATER SOUND PROJECTOR
(R. W. Hutchins, Huntec)

D. POSSIBLE ENERGY SOURCE FOR DEEP SOURCES
(S. Selwyn, LDGO)

SUMMARY OF CONCLUSIONS

1. From a signal physics point of view (i.e., disregarding cost factors and technical problems associated with source design), the conclusion favors a conventional transducer capable of providing a 500-millisecond pulse with a 200 Hz bandwidth. This will give a time-bandwidth product of 100 as opposed to a time-bandwidth product of approximately one for sources whose bandwidths are controlled primarily by the pulse duration. However, one of the problems associated with a long pulse is that signal returns must be coherent with the transmitted acoustic signal. This is expected to be true for small grazing angles and for angles of incidence close to normal. However, at angles close to the "critical" angle, degradation of coherence is expected. Where such degradation of coherence occurs, the degree of degradation may depend upon the type modulation used to achieve the desired bandwidth. For this reason, phase (or frequency) modulation is favored. There does not appear to be any reason why this should be a linear FM slide. The primary requirements would be that it have no envelope modulation and that it is repeatable from transmission to transmission; and the actual noise-free acoustic waveform is available for correlation processing. The suggested way of achieving this with a conventional projector is to use a digital function generator with an appropriate D/A convertor to drive the projector. This would negate the need for input shaping circuits.

2. It has been determined that no existing CW transducer is capable of meeting the minimally acceptable requirements of the deep tow application. Some types of transduction mechanisms have been excluded from serious consideration because they share a common requirement; ie, they all require a means of providing compensation for hydrostatic pressure or internal pressure release. Excluded types include: bender bar, flextensional, moving coil, electromechanical, ceramic flexural disc, and hydroacoustic flexural disc.

3. An approach can be recommended that is within the present state-of-the-art; the Helmholtz "boosted" piezoelectric ceramic ring array. It is believed that this type of transducer can meet essentially all of the requirements of the deep tow application at a relatively low cost. It should be kept in mind that all of the transduction types addressed were considered strictly in terms of the NORDA deep tow requirements. If some of the requirements (primarily depth, size, and weight) were compromised, approaches other than the Helmholtz resonator may also become attractive.

BACKGROUND AND ACKNOWLEDGEMENTS

1. The Underwater Sound Reference Detachment of the Naval Research Laboratory was tasked by the Naval Ocean Research and Development Activity to assess the state-of-the-art in high power low-frequency acoustic sources for a deep towed application. A summary of the requirements is shown in Table 1.

2. Due to the unusually quick reaction time required, it was necessary to divide the work in the task among several of USRD's personnel. Those contributing include:

I. D. Groves, Jr.; Head, Transducer Branch
T. A. Henriquez; Head, Transducer Development Section
G. D. Hugus; Mechanical Engineer
A. C. Tims; Research Physicist
A. M. Young; Research Physicist

The analysis of the proposed approach was done by T. A. Henriquez.

INTRODUCTION

Transducer designers often have the feeling that users do not appreciate the difficulties encountered in attempting to meet their specifications for high power low-frequency sources. With that in mind, perhaps the best place to begin an assessment of low-frequency acoustic projector "state-of-the-art" is with a short general review of the radiation problem itself.

1. Within the size, weight, and frequency constraints of the deep tow application, any radiator will be small when compared to the acoustic wavelength in the medium. Inherent to this condition is a very low radiation efficiency. More specifically, as the ratio of the radiator's principal acoustic dimension to the wavelength in the water decreases, the radiation impendance acting on the radiator becomes increasingly reactive. Therefore, an increasingly smaller percentage of the total input power is dissipated in the form of acoustic radiation and a larger percentage is used to simply "move water" (analogous to the electrical and mechanical conditions of supplying power to a reactive load).

2. The power radiated from an "acoustically small" source is determined by the radiation resistance acting on, and the volume velocity generated by, the radiating surface. As previously discussed, the radiation resistance becomes increasingly small with decreasing frequency, thus leaving the inherent requirement of all high power low-frequency acoustic sources, a large volume velocity. By definition then, the final compromise left to the transducer designer is between the radiator surface area and surface velocity. Since virtually all transduction mechanisms quickly become displacement limited, the surface area of the radiator increases rapidly with requirements for higher output power and lower frequencies.

The increased surface area of the radiator means the forces due to hydrostatic pressure are also increased, and a heavier device often results from the required pressure compensation mechanism or increase in the volume of structural materials required. Finally, the requirement for large volume velocities means that high power low-frequency sources are inherently large force devices and, as such, are generally less reliable than transducers designed to operate at higher frequencies.

3. The overall efficiency of an acoustic source may be expressed as the product of the radiation efficiency and the efficiency of the transduction mechanism. It should be obvious from the previous discussion that, even if the transduction mechanism is reasonably efficient, the overall efficiency will still be low. The efficiency can, of course, be substantially increased by making the device resonant; to do so, however, would severely limit the useful bandwidth.

4. In summary, the undesirable characteristics of high power low-frequency acoustic sources may be shown to be direct results of the physics of the radiation problem itself. In the deep tow application, however, the restraints on the transducer do allow for feasible approaches to the problem. These approaches are addressed in the succeeding sections of this report.

DISCUSSION OF TRANSDUCTION MECHANISMS AND TRANSDUCER TYPES

Many types of transducers could conceivably be used to generate the required sound pressure levels for the deep tow application. Most types, however, either can not operate to the depths required, or the modifications required to make them operable render them unsatisfactory. A few other types require no compensation for hydrostatic pressure or internal pressure release, but their physical size makes them unsatisfactory.

Bender Bar Transducers

1. This type of transducer typically consists of multiple "bars" arranged in a "barrel stave" configuration around a cylindrical housing. Each bar is made of two segmented layers of ceramic and is hinged at each end. The two layers of ceramic are polarized (or driven) in opposition to produce motion in a bending mode.

2. The "barrel stave" configuration of the transducer results in a central cavity which is oil filled to compensate for hydrostatic pressure. A number of compliant tubes (sealed, air filled metal tubes) are normally inserted into the cavity to increase its' compliance and to provide a pressure release mechanism for radiation from the inner surfaces of the bars. This type of pressure release mechanism is not considered feasible for the depths required in this application.

3. For high power low-frequency applications, bender bar transducers become very large and heavy; far beyond the size and weight limits of the deep tow application.

Flextensional Transducers

1. The flextensional transducer consists of a elliptically shaped housing with a longitudinally vibrating ceramic stack along its' major axis; ie, the housing, or shell, is the radiating surface. The shells may be stacked in a line configuration and the ends of the stack sealed at the end plates. In this configuration, the flextensional transducer becomes a relatively efficient low-frequency source due to the large radiating area.

2. Conceivably, flextensional transducers can be made relatively small and light for their output power capability. They do, however, require a method to compensate for hydrostatic pressure and to provide a pressure release mechanism for the interior of the shell. Most commonly, the interior of the shell is either air filled or oil filled with compliant tubes inserted. Neither approach is considered feasible for this application.

Moving Coil Transducers

1. The moving coil (electrodynamic) transducer derives its driving force from the interaction between an ac current moving in a conductor and a large magnetic field. In the most common configuration, the force is used to drive a rigid piston with the advantage of relatively large permissible displacements. This type of transducer has a long history of successful use in generating moderately high sound pressure levels at low frequencies over a relatively large bandwidth. Unfortunately, moving coil transducers use an air or gas compensation system.

Electromechanical Transducers

1. Although most electromechanical transducers are very old designs, this type of transducer can generate high acoustic output levels at very low frequencies. In a common form, a large electric motor drives two opposing pistons through eccentrics on a crank shaft. In this form, however, electromechanical transducers are inherently narrow bandwidth devices and also use air as a pressure compensation/pressure release mechanism.

Ceramic Flexural Disc Transducers

1. The trilaminar configuration of the ceramic flexural disc transducer lends itself reasonably well to the high power low-frequency requirement. In the trilaminar configuration, an inactive disc (normally steel or aluminum) is laminated between two ceramic disc composites; when the two ceramic disc are driven in opposition a flexing motion is produced in the trilaminar structure.

2. Since the two sides of the trilaminar disc are 180° out of phase, one side of the disc must be pressure relieved. In most applications, two trilaminar plates are mounted back-to-back with a spacer ring between them. The space between the discs may either be gass filled or oil filled with compliant tubes inserted to provide the necessary pressure release. This double trilaminar disc configuration can actually be simply oil filled, but since the resonance frequency is strongly dependent upon the compliance of the internal cavity, this is applicable only for frequencies higher than those under consideration here or for larger allowable sizes.

3. The ceramic flexural disc can offer a good power-to-weight ratio and a potentially high efficiency for some applications, but the design suffers from the same pressure compensation and pressure release problems as do most others.

Hydroacoustic Flexural Disc Transducers

1. In its common form, the hydroacoustic flexural disc transducer consists of two opposing flexural discs driven by a central hydraulic amplifier. A low level electrical signal with the desired acoustic waveform is used to control the hydraulic amplifier while the hydraulic power is supplied by an electrically driven pump. The hydraulic system can essentially be housed within the transducer module, eliminating the need for handling high pressure hydraulic lines from the surface.

2. For very low-frequency high power applications, this type of transducer represents one of the few feasible alternatives. In terms of the deep towed source requirements, however, the advantages of the hydroacoustic flexural disc are a relatively high overall efficiency and broad attainable bandwidth, while its disadvantages are a low power-to-weight ratio and a limited depth capability.

Helmholtz Resonator Transducers

1. The transducer considered here essentially consists of a Helmholtz cavity and orifice driven by a piezoelectric ceramic driver. One surface of the ceramic drives the Helmholtz cavity while the other surface radiates directly into the medium. At the Helmholtz resonance frequency, the radiation from the orifice and the exposed surface of the ceramic driver are in phase. The purpose, then, of the Helmholtz resonance is to "boost" the low frequency response of the ceramic driver; that is, below its first resonance, the transmitting voltage response of the ceramic driver has a 12 dB per octave slope, positioning the Helmholtz resonance at the lower end of the frequency band to be covered provides a significant increase in the response.

2. In terms of the deep tow application, the Helmholtz "boosted" ceramic driver can be configured within the size and weight constraints of the specifications and provide the required sound pressure level and

bandwidth. The cavity may be free-flooded with seawater and the transducer requires no pressure compensation/pressure release mechanism.

Impulse Sources

1. Impulse sources offer some advantages over conventional sources for high power applications; their size and weight are generally small for the obtainable sound pressures, and in some forms they can be relatively inexpensive. For the deep tow application, however, most of the available impulse sources pose severe handling problems; for example, control over deployment of explosives, very high voltages required for spark gap devices, and high pressure air lines for air guns.

2. One impulse source which does seem to have potential for this application is the "cocked" piston. In this type of device, a piston is forced outward ("cocked") against the ambient hydrostatic pressure; when the piston is suddenly released, the resulting implosion generates very large negative acoustic pressures.

3. The primary reason for not using the cocked piston in the deep tow application comes from signal processing considerations. The low time-bandwidth product obtained considerably reduces the advantage of the obtainable sound pressure levels. This conclusion is discussed in detail in the next section of this report.

ASSESSMENT OF PULSED CW, PULSED FM, AND IMPULSE SOURCES

This section will provide a cursory examination of the signal physics associated with a deep-ocean bottom-profiling system. It will deal with the signal physics both from the standpoint of information-gathering potential and the ability to achieve desired waveforms at the desired depth. The pulsed CW analysis will treat primarily the more conventional transducer systems that are driven by pulsed CW waveforms, where the resolution is achieved primarily by a separation of signal returns directly in the time domain. The analysis of the impulse sources will treat the more unconventional sources such as explosive charges, air guns, spark discharges, etc., where again the resolution is obtained primarily by separations of signal returns directly in the time domain. The analysis of the FM pulses will treat pulses of longer duration where the bandwidth (and subsequent resolution capability) is not related to the signal duration. In this case, the resolution will be achieved by signal processing techniques such as matched filtering or the cross-correlation of complex signal returns with a noise-free prototype of the transmitted signal. The analysis will not limit itself to the FM process to achieve the desired bandwidth. As a general rule, the short CW pulses and the impulse sources will require the more simple processing but will yield less information, at least in the ideal case. On the other hand, the longer pulses will require more sophisticated processing, but will ideally yield more information.

In examining the pulsed CW source, we will consider a CW signal with an integral number of cycles with the initiation of the pulse being synchronized with positive-going axis-crossing of the CW signal. It is important that this synchronization occur so as to avoid higher frequencies generated by finite discontinuities that might be associated with the signal. The integral number of cycles is desirable so that the time integral of the pulse is zero and thus contains no d.c. component. Such a pulsed signal is expressed below as

$$g(t) = \sin \omega_o t \, [U(t)-U(t - \frac{n}{f_o})] \, , \, \omega_o = 2\pi f_o \qquad (1)$$

where fo is the frequency of the CW signal, n is the number of cycles, and U(t) is the unit step function. The normalized energy spectral density of g(t) is given by

$$E_n(f) = \frac{4}{n^2\pi^2[1-(\frac{f}{f_o})^2]} \quad \sin^2\pi n\frac{f}{f_o} \quad . \qquad (2)$$

From the parameter guide given in the description of work, a 400 Hz CW signal of two cycle duration is suggested. The energy spectral density of this signal is shown plotted as a solid line on Fig 1, where f_o is considered equal to 400 Hz. If the transmitted acoustic signal in the water is that described by Eq. (1), the simplest processing would be to feed the return signals through a bandpass filter with a bandpass of approximately 200 Hz and centered at 400 Hz. The output would then be recorded and observed. The first level of sophistication would be to feed the filter output signal through a square-law detector with a post-integration time constant of approximately 5 milliseconds. This output would then be recorded and observed. (A linear detector could be substituted for the square-law detector with very little degradation of results). However, the probability of achieving this signal waveform with conventional projectors at the required depth is small. To approximate the signal waveform would require the shaping of the drive signal to the projector to compensate for response characteristics of the projector. This shaping could take the form of an appropriate filter on the input of the projector or a generation of the desired waveform shape directly in the driving signal function generator. Furthermore, even if the ideal pulsed CW signal were achievable as a transmitted acoustic signal, it is not believed to be the most desireable waveform. A more desireable waveform is thought to be a pulsed CW signal with a truncated Gaussian envelope. The reasoning behind the selection of a Gaussian envelope is that the Fourier transform of a Gaussian envelope also has a Gaussian shape. The reason for truncation is to impose real time limiting on the signal for practical purposes. An expression for such signal is given by

$$g(t) = e^{-b^2t^2} \sin \omega_o t \, [U(t + \frac{n}{f_o}) - U(t - \frac{n}{f_o})]. \qquad (3)$$

Note that the initiation of g(t) is at $t = -\frac{n}{f_o}$ rather than zero and that the unit step functions insure the truncation is synchronous with the carrier. The parameter, b, is directly related to the bandwidth. The energy spectral density of g(t) may be calculated by convolving the autocorrelation function of $\sin \omega_o t$ and the autocorrelation function of the truncated Gaussian envelope. This is probably the most desireable pulsed CW waveform. However, again, signal shaping and/or direct control of the driving signal function generator will be required to achieve an approximation of the acoustic waveform.

While simple processing may be used, it is more desirable to have a noise-free prototype of the acoustic signal available and to cross-correlate it with the signal returns. This is equivalent to a matched filter processing. Considering the above as optimal processing is contingent upon the interfering noise signal being flat across the processing bandwidth. Since this is obviously not the case, preconditioning of the signal returns (plus noise) is desireable before correlation processing. As a result of this preconditioning, some modifications to the transmitted acoustic waveform may be desirable. Maximum information will exist when both signal power and noise power are flat across the processing frequency band.

In the analysis of impulse sources, it is clear that fewer problems normally exist (in an acoustic sense) in achieving high level sound sources. However, control over these sources is generally at a minimum. We believe that proper control over charge size and detonation depth will result in good repeatability for underwater explosive charges. This certainly seemed to be the case with 0.23kg (½ lb) charges detonated during NEAT II experiments (1972) at depths up to 2700 meters (9000 ft). Energy spectral densitities of these charges (including bubble pulses) peaked at 400-500 Hz with very little energy below 100 Hz. Repeatability of the shots were good with differences being attributed primarily to slight differences in detonation depths. At 4000 meters, the bubble pulse interval for a 0.23kg (½ lb.) charge of TNT is approximately 1.28 milliseconds, giving a midband frequency of approximately 780 Hz in the energy spectrum. Obtaining a 400 Hz midband frequency at 4000 meters would require a charge size of almost 1.81kg (4 lbs.). While this would probably give satisfactory signals, the primary (and probably insurmountable problem) would be that of logistics. Sink time and laterial excursions due to currents would rule out charges dropped from the surface. Carrying and deploying the number of charges required at depth would appear to present an insurmountable logistics problem as well as an unacceptable safety problem.

Based on the limited information available to us, the use of air guns at this depth has no potential, particularly the type air guns with which we are familiar.

We have conducted a very limited "scan" of available literature on spark gap discharges. While conclusions are not definite, the opinion

is that expected energy spectral densities achievable along with the very high voltages required will make the potential of such sources negligble for this application.

The only impulse source reviewed that appears to have potential for this application is the hydraulically-cocked piston of Hydroacoustics, Inc. The only disadvantage of this approach from the signal physics standpoint is lack of control of the acoustic waveform in the water. As is the case with the short CW pulse, the time-bandwidth product of the signal is approximately unity. Processing of the bottom returns would probably be best achieved by cross-correlation techniques where the interferring noise (ambient) is pre-whitened over the bandwidth of interest.

Initial reaction to the pulsed FM source (and other sources where the signal bandwidth is not directly related to pulse duration) was negative. However, after analysis and reflection, this type signal was considered to be the best proposed from a signal physics point of view. This is primarily due to obtaining a signal time-bandwidth of 100 as opposed to unity for impulse and short CW pulses. This basically means that for the same signal levels, the longer pulse has the potential to provide 100 times the information as do the short pulses. However, while less sophisticated processing may be used with the shorter pulses (i.e. square-law and linear detection followed by post-detection filtering), the longer pulse will require cross-correlation processing (or its equivalent). When cross-correlation processing is used, bottom returns are required to be coherent with the transmitted signal. This is expected to be the case for small grazing angles and for angles of incidence close to normal. However, at grazing angles close to the "critical" angle, degradation of the coherence of bottom returns is expected. A general expression for a long pulse system whose bandwidth is not directly related to the pulsewidth is given by

$$g(t) = A(t) \cos [\omega_o t + \phi(t)]\{U(t) - U(t-T)\} \quad , \qquad (4)$$

where T represents the pulse duration and where the bandwidth is derived from the amplitude modulation, A(t), and the phase modulation, $\phi(t)$. Three types of signals then can exist: (1) where amplitude modulation alone exists, (2) where phase modulation (or frequency modulation) alone exists, or (3) where both amplitude and phase modulation exists. For a pseudo-noise signal or a real noise signal, case (3) applies and generally A(t) and $\phi(t)$ are independent with more or less identical first-order statistics. When a signal defined by Eq (4) is transmitted, a degradation of coherence may result both in propagation and reflection which is not equally dependent upon A(t) and $\phi(t)$. Therefore, the choice of a waveform can conceivably effect the degree of degradation of coherence. Based on experience and intuition, case (2) is favored for the bottom-profiling application because we would expect less degradation of coherence from the signal with phase modulation alone. However, it should be remembered that the waveform of all transmitted pulses must be true replicas. In a conventional modulation process, this

requires that the carrier and modulating signals be synchronous. However, this is probably best achieved with a digital function generator using an digital-to-analog convertor and approriate filtering.

From a signal physics point of view, a conventional projector using a phase-modulated signal to achieve the required bandwidth and with a pulse length of 500 milliseconds is favored. Signal conditioning prior to processing and cross-correlation processing (or its equivalent) is recommended.

RECOMMENDED APPROACH FOR A DEEP TOWED LOW-FREQUENCY ACOUSTIC SOURCE

1. Based on the conclusion that a conventional source is required for this application, we have concluded that a Helmholtz boosted ceramic projector is best suited to the overall requirements. When discussing such devices, two types of ceramic drivers are usually considered; the trilaminar flexural disc and the segmented ring. For the same radiating area, the flexural disc produces the greater volume displacement, but if the resonator is more constrained as to the available space, the ceramic rings become more attractive. Within the size constraints of this application, a larger radiating area may be achieved by using a stack of segmented ceramic rings.

2. A conceptual design of the recommended transducer is shown in Figure 2. Actually, two transducers are addressed in this approach; one which we believe to be feasible and will meet all of the requirements, and a second more conservative design using twice the ceramic volume which would be slightly beyond the size and weight limits. The advantages and disadvantages of each will become obvious in the following discussions.

3. The basic element in both approaches is a 0.5m outside diameter by 0.18m high segmented Navy Type I ceramic ring. The individual rings are radially prestressed by a glass fiber/epoxy composite. The first design contains five rings for an overall ceramic length of 0.9m, while the second design contains ten rings for an overall active length of 1.8m. The calculated maximum source level for each configuration is compared to the minimum requirement in Figure 3. The figure shows the additional margin of safety provided by the more conservative approach; ie, a larger margin for error between the minimally acceptable source level and the maximum voltage limit on the ceramic.

4. Figure 4 shows, for each configuration, the electrical power required to generate the minimum 204 dB source level. The advantage of the larger ceramic volume in the conservative approach is obvious. We feel, however, the curves in the figure may be somewhat misleading. Since the electrical power is mostly reactive, some reduction in the required power may be possible by tuning the capacitive reactance with an inductor. An equivalent circuit model of the transducer(s) was used to calculate the input impedance and volt-amperes required for both configurations. The model was also used to estimate the effects of the cable and the series tuning inductor. Figures 5 and 6 show the input impedance of the untuned transducers with and without the RG8/U cable. The marked effect of the cable resistance and capacitance is obvious and was included in the further analysis. The input impedance of both configurations tuned to the mid-band frequency of 400 Hz is shown in Figures 7 and 8. Figures 9 through 11 depict the volt-amperes required to generate the 204 dB source level; Figures 9 and 10 address the untuned configurations while Figure 11 addresses the tuned transducers.

5. In terms of the power handling capabilities of the RG8/U cable; the maximum voltage limit on the ceramic is the same as that for the cable, 5 kilovolts (RMS). For the low duty cycles required, the average power for either transducer configuration is relatively low and represents no limitation by the cable's current carrying capacity. We see no particular advantage in changing the cable type. The cable resistance will be considerable for 5700m of any practical cable type.

6. A summary of characteristics of the two approaches is shown in Table 2.

7. Assuming the required source level may be compromised slightly, the smaller source would be the logical choice on the basis of cost. If the source level can not be compromised, the choice will have to be made on the basis of risks versus cost; ie, the risk of not meeting the required source level will be slightly higher with the small source, but it costs approximately half as much.

BIBLIOGRAPHY

1. Ralph S. Woollett, "Underwater Helmholtz-Resonator Transducer: General Design Principles," NUSC Technical Report 5633, 5 July 1977.

2. T. A. Henriquez, "The USRD Type F39A 1-kHz Underwater Helmholtz Resonator," NRL Report 7740, 10 April 1974.

3. Claude E. Sims, "Bubble Transducers for Radiating High-Power Low-Frequency Sound in Water," J. Acoust. Soc. Am. 32, 1305 (1960).

4. G. D. Hugus III, "Pressure-Compensating Systems for Underwater Gas-Filled Electroacoustic Transducers," NRL Memorandum Report 2955, 1 Dec 1974.

5. I. D. Groves, Jr., "Twenty Years of Underwater Electroacoustic Standards," NRL Report 7735, 21 Feb 1974.

6. Irving Weisman and Seymour Adler, "Locked Frequency Modification of A MARK 6 (b) Source," Technical Report No. 165, Jan. 1969, Hudson Laboratories of Columbia University.

7. Ralph S. Woollett, "VLF Flexural Disk Transducers Using Disks 1 Meter in Diameter," NUSC Technical Report 5509, 3 Dec 1976.

8. H. L. Rathun, Jr., and E. J. Parssinen, "Low-Frequency Flexural Disk Transducers", J. Underwater Acoust. Vol. 12-No. 3, July 1962.

9. John V. Bouyoucos, "Hydroacoustic Transduction", J. Acoust. Soc. Am. 57, 1341 (1975).

10. John V. Bouyoucos, "Flexural Disc Transducer," U. S. Patent No. 3,382,841 (14 May 1968).

11. A. M. Young, "Proposal for the Development of a High-Power, Low-Frequency Underwater Acoustic Source," NRL Memorandum Report 2897, 1 Nov 1974.

12. "Proceedings of the Workshop on Low-Frequency Sound Sources," 5, 6, 7 Nov 1973, NUC TP 404 Vol I, Sept 1974.

13. "Lectures on Marine Acoustics" Vol II Ed. by Jerald W. Caruthers, Sea Grant Publication No. TAMU-SG-71-404, June 1971, College Station Texas.

14. "Handbook of Acoustic Projector Technology," Vol I; L. Grantner, F. Kubick, R. Williams; Ocean and Atmospheric Science, Inc., Tech. Rept. TR-76-325, October 1976.

TABLE 1 - SUMMARY OF NORDA DEEP TOW SOURCE REQUIREMENTS

SOURCE LEVEL	220 dB re 1 μPa at 1m (MAXIMUM) 204 dB re 1 μPa at 1m (MINIMUM)
FREQUENCY	≤ 500 Hz
BANDWIDTH	≥ 200 Hz
PULSE LENGTH	5 msec (PULSED CW) 125/250/500 msec (PULSED FM)
PULSE REPETITION RATE	15 sec (MAX) 30 sec (DESIRED)
PHASE RESPONSE (FM)	LINEAR
POWER	COMPATIBLE WITH 5700m OF RG8/U COAXIAL CABLE
SIZE	0.6m DIAMETER X 1.8m LONG
WEIGHT	460 kg
OPERATING DEPTH	3000m (MINIMUM) 4000m (DESIRED) 6000m (MAXIMUM)

Naval Research Laboratory
UNDERWATER SOUND REFERENCE DIVISION
P. O. Box 8337, Orlando, Florida 32806

USRD No. 19

Date:

Water temp. °C

Hydrostatic Pressure kPa

FIGURE 1

NORMALIZED ENERGY SPECTRAL DENSITY OF 2 CYCLE PULSE

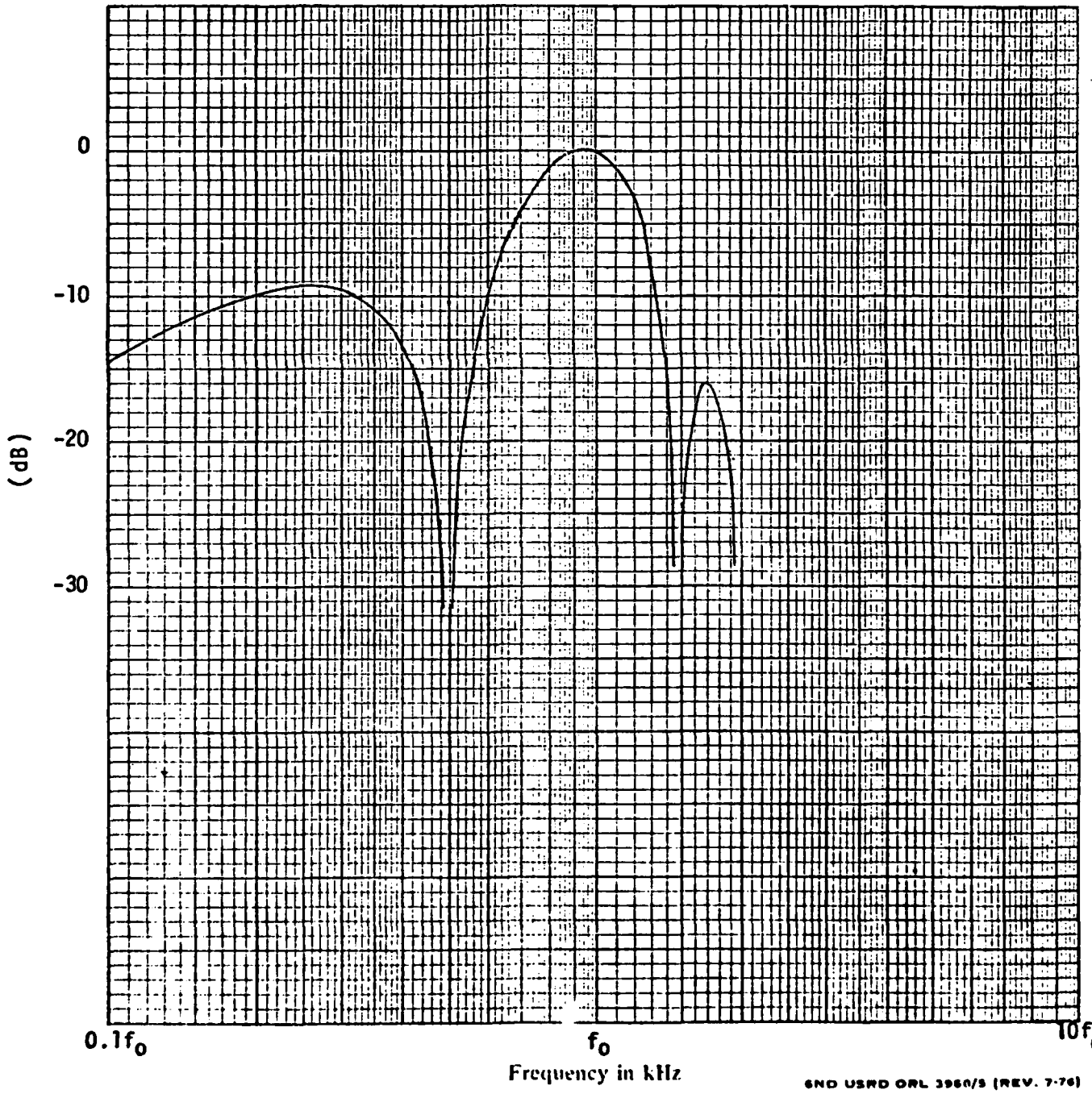

CONCEPTUAL **DESIGN FOR LOW** FREQUENCY **DEEP TOW SOURCE**

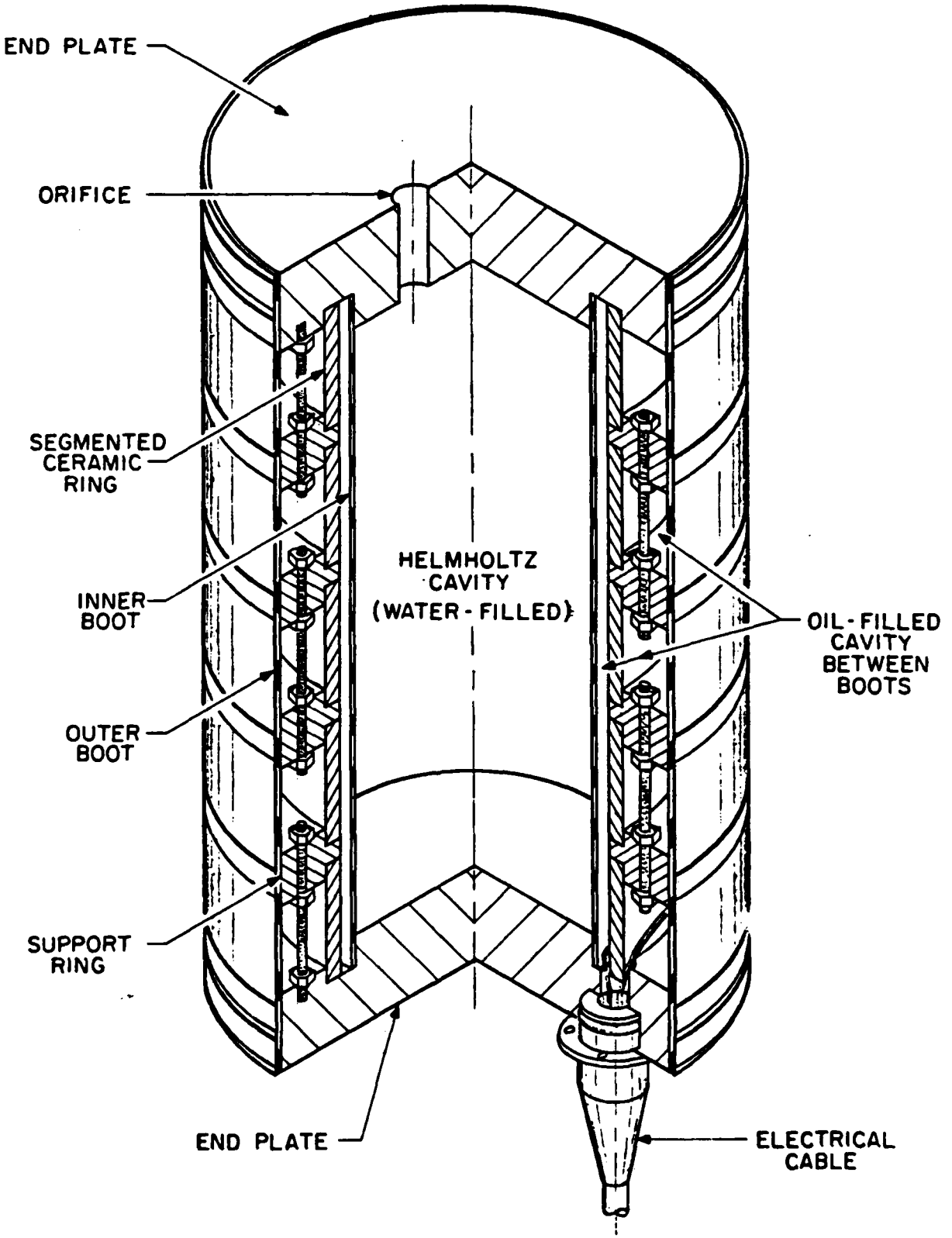

FIGURE 3

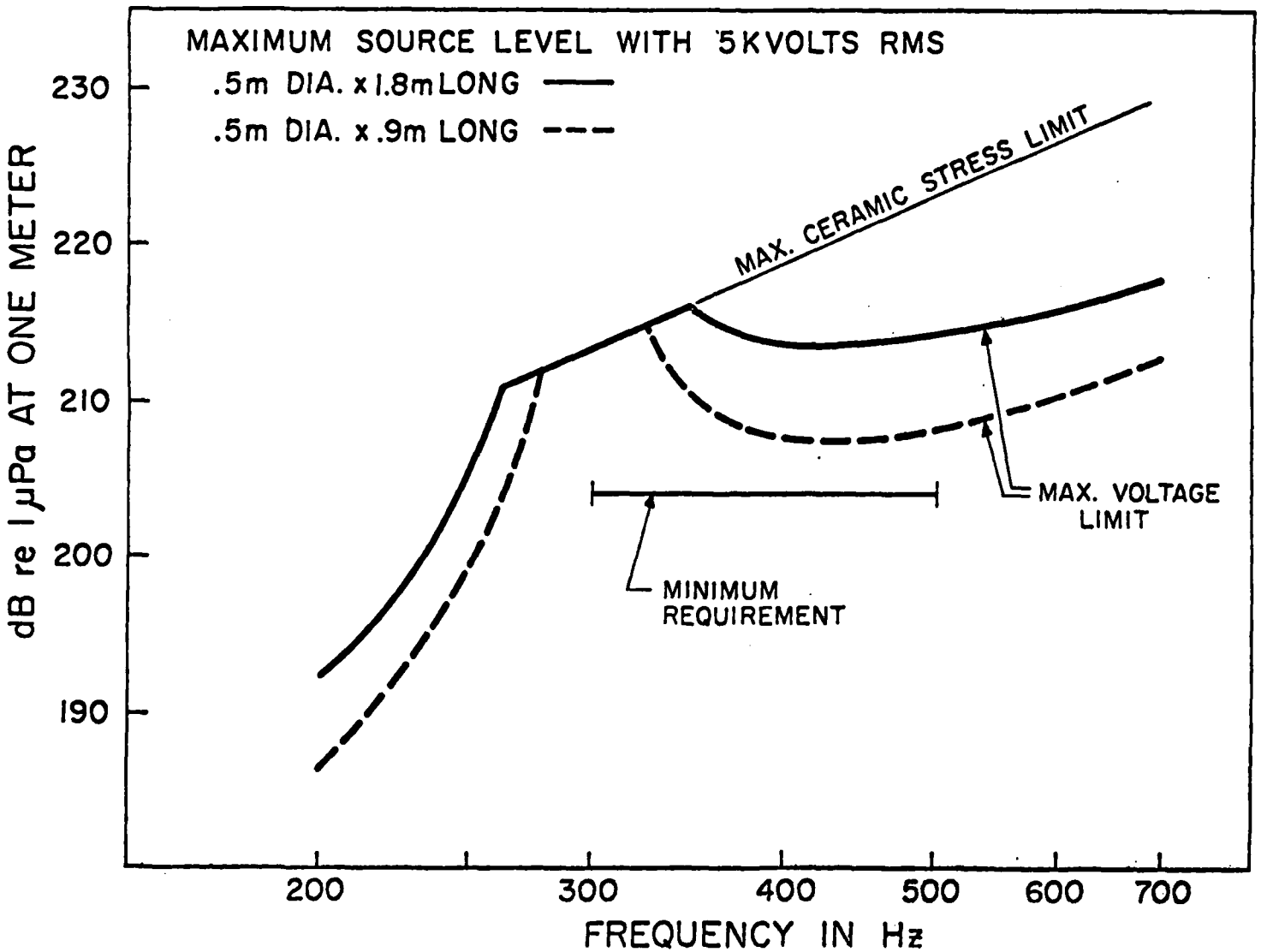
MAXIMUM SOURCE LEVEL WITH 5KVOLTS RMS
.5m DIA. x 1.8m LONG
.5m DIA. x .9m LONG
MAX. CERAMIC STRESS LIMIT
MAX. VOLTAGE LIMIT
MINIMUM REQUIREMENT
dB re 1 μPa AT ONE METER
230
220
210
200
190
200
300
400
500
600
700
FREQUENCY IN Hz

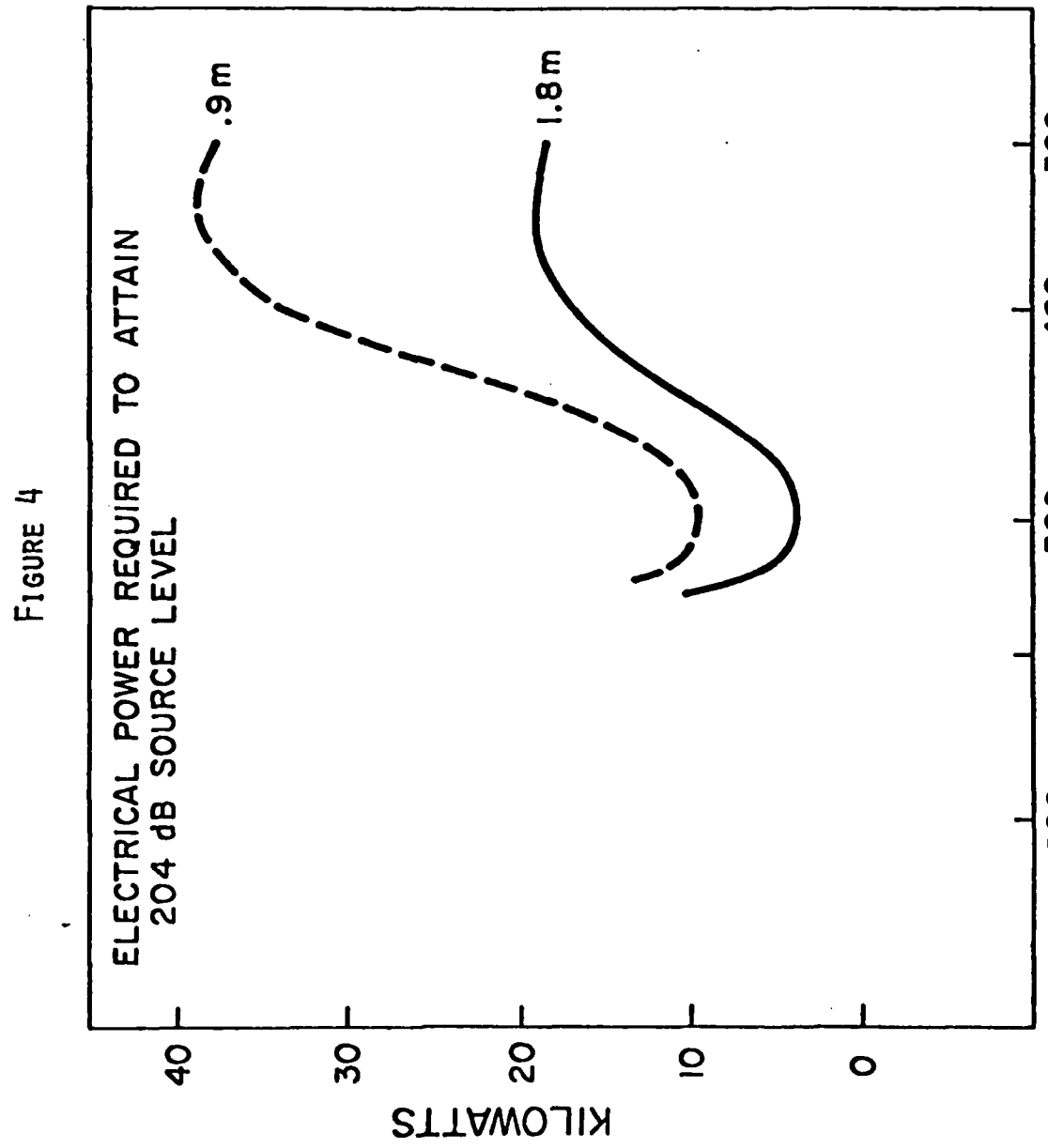
ELECTRICAL POWER REQUIRED TO ATTAIN
204 dB SOURCE LEVEL
.9m
1.8m
KILOWATTS
0
10
20
30
40
200
300
400
500
FREQUENCY IN Hz

FIGURE 4

Naval Research Laboratory
UNDERWATER SOUND REFERENCE DIVISION
P O. Box 8337, Orlando, Florida 32806

INPUT IMPEDANCE

0.9M LONG HELMHOLTZ RESONATOR

_____ WITHOUT CABLE

- - - - WITH 5700M. OF RG8/U CABLE

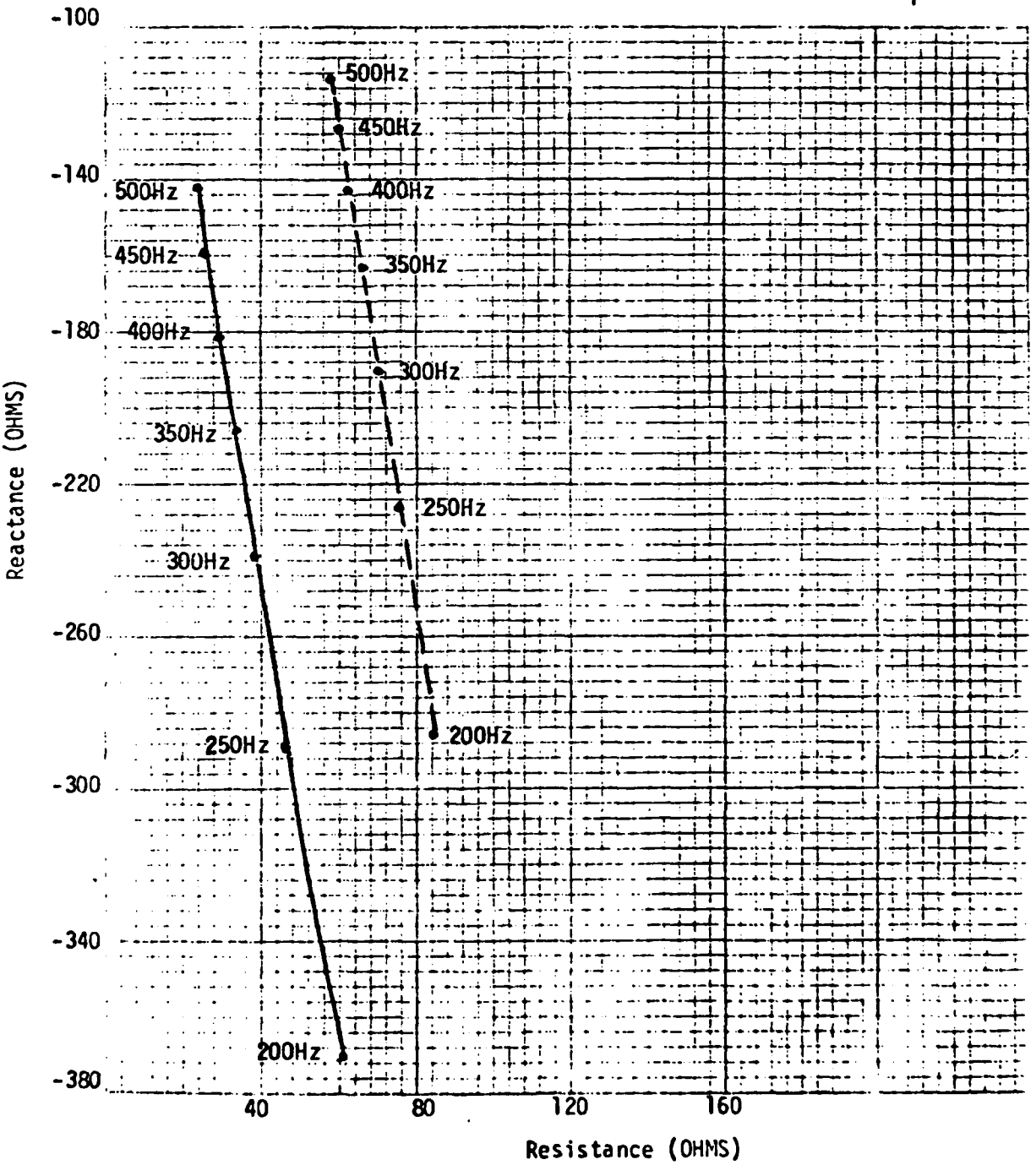

Figure 5

Naval Research Laboratory
UNDERWATER SOUND REFERENCE DIVISION
P. O. Box 8337, Orlando, Florida 32806

INPUT IMPEDANCE

1.8M LONG HELMHOLTZ RESONATOR

_____ WITHOUT CABLE

- - - - WITH 5700M OF RG8/U CABLE

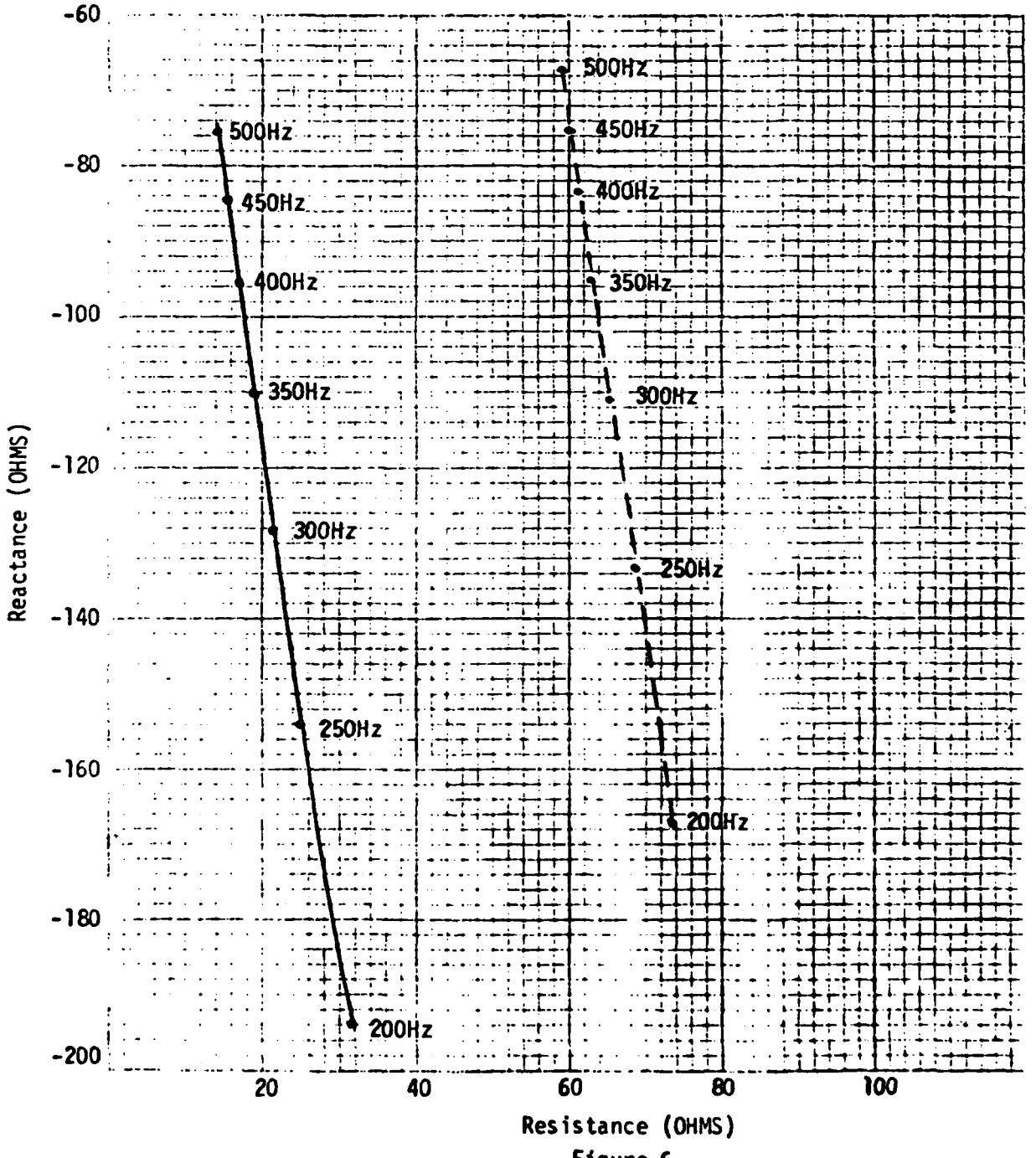

Figure 6

Naval Research Laboratory
UNDERWATER SOUND REFERENCE DIVISION
P. O. Box 8337, Orlando, Florida 32806

INPUT IMPEDANCE

TUNED 0.9M LONG HELMHOLTZ RESONATOR WITH 5700M OF RG8/U CABLE

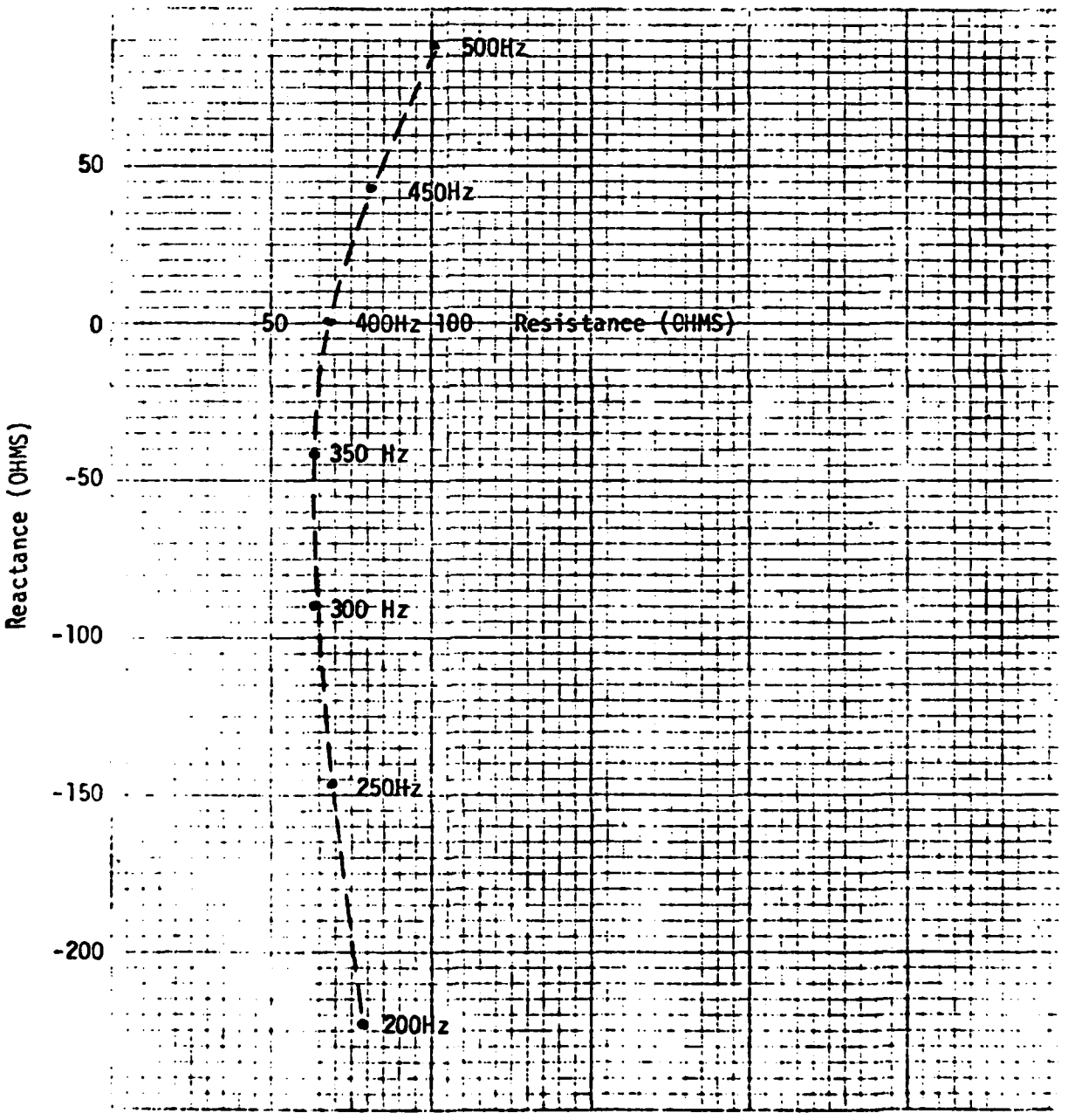

Figure 7

Naval Research Laboratory
UNDERWATER SOUND REFERENCE DIVISION
P. O. Box 8337, Orlando, Florida 32806

INPUT IMPEDANCE

TUNED 1.8M LONG HELMHOLTZ RESONATOR WITH 5700M OF RG8/U CABLE

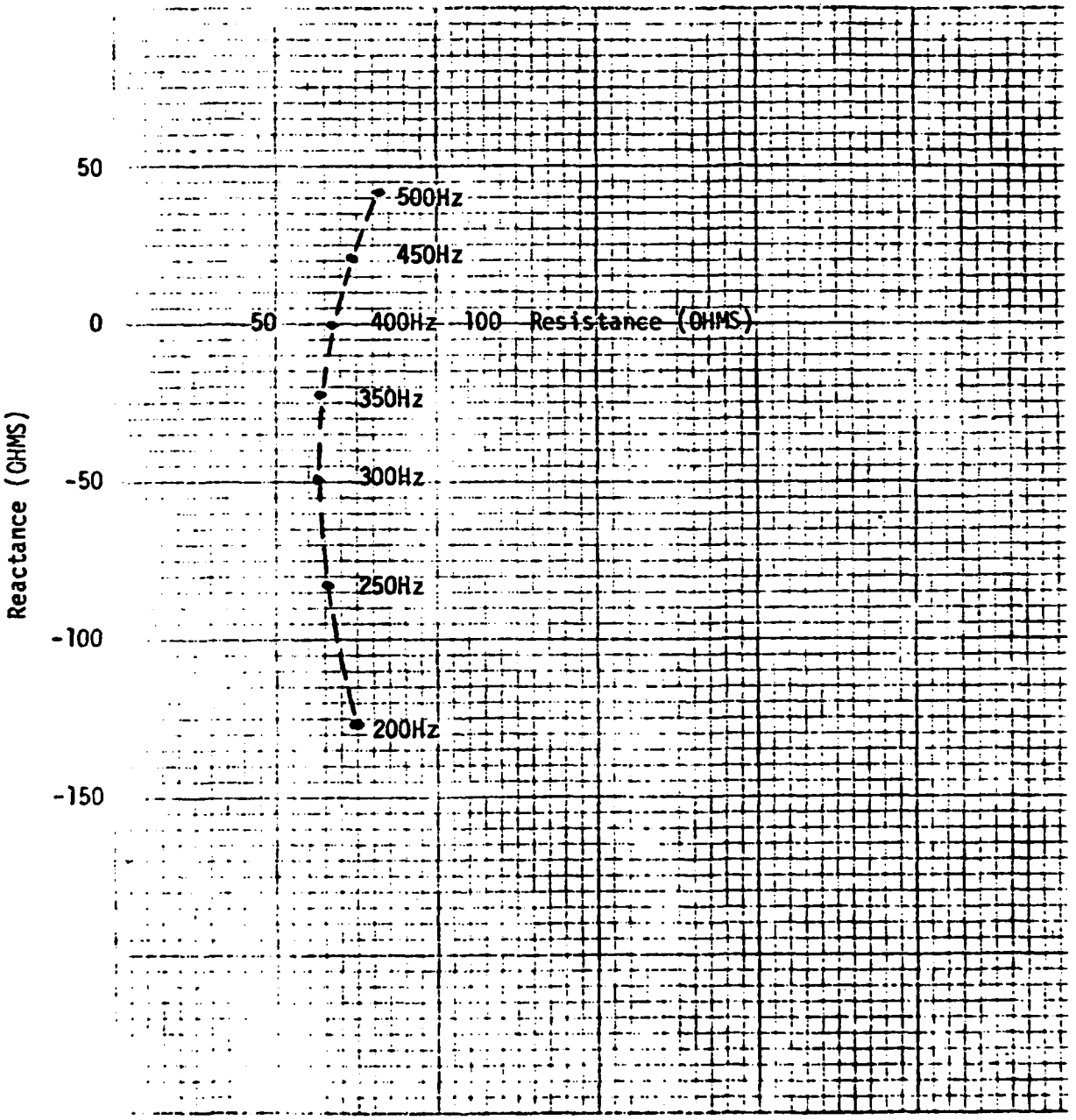

Figure 8

Naval Research Laboratory
UNDERWATER SOUND REFERENCE DIVISION
P. O Box 8337, Orlando, Florida 32806

UNTUNED 0.9M HELMOLTZ RESONATOR WITH
5700M OF RG8/U CABLE.

VOLT-AMPERES REQUIRED TO GENERATE
204 DB RE 1 µPA AT 1M

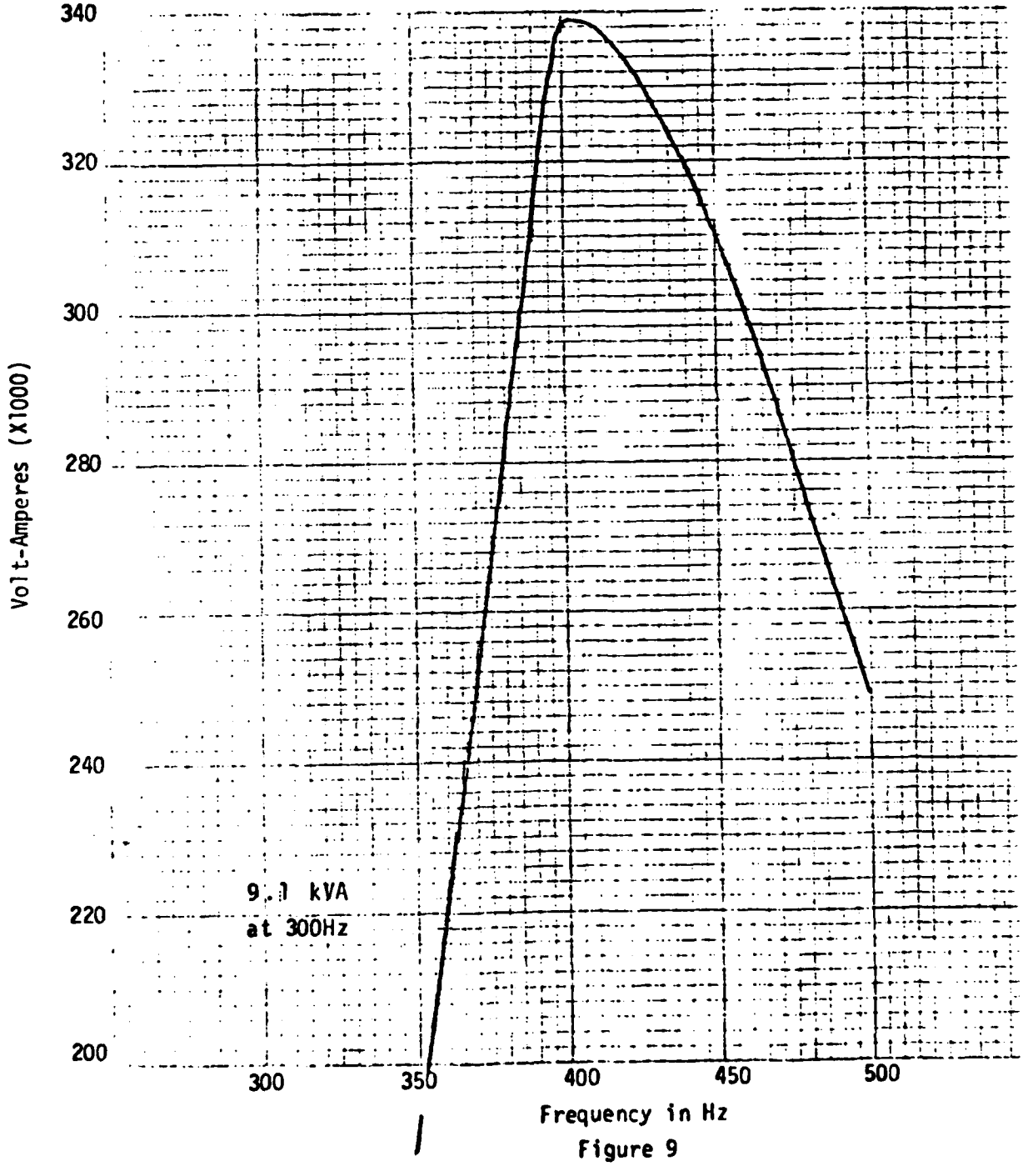

Figure 9

Naval Research Laboratory
UNDERWATER SOUND REFERENCE DIVISION
P. O. Box 8337, Orlando, Florida 32806

UNTUNED 1.8M LONG HELMHOLTZ RESONATOR WITH 5700M OF RG8/U CABLE

VOLT-AMPERES REQUIRED TO GENERATE 204 DB RE 1 μPA AT 1M

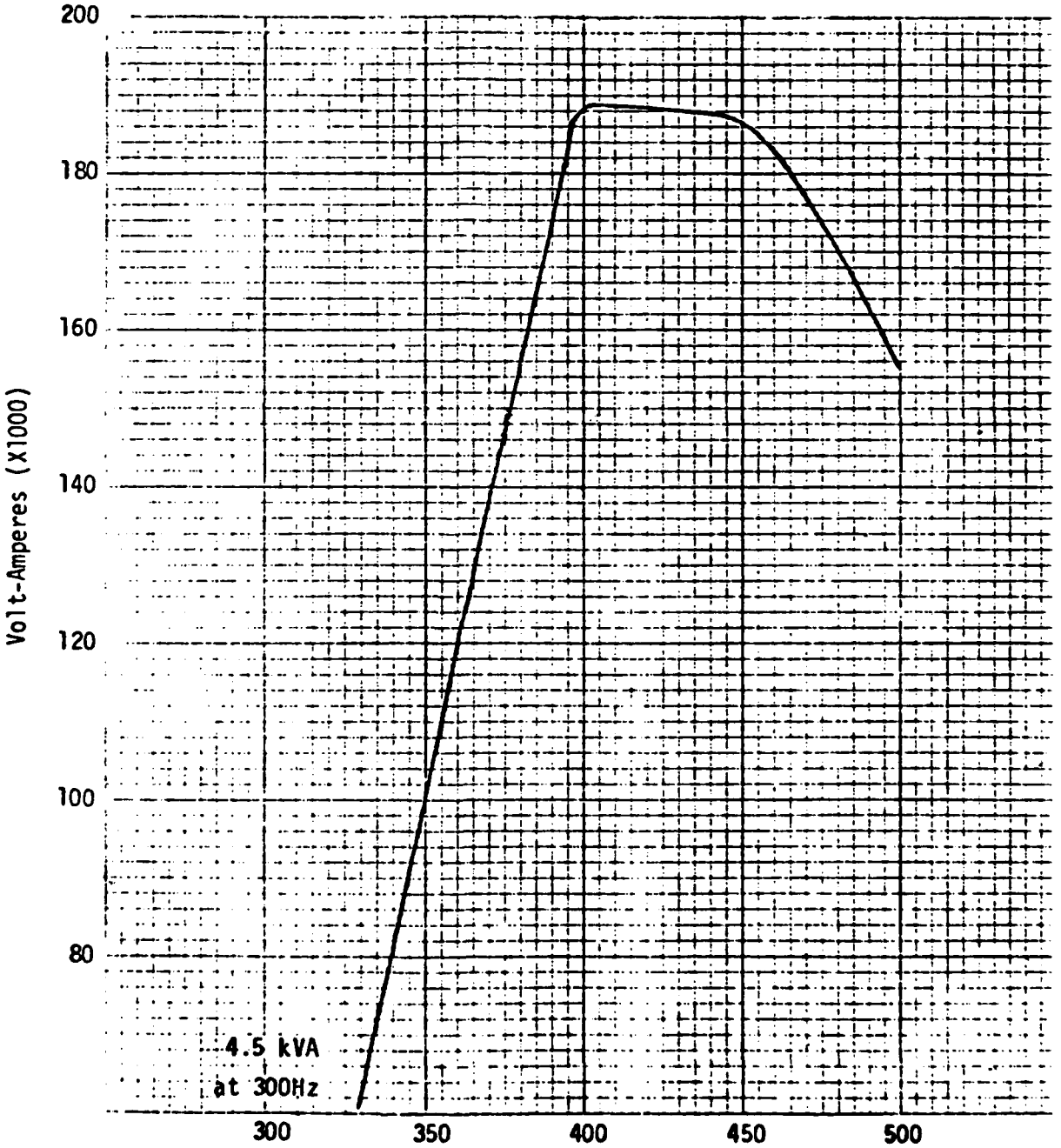

Figure 10

Naval Research Laboratory
UNDERWATER SOUND REFERENCE DIVISION
P. O. Box 8337, Orlando, Florida 32806

VOLT-AMPERES REQUIRED TO GENERATE
204 DB RE 1 μPA AT 1M

_____ TUNED 1.8M LONG HELMHOLTZ RESONATOR WITH 5700M OF RG8/U CABLE

- - - - TUNED 0.9M LONG HELMHOLTZ RESONATOR WITH 5700M OF RG8/U CABLE

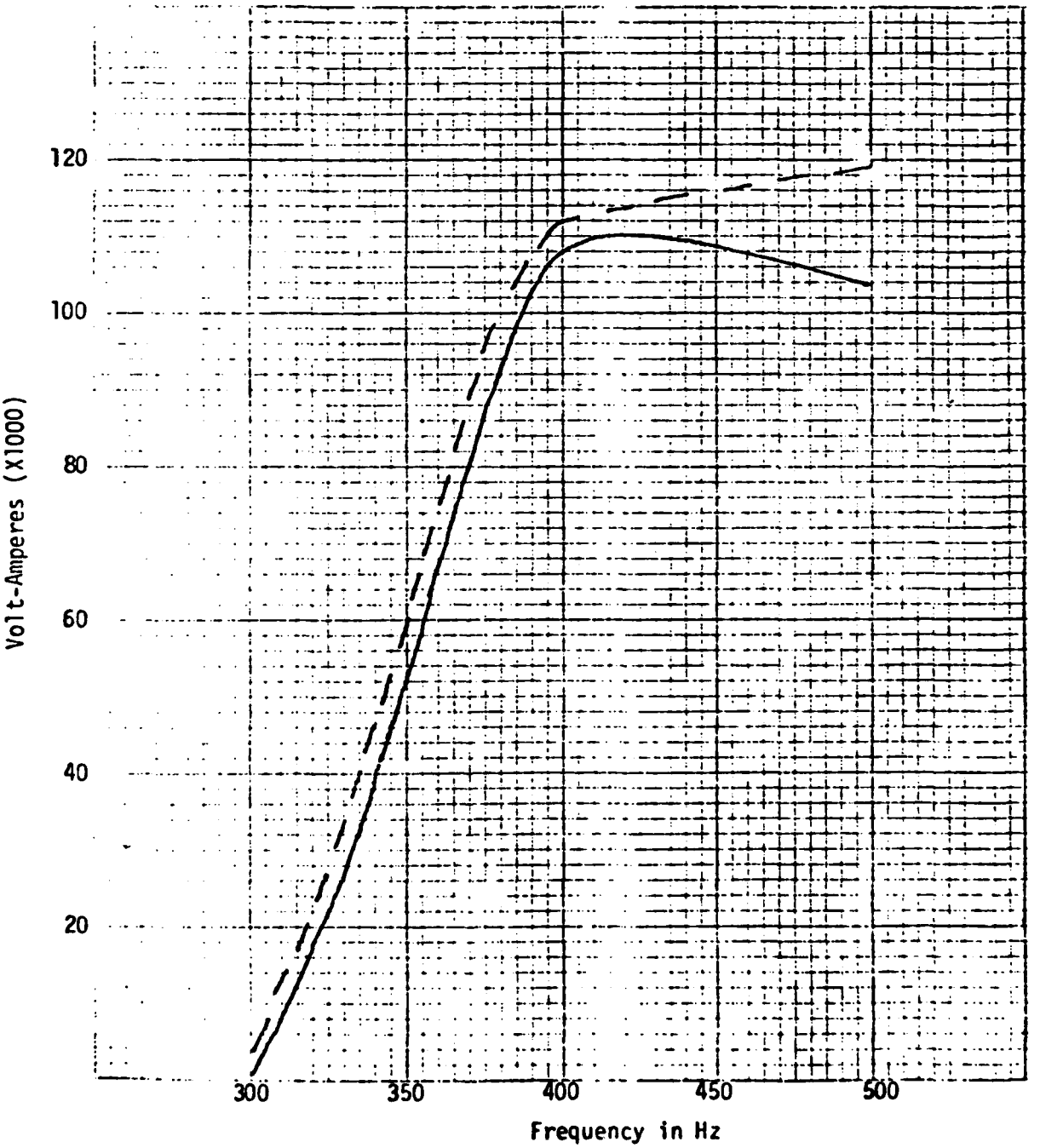

Figure 11

TABLE 2

SUMMARY OF CHARACTERISTICS: RECOMMENDED APPROACH

DIAMETER	0.5m	0.5m
LENGTH	0.9m	1.8m
WEIGHT (IN AIR)	500 kg.	1020 kg.
WEIGHT (IN WATER)	380 kg.	775 kg.

IV.B. A DEEP TOWED 3KHz PARAMETRIC SOURCE

James Kosalos, INCO U.S. Inc.

ABSTRACT

During September and October 1978, INCO United States, Inc. deployed a prototype deep towed survey system to chart distributions of manganese nodules for an ocean mining consortium directed by Ocean Management, Inc. (OMI). The survey system's acoustic sensors included a bilateral side looking sonar and a 3KHz parametric source for sub-bottom profiling beneath the survey vehicle. Profiling records produced by this system were much improved over those achieved with a 3.5 KHz source towed on the surface and received either there or on the deep towed vehicle. An average of 100 ms bottom penetration time was achievable with both systems. Although the quality of the parametrically produced profiles was flawed by signal strength variations induced by pitching of the towed vehicle, the narrow source beam width (4^{o} fore and aft and 20^{o} thwartwise) provided provoking high resolution views of sub-bottom structure.

SYSTEM EVOLUTION AND DESCRIPTION

The need for sub-bottom profiling capability in the deep towed survey system was identified early in the design phase and various methods of achieving this were investigated. Since an appropriately designed sub-bottom profiler would also provide microtopographic structure beneath the survey vehicle, a parametric means of generating the required acoustic energy seemed attractive because of the narrow beam-patterns achievable: Non parametric low frequency sources designed to operate at full ocean depths cannot yield moderate beam patterns or particularly good front to back ratios without becoming unattractively large and heavy.

An early solution utilized a parametric source which was a concomitant product of a specially designed side looking sonar, to wit the side looking transducers were to have side lobes in the vertical plane which could be overlapped beneath the towed vehicle to produce a region of acoustic "mixing" without an additional projector (Kosalos & Cooke, U.S. patent #4075599). Thus the parametric source frequency would be given by the difference between those selected for the side looker, and the receiving system would be a separate hydrophone optimized for this task. This concept was eventually abandoned because of fears about the colinearily of the primaries and the potentially high design and development cost of the specialized projectors. A solution involving a third projector for the parametric source was subsequently chosen.

The selected configuration utilized three identical transducers designed to yield appropriate vertical patterns for both the side looker and the parametric source. They were chosen to have four vertically stacked horizontal rows of elements which

could be connected in different configurations. Thus, when arranged for exitation by a single frequency source, they yielded a suitable side look beam pattern and when driven by a dual frequency source they could provide the colinear acoustic beams necessary for parametric generation of 3 KHz sub-bottom profiling signals. Horizontal beam pattern problems caused by attempts at interdigitating array elements dictated utilization of only entire horizontal rows of elements to implement both configurations of the transducers. Computer drawn theoretical beam patterns matched those measured to within a few db and provided the means with which to iterate on an acceptable solution.

The 3 KHz sub-bottom profiling signals were received on a separate transducer on the towed vehicle and telemetered to the surface for display.

SYSTEM DEPLOYMENT AND OPERATION

The parametric source and the separate low frequency receiving transducer were installed on a neutrally buoyant tow vehicle which followed a two ton depressor at the end of the single coaxial tow cable. This configuration proved to be reasonably stable with ship heave induced motion confined nearly totally to the depressor. Vehicle roll was nearly non-existent (less than 0.4^{o}), yaw stability was also reasonably good, but pitching proved to be bothersome with excursions greater than 4^{o} being observed reasonably often. Pitch period was around eighteen seconds and the profiling records clearly show both signal strength fading, as the vehicle's receiver moved out of the narrow acoustic beam, and ficticious vehicle altitude variation caused by pitch induced errors in narrow beam altitude measurements made using the primary frequencies.

The acoustic profiles generated with this system indicate pelagic sedimentary processes are not as simple as once thought. Although smooth sedimentary blanketing of rough topographic features was observed (some submarine hills were unveiled as rugged rock outcrops several hundred meters high), large, generally uninteresting, flat areas were found to contain a variety of discontinuous sedimentary horizons. Some of these features would have been visible with a deep towed 3KHz broad beam profiler but the narrow beam parametric source provided unambiguous information in areas where a conventional source would have failed.

COMPUTER SIMULATION MODEL OF A TRANSIENTLY EXCITED UNDERWATER SOUND PROJECTOR

R.W. Hutchins
Huntec (70) Limited
Toronto, Ontario, Canada

Summary

A computer simulation model of a transiently excited plane piston underwater sound projector is developed, which yields solutions of the acoustic performance of the transducer system to three figure accuracy, at a cost of about $30.00 per case. The methodology outlined, is capable of dealing with the non linearities of an electro-dynamic source of the "boomer" type, and in addition, is particularly suitable for mechanically "stiff" systems, where the time constants of the electrical equation of motion are some three orders of magnitude shorter than the time constants of the mechanical equation of motion.

It is shown that the convolution integral representing the transient radiation loading of the medium on the piston appearing in the mechanical equation of motion, may be dealt with by decomposing the electro-mechanical system equations, into two coupled sub systems, the first of which is solved by the method of state variables, and the second, which is solved by direct integration using Simpson's method.

A comparison of experimental data and data predicted by the model, agree within the experimental error, in this case about 10%.

The model is completely general, and may be adapted to yield both the transient and steady state solutions for any type of transducer, including sonar type projectors.

List Of Symbols

- A - Area of the piston square meters
- a - Radius of the piston in meters
- C - Capacity of energy storage capacitor in farads
- C_o - Velocity of sound in the medium (Water) meters per second
- d - Density of medium, Kilograms per cubic meter
- E - Initial voltage on the capacitor Volts
- $F(t)$ - Reaction force imposed by the medium on the moving piston Newtons
- g - Acceleration due to gravity meters per second
- $H(t)$ - Heaviside unit step function
- $h_m(t)$ - Impulse response function of the piston
- $i(t)$ - The time dependant coil current
- k - The spring constant of the piston suspension Newtons per meter
- $\ell(x)$ - The effective circuit inductance, dependant upon the piston position, Henries
- $\ell(0)$ - The value of the circuit inductance with the piston in its initial position, Henries
- m - Mass of the piston in kilograms
- $p(z_o,t)$ - The time dependant pressure at a distance of z_o meters from the piston along the piston axis. Newtons per square meter
- $r(x)$ - The effective circuit resistance, dependant upon the piston position, Ohms
- t - Time in seconds
- $v(t)$ - The time dependant piston velocity in meters per second
- $x(t)$ - The time dependant displacement of the piston from the coil, in meters
- x_o - Initial distance of the plane of the piston from the coil
- z_o - Distance measured along the piston axis from the piston to the field point in meters
- γ - Depth of immersion of the piston in meters.

Introduction

The application of acoustic methods to an increasing variety of engineering problems associated with the sea bed, and near sub-surface, has grown rapidly in recent years.

Some examples of instrument systems utilizing acoustics, include the familiar echo sounder or fathometer; side scan sonar; and sub bottom profilers, the latter having been adapted from deep seismic exploration experience.

The distribution of pressure versus time (pressure signatures) that are desired for various applications are usually known, or can be determined, and the problem facing the designer of underwater sound generators, of whatever form, is to devise an apparatus which produces an adequate approximation to the desired sound field.

The usual procedure is to solve the equation of motion of the transducer to obtain the steady state velocity of the radiating surface. From this, the velocity potential may be derived by convolving the velocity function with the impulse response of the transducer. Finally, the far field pressure signature is obtained by taking the time derivative of the velocity potential.

The above procedure cannot be easily applied to obtain the transient solution, since the loading of the radiating surface by the medium is time dependant, and the

electro-mechanical equations of motion cannot be directly solved to yield the required velocity function.

This paper outlines a method of obtaining a solution to the problem of predicting both the near field and far field acoustic pressure signatures of a "boomer" type[1] of seismic sound source, when it is impulsively excited by the discharge of a capacitor.

This has made it possible to formulate the associated transducer design problem in such a way that the transient behaviour of the complete system is readily obtained with the aid of a digital computer.

These computer solutions are sufficiently cheap($30.00 per case) that search procedures can be used to arrive at a set of system parameters that produce the desired pressure signatures, and, at the same time, maximize the electric to far field acoustic conversion efficiency.

The design method is completely general and can therefore be used to obtain both the transient and steady state solutions of the system equations for any class of underwater sound generator, including impulsively excited sonar type projectors.

The Electro-Mechanical Equations

One form of an electro-dynamic sound projector, sometimes referred to as a boomer, utilizes the Lorentz forces arising from the interaction of eddy currents induced in an electrically conducting sheet which serves as a piston, and a driving current flowing through an adjacent flat pancake coil.

The mechanical equation of the forces acting upon the piston, include a radiation term given by

$$F(t) = dc_0 A \int_0^t h_n(t-\tau) \frac{d^2}{d\tau^2} x(\tau)\, d\tau \qquad \ldots\ldots\ldots\ldots (1)$$

The impulse response function $h_n(t)$ for a plane piston in an infinite baffle is given by[2] as

$$h_n(t) = \frac{2}{\pi}\left\{ \cos^{-1}\left(\frac{c_0 t}{2a}\right) - \frac{c_0 t}{2a}\left[1-\left(\frac{c_0 t}{2a}\right)^2\right]^{\frac{1}{2}} \right\} \times H(2a - c_0 t) \qquad \ldots\ldots\ldots\ldots (2)$$

Where $H(2a - c_0 t) = 0$ for $t < \frac{2a}{c_0}$

$= 1$ for $t > \frac{2a}{c_0}$

The driving force may be represented by the product of the current squared, and the derivative with respect to the piston displacement x of the circuit inductance[3]. The form of the mechanical equation is thus

$$m\frac{d^2x}{dt^2} + dc_0 A \int_0^t h_n(t-\tau)\frac{d^2}{d\tau^2} x(\tau)\, d\tau + k\,x(t) + (mg + dg_j A) = \frac{1}{2}\frac{d}{dx} l(x)\left[i(t)\right]^2 \qquad \ldots\ldots\ldots\ldots (3)$$

The first term represents the inertia due to the mass of the piston, the second term the radiation loading, the third the restoring force due to the supporting spring, the fourth a constant due to the static pressure of the fluid and the weight of the piston (transducer pointing downwards).

The electrical equivalent circuit of the transducer, as seen at the coil terminals may be considered as an inductance in series with a resistance, the values of which depend upon the position of the piston relative to the coil.

The coil is connected through a crowbar switch to a capacitor, charged to an initial voltage. When the capacitor is discharged through the transducer, the equivalent circuit inductance and resistance consists of the leakage inductance of the transducer, the a-c resistance of the coil, the external circuit inductance and resistance, and a displacement dependant inductance and resistance arising from the variable coupling between the coil and the circuit represented by the moving piston.

These parameters may be lumped together, to produce an equation of the form

$$\frac{d}{dt}\left[l(x)\, i(t)\right] + Y(x) i(t) + \frac{1}{C}\int i(t)\, dt = 0 \qquad \ldots\ldots\ldots\ldots (4)$$

Equations (3) and (4) must be solved for the time dependant current $i(t)$ and the corresponding piston displacement $x(t)$ and velocity $\dot{x}(t)$, for the following initial conditions

$$i(0) = 0 \qquad \ldots\ldots\ldots\ldots (5)$$

$$\frac{d}{dt} i(0) = -\frac{E}{l(0)} \qquad \ldots\ldots\ldots\ldots (6)$$

$$x(0) = x_0 \qquad \text{.....(7)}$$

$$\frac{d}{dt}x(0) = 0 \qquad \text{.....(8)}$$

Equations (3) through (8) inclusive may be expressed in normal form* by the following substitutions

$x(t)$ is represented by x_1

$\frac{d}{dt}x(t)$ is represented by x_2

$i(t)$ is represented by x_3

$\frac{d}{dt}i(t)$ is represented by x_4

to yield

$$\dot{x}_1 = x_2 \qquad \text{.....(9)}$$

$$\dot{x}_2 = -C_2 x_1 - C_3 + C_4 g_7(x_1) x_3^2 - C_5 \int_0^t h_4(t-\tau) \frac{d}{d\tau} x_2(\tau) d\tau \qquad \text{.....(10)}$$

$$\dot{x}_3 = x_4 \qquad \text{.....(11)}$$

$$\dot{x}_4 = \begin{bmatrix} - g_1(x_1) x_2^2 - g_2(x_1) x_2 \\ - g_3(x_1) - g_4(x_1) \dot{x}_2 \end{bmatrix} x_3 - g_5(x_1) x_2 x_4 - g_6(x_1) x_4 \qquad \text{.....(12)}$$

where

$$C_2 = \frac{k}{m}$$

$$C_3 = \frac{mg + dg_3 A}{m}$$

$$C_4 = \frac{1}{m}$$

$$C_5 = \frac{d C_0 A}{m}$$

$$g_1(x_1) = \frac{1}{\ell(x_1)} \frac{d^2}{dx_1^2} \ell(x_1)$$

$$g_2(x_1) = \frac{1}{\ell(x_1)} \frac{d}{dx_1} \ell(x_1)$$

$$g_3(x_1) = \frac{1}{C \ell(x_1)}$$

$$g_4(x_1) = \frac{1}{\ell(x_1)} \frac{d}{dx_1} \ell(x_1)$$

$$g_5(x_1) = \frac{2}{\ell(x_1)} \frac{d}{dx_1} \ell(x_1)$$

$$g_6(x_1) = \frac{V(x_1)}{\ell(x_1)}$$

$$g_7(x_1) = \frac{d}{dx_1} \ell(x_1)$$

and the initial conditions are

$$\dot{x}_1(0) = x_0 \qquad \text{.....(13)}$$

$$\dot{x}_2(0) = 0 \qquad \text{.....(14)}$$

$$\dot{x}_3(0) = 0 \qquad \text{.....(15)}$$

$$\dot{x}_4(0) = -\frac{E}{\ell(0)} \qquad \text{.....(16)}$$

Equations (9) through (16) inclusive constitute the state equations of the transducer system.

For practical transducer systems of this type, the time constants of the electrical equation are faster than the time constants of the mechanical equation, by about three orders of magnitude, and thus the coupled equations represent a "stiff system" in terms of its numerical solutions.

Conventional methods of numerical solution such as Runge-Kutta are not satisfactory unless a very small time step of integration is used to preserve numerical stability, thereby making the computation time to solve such a system on a digital computer prohibitive.

Davison[5,6] has developed a method of numerical solution which deals with "stiff systems" and allows a large time step of integration to be used. His algorithm[5] may be applied to the solution of the state equations (9) through (16) by considering these equations as representing two coupled sub systems S1 and S2 shown in figure 1.

We define a function $Y(t)$ as

$$Y(t) = \dot{x}_2 = -C_2 x_1 - C_3 + C_4 g_7(x_1) x_3^2 + U(t) \qquad \text{.....(17)}$$

and substitute into equation (10) to obtain

$$\dot{x}_2 = -c_2 x_1 - c_3 + c_4 g_7(x_1) x_3^2 + v(t) \quad \ldots\ldots\ldots(18)$$

and substitute for $\dot{x}_2$ from equation (18) into equation (12) to obtain

$$\dot{x}_4 = \left\{ \begin{array}{l} -g_1(x_1) x_2^2 - g_3(x_1) x_2 - g_3(x_1) \\ -g_4(x_1) \left[\begin{array}{l} -c_2 x_1 - c_3 \\ \quad + c_4 g_7(x_1) x_3^2 + v(t) \end{array} \right] \end{array} \right\} x_3$$

$$- g_5(x_1) x_2 x_4 - g_6(x_1) x_4 \quad \ldots\ldots\ldots(19)$$

We now consider sub system S1 whose equations are (9), (11), (18) and (19). and a second sub system S2 whose equation is given by

$$v(t) = -c_5 \int_0^t h_n(t-\tau) y(\tau)\, d\tau \quad \ldots\ldots\ldots(20)$$

The algorithm of [5] may now be used to solve the equations of sub system S1 subject to the initial conditions (13), (14), (15) and (16). Sub system S2 represented by equation (20) may be integrated directly by Simpson's method.

In this manner, the system equations may be simulated on a digital computer to obtain the coil current $x_1(t)$ and the piston velocity $v(t)$.

The Acoustic Pressure Field

The pressure amplitude at any field point is the time derivative of the velocity potential The velocity potential is obtained by convolving the impulse response of the piston with the piston velocity function[7].

Carrying out these operations, the on axis pressure amplitude for a plane baffled piston is

$$p(z_0,t) = dc_0 \left\{ \begin{array}{l} V\left(t - \frac{z_0}{c_0}\right) H\left(t - \frac{z_0}{c_0}\right) \\ -V\left[t - \frac{(z_0^2+a^2)^{\frac{1}{2}}}{c_0}\right] \cdot \\ H\left[t - \frac{(z_0^2+a^2)^{\frac{1}{2}}}{c_0}\right] \end{array} \right\} \quad \ldots(21)$$

Where $V(t)$ is the time dependant piston velocity and z_0 is the distance to the field point along the piston axis.

From equation (21) we observe that if the time duration of the velocity function is less than the path difference between the piston centre to the field point, and the piston edge to the field point, then we may expect to observe two separate pulses, one positive, and one negative.

Pulse Shape Synthesis

Figures 2A and 2B are two arbitrary velocity functions for a plane piston transducer, together with the normalized pressure pulses obtained from equation (21).

To obtain the pressure pulse shape, it is simply necessary to add the mirror image of the velocity function, delayed by an amount equal to the differences in path length.

The negative pressure peak of Figure 2A is about equal to the positive pressure amplitude. Providing the negative absolute pressure does not exceed the cavitation threshold at some position in the near field, this is a desirable pulse shape for a high resolution seismic source.

When high peak intensities are required, it is desirable to suppress the negative pressure peak to avoid cavitation. This can be accomplished by modifying the shape of the piston velocity function as shown in Figure 2B.

The positive pressure of the far field on axis pulse will be maximum when the piston acceleration is maximized, and the negative peak pressure amplitude will be diminished if the piston is gradually brought to rest.

Practical Application of the Model

The design variables of this form of transducer system are reflected in the mechanical parameters represented by the constants C_2 to C_5 inclusive, and in the electrical parameters of the transducer proper and of the external driving circuit, which includes the transmission line from the energy storage capacitor to the transducer. The lumped electrical parameters are represented by the functions $g_1(x_1)$ to $g_7(x_1)$ inclusive.

Whilst the derivation of the explicit forms of these functions in terms of the electrical design variables of the transducer and driving circuit are beyond the scope of this paper, numerical methods have been developed [8] which may be applied to optimization of both mechanical and electrical design variables to achieve some worthy criterion such as maximization of the ratio of the far field acoustic energy, to the electrical energy stored in the capacitor.

At the same time, the velocity function of the piston may be shaped by a variety of methods, to yield only positive pressure pulse signatures in the far field, with little or no excursions into the negative

pressure regions, thus making possible the use of superposition of the output's of several such transducers in an array configuration, with variable delay triggering, to provide a variable spectral source.

The computer program has been written to provide the main beam pressure signature at a specified distance in the far field; the total work done by the piston on the water; the piston velocity and displacement; the coil current, and the radiation loading on the piston by the medium.

A number of computer runs of the system were carried out using different integration step sizes. The computed solution using a step size of $.5 \times 10^{-6}$ seconds agreed with the computed solution using a step size of 2×10^{-6} seconds to at least 2 figure accuracy over a time interval of zero to 500 micro-seconds. The cost of the computation with the smaller step size being approximately $31.10 per case.

A standard model ED-10A transducer that has been in production for some years by the company, was modelled by the above procedure. The comparison between actual field measurements and the computed results are shown in Figure 3. An experimental error of about 10% may be expected in the measured results.

Conclusions

The computer simulation model of a transiently excited underwater sound projector has made it possible to systematically investigate the affect of the various electrical and mechanical design parameters of the transducer, upon its acoustic performance. The mathematical techniques involved in developing the model are borrowed from modern automatic control theory, and have not to the author's knowlege, been applied to this particular kind of problem before.

The method is an extremely powerful design aid, due to the rapidity at which alternative designs may be evaluated at nominal cost.

This model is now being applied to the design of a new family of high intensity seismic sources, of greatly improved performance.

Acknowlegements

I am indebted to E.J. Davison for his algorithms, and for his suggestions as to how to deal with the inconvenient presence of the convolution integral in the equations of motion. I wish also to acknowlege the many valuable contributions of K. Hruska and N.D. Thai to this particular problem.

This work is being supported jointly by the company, and by the Defence Research Board of Canada. The development of commercial transducer systems is being supported in part by the Department of Industry Trade and Commerce, under the Program for the Advancement of Industrial Technology, and by the company.

References

1 Edgerton, H.F. and Hayward, G.C. "The Boomer Sonar Source for Seismic Profiling" J. Geophysics RES, VOL 69 pp 3033-3042, 1964.

2 Stepanishen, P.R.: "The Time Dependent Force and Radiation Impedance on a Piston in a Rigid Infinite Planar Baffle" J. Aco. Soc. A Vol. 49 No. 3 (part 2) pp. 841-849, 1971.

3 Panofsky W.K.H., and Phillips M., "Classical Electricity and Magnetism" Second Edition Chapter 10 Addison-Wesley Publishing Company Inc.

4 Tou, Julius,"Modern Control Theory" McGraw-Hill, 1966.

5 Davison E.J. "An Algorithm for the Computer Simulation of Very Large Dynamic Systems", Dept. of Electrical Engineering, University of Toronto, Central Systems Report No. 7208, May 1972.

6 Davison, E.J., "A High Order Crank-Nicholson Technique for Solving Differential Equations" Computer J. Vol 10, No 2 August 1967 pp 195-197.

7 Stepanishen, P.R. "Transient Radiation from Pistons in an Infinite Planar Baffle": J.Aco. Soc. A., Vol. 49 No. 5 (Part 2), pp 1629-1638, 1971.

8 Davison, E.J., and Alas, R, "Numerical Optimization of Large Interconnected Systems" AIChE Journal Vol 15 No. 2 pp 267-281 March 1969.

(Presented at Ocean '74, IEEE Int. Conf. on Engineering in the Ocean Environment, Halifax, Nova Scotia, August 21-23, 1974)

Top

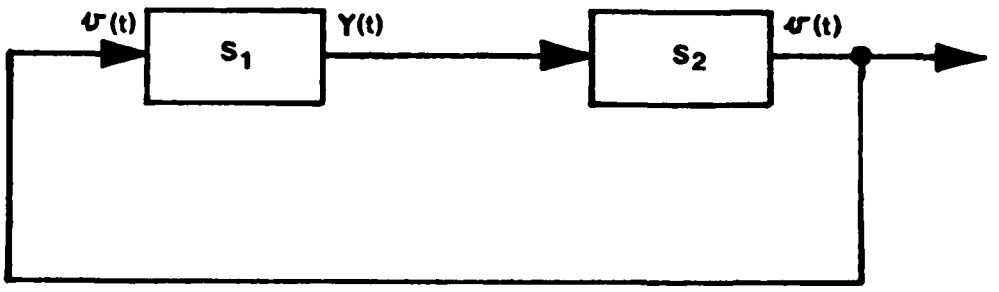

FIGURE 1

COMPUTER SIMULATION MODEL
OF ELECTRO-MECHANICAL
STATE EQUATIONS

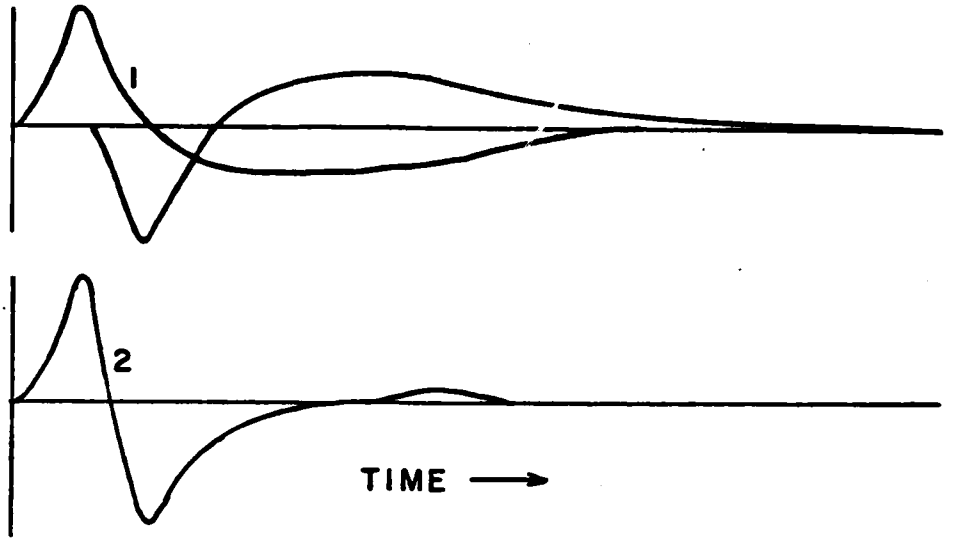

A

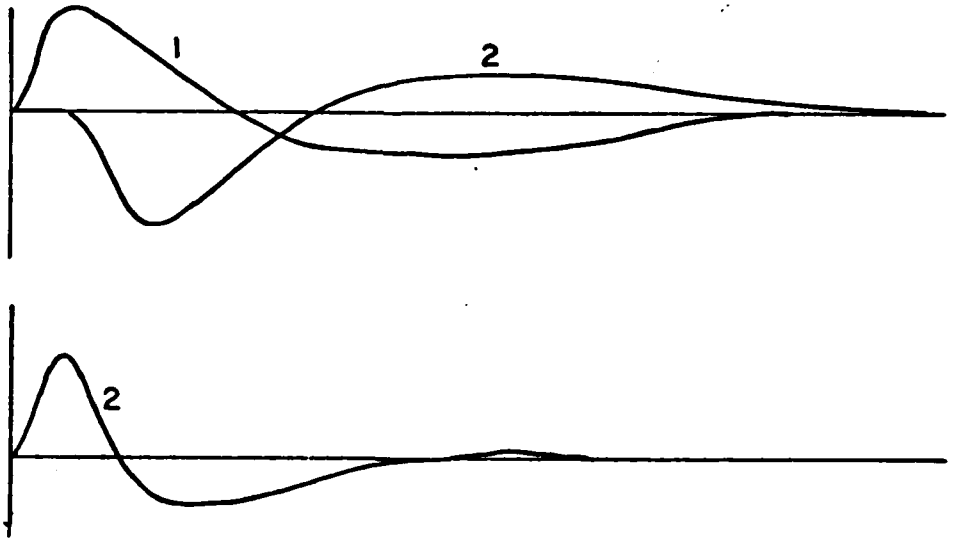

B

FIGURE 2

NORMALIZED ON-AXIS PRESSURE SIGNATURES (2) ARISING FROM AN ARBITRARY PISTON VELOCITY FUNCTION (1)

A - RAPID DECELERATION
B - GRADUAL DECELERATION

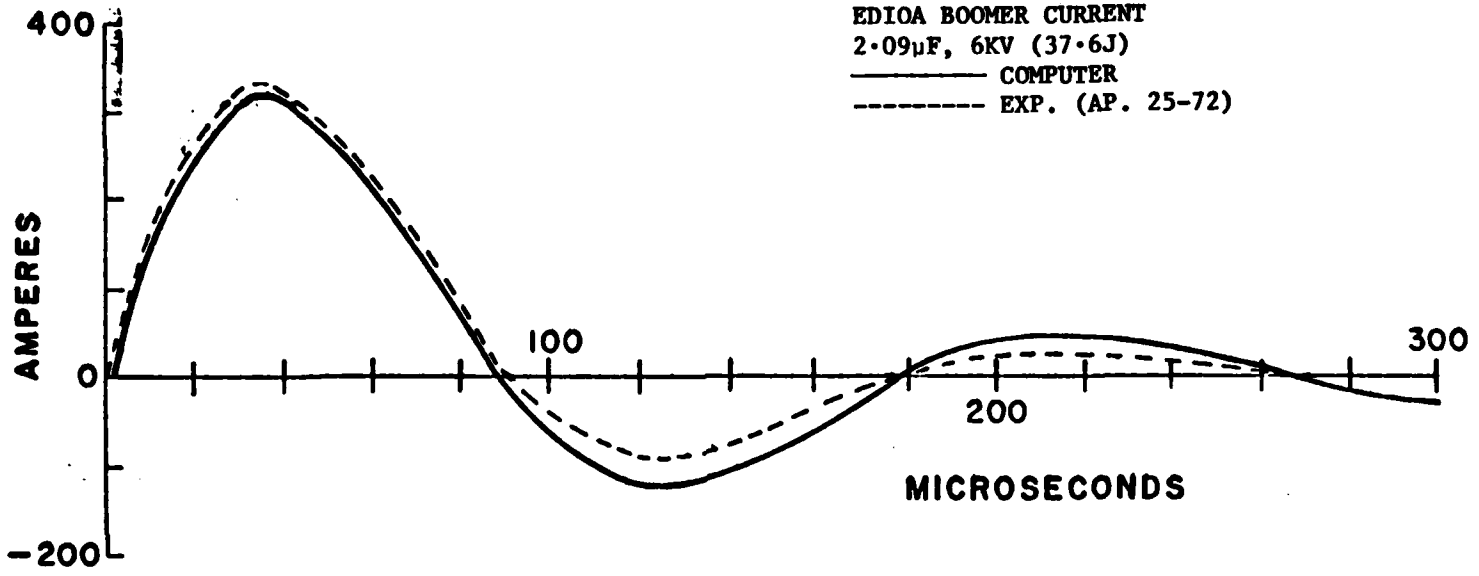

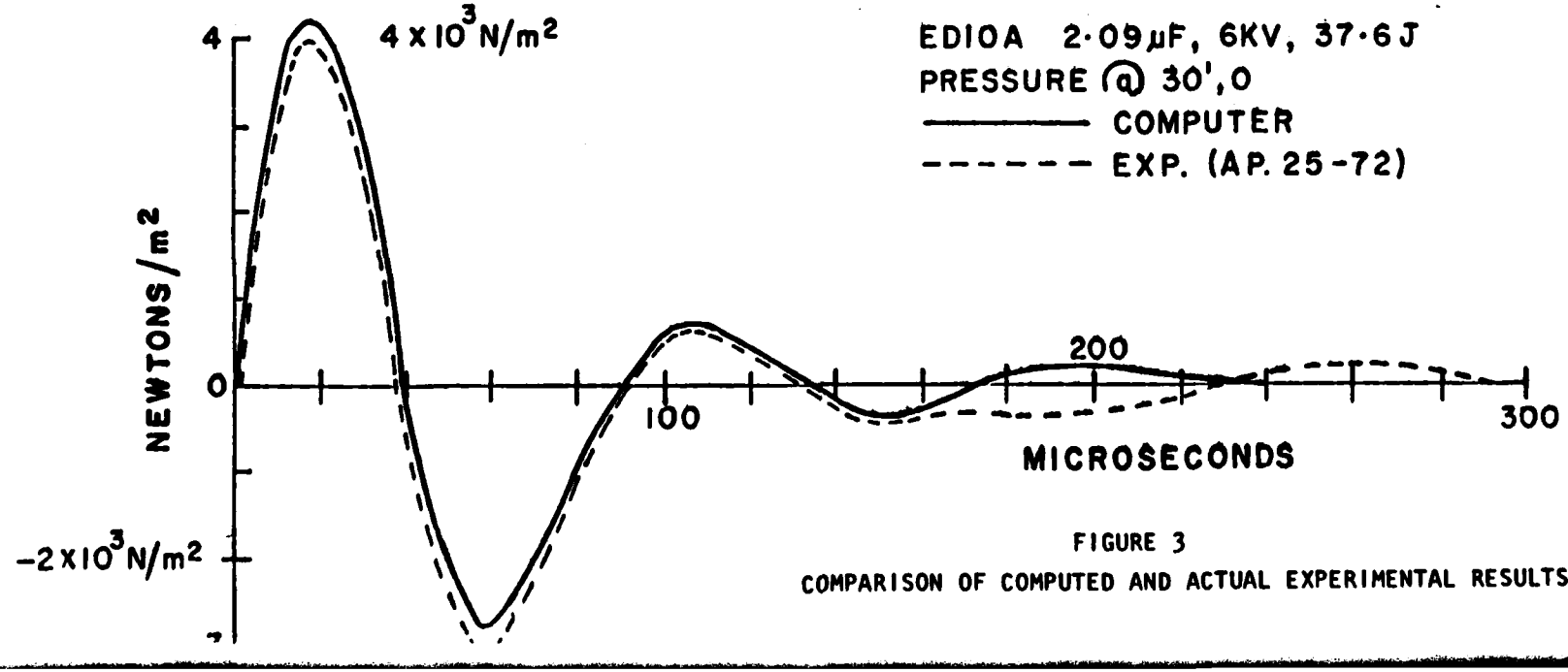

FIGURE 3
COMPARISON OF COMPUTED AND ACTUAL EXPERIMENTAL RESULTS

IV.D. POSSIBLE ENERGY SOURCE FOR DEEP SOURCES

S. Selwyn, LDGO

The concept of a remote energy source usable in the deep sea without umbilical hoses, electrical wires, or additional control cables is appealing and desirable for operating equipment such as corers, rock drills, anchoring devices, or, for functioning as a low frequency sound source. Specialized conduits transmitting electricity, pneumatic pressure, or hydraulic fluids are the most commonly used methods for conveying energy or providing control to equipment at depth from surface vessels. Power losses due to friction or electrical resistance can be significant, especially at deeper depths; handling difficulties on deck with multiple cables and tubes and winches, not to mention entanglement problems with the main lowering cable during lowerings, compound the problem of controllable energy sources in the deep ocean. Impact or remotely triggered powering devices isolated from the tending vessel provide only brief sources of energy.

In bottom sampler designs, for example, portable power units where energy is derived from either surface vessels or from self-contained storage systems have been used in the vibro-corer, an air-driven, vibrating sampler, or in the "SEACORE 50", an electrically driven rotary drill usable only to 1,000 ft. water depths. The severe restrictions in using this equipment at deeper water depths due to line losses through electrical cables or hydraulic lines, in addition to high costs of purchasing and using cables and lines, severely limit their effectiveness. At extreme water depths, an additional problem arises for surface-supplied, pneumatically- or hydraulically-driven devices -- pressure differentials are reduced leading to a significant reduction in their inherent efficiency. To overcome line losses, self-contained power sources on sediment samplers have utilized energy stored in the form of compressed air, springs, electrical batteries, hydraulic accumulators, stretched rubber bands, or explosives. None of these has proven completely successful; as one example, the Norwegian Geotechnical Institute Gas-Operated, Sea-Floor Sampler was driven into the sea-floor by igniting rocket propellent but after a few tests has not seen extensive use.

Hydrostatic pressure differentials have been used but so far are capable of providing only brief pulses of usable power. A rotary rock drill, which has successfully drilled short cores in igneous rocks from the Mid-Atlantic Ridge has utilized hydrostatic pressure to drive a rotary hydraulic motor developing 3 h.p. for ten minutes from an air chamber initially pressurized at 15 p.s.i. Yet the hydrostatic pressure differential represents an enormous source of potential energy - a source that is inherent to the oceans, inexhaustable, although constrained by water depth.

Our goal to design an improved bottom sampler, one that does not simply scale-up existing designs and does not rely entirely upon momentum gained during free-fall for complete penetration, has resulted in the Hydrostatic Motor now under development at the Lamont-Doherty Geological Observatory. It utilizes hydrostatic pressure differentials as a source for extended and controllable power. While our immediate application of the Hydrostatic Motor will be for driving corers into bottom sediments

to sample longer stratigraphic sections than those now obtainable by conventional piston corers, the concept could have wide applicability. We present here our fundamental design for the Hydrostatic Motor; discussion of the Hydrostatic Corer will be presented later in other publications.

DESCRIPTION OF THE EQUIPMENT

The utilization of hydrostatic pressure requires only that a pressure differential between atmospheric (or near atmospheric) conditions in the upper water column and those encountered at depth be established between two chambers, both connected in such a way that controlled pressure equalization will force a movable piston to provide harnessable mechanical energy. Oceanic pressure gradients are approximately 0.5 p.s.i. for every one foot increase in water depth. It is not a linear increase due to small changes in sea-water density, but, as an approximation, every foot of submersion in sea water would produce an increase of about 0.5 p.s.i. Thus any object lowered to a depth of 30,000 feet will be at an ambient external pressure of approximately 15,000 p.s.i.

Transfer of this high pressure to a chamber maintaining lower near-surface pressures results in a tremendous work availability. In our design (Figure 1) five principle components would control pressure equilization and convert this potential energy to mechanical work: chambers [1] and [2] are hollow, rigid, and connected chambers capable of withstanding ambient external pressure. Chamber [2] senses higher hydrostatic pressures by either being open to sea-water, as pictured in Figure 1, or through a sealed membrane if hydraulic oils are used. Chamber [1] retains near-surface, lower, pressures. In our example, the piston [3] is free to slide within chamber [2], unless mechanically restrained. Valves [4] and [5] are wide orifice valves. When mechnically released under the influence of high hydrostatic pressure, piston [3] tends to move to the right (with proper constraints to prevent excessive impact and damage, in this case a spring) into the region of lower pressure providing the power stroke. The piston is returned to its initial position by opening valve [4] and allowing high ambient pressure water to enter behind the piston which is now exposed to equal water pressure on both faces and is again mechanically restrained. Valve [5] is then opened thereby allowing water to drain from chamber [1] into the low pressure chamber [2], thus re-establishing a low pressure area behind the piston and completing the cycle.

The unit will continue to operate provided the valves are properly sequenced and piston restraint continues until the low pressure chamber is nearly filled with water. The number of cycles is approximately equal to the ratio of the volumes of the cylinder to the low pressure chamber. Cycling of valves would be controlled by piston movement.

At 15,000 feet with chamber [2] at 15,000 p.s.i. assuming an internal pressure in chamber [1] of 15 p.s.i. corresponding to near-surface hydrostatic pressures, an increase of one thousand fold in the force per unit area would be available to the movable piston [3] between

this chamber and the ambient pressure field at depth. If the piston has, for example, an area of 10 square inches, the total force differential would be 15,000 p.s.i. x 10 $in.^2$, or 150,000 pounds. By applying this force for a single piston stroke of 10 inches, the work done on the system would be 1,500,000 inch pounds and the storage capacity consumed in the sealed low pressure cylinder would be 100 cubic inches.

If chamber [2] has a total capacity of 2000 cubic inches (slightly more than 1 cubic ft., 20 power strokes could be made. The number of power strokes is approximately equal to the storage volume divided by the displacement per stroke, or:

$$\text{no. of piston strokes} = \frac{\text{storage volume at lowered pressure}}{\text{stroke displacement}}$$

The total work available to the system would be: (external pressure) x (piston area) x (length of the stroke) x (number of strokes). There would thus be:

$$\text{work available} = \frac{\text{external pressure}}{\frac{15{,}000 \text{ lb.}}{\text{in.}^2}} \times \text{piston area } 10 \text{ in.}^2 \times \text{stroke length } 10 \text{ in.} \times \text{no. of strokes } 20$$

$$\text{or} \quad 30 \times 10^6 \text{ in. lb.}$$

$$\text{or approximately } 2.5 \times 10^6 \text{ ft. lb.}$$

Because the total work which can be done by the device is equal to the force applied to the piston times the total distance, piston travel is not a function of piston area or the length of the cylinder, and the energy stored is only a function of the volume of chamber [2] and the ambient pressure. Thus at 15,000 pounds per square inch a one cubic foot chamber would store 2,500,000 foot-pounds of energy, regardless of the piston configuration. It is interesting to note that one SCUBA air tank would approximately provide this volume.

As noted earlier, our immediate goal is to couple the Hydrostatic Motor to a piston corer, perhaps either as a drop-hammer type of pile driver or as a vibrator, thereby greatly increasing corer penetration without having to rely upon larger and heavier momentum-type samplers and correspondingly larger ships. Consequently, a conventional oceanographic vessel would be capable of sampling larger stratigraphic sections in the deep sea. However, since an enormous work capability could be made available in a relatively small package constructed from commercially available components, we envision that the Hydrostatic Motor will have wide applicability within other oceanographic disciplines.

The Hydrostatic Motor represents an effective method for converting hydrostatic pressure gradients into usable energy. By simply raising the device to shallower depths the system will be recharged. Energy losses in transferring the equipment, by winches, for example, vertically through pressure gradients, prohibit any large-scale use for manufacturing significant power, such as in the generation of electrical power for use on land, although naturally occurring hydrostatic pressure changes while the Hydrostatic Motor remains in place such as perhaps produced by internal waves might even make this feasible. At the moment, we do see immediate application to power requirements necessary for deep-ocean instrumentation.

ACKNOWLEDGMENTS

Preliminary design was financed through the Office of Naval Research (contract N00014-75-C-0210) and the National Science Foundation (contract OCE76-18049) as part of their support to the Lamont-Doherty Geological Observatory Core Laboratory and Repository. Prototype development is now supported by the Office of Naval Research through contract N00014-75-C-0210 (Hydrostatic Corer). We appreciate comments by R. Stoll and N. Opdyke. Original concept covered under patent to S. Selwyn with appropriate releases and usage for scientific research given according to National Science Foundation and Office of Naval Research stipulations.

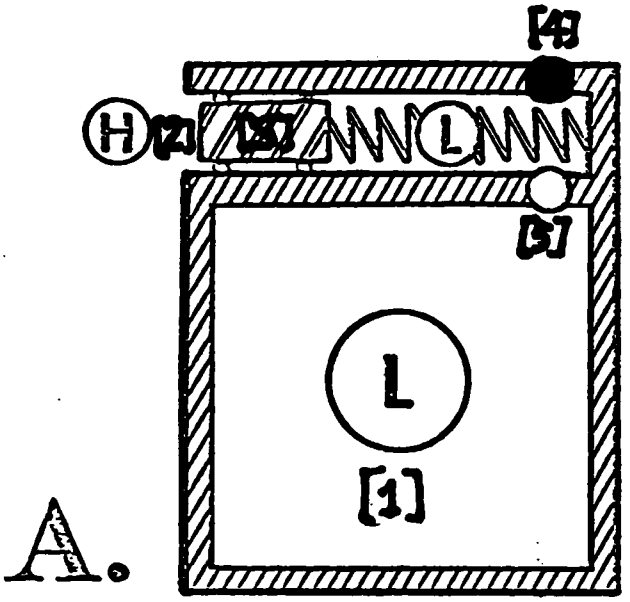

A.

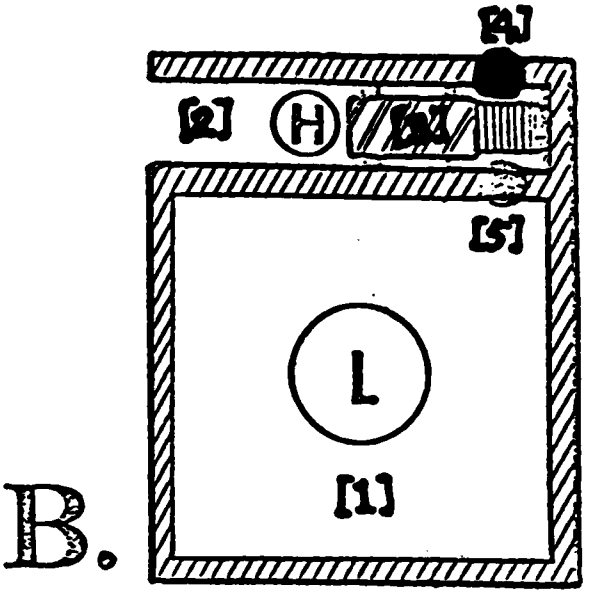

B.

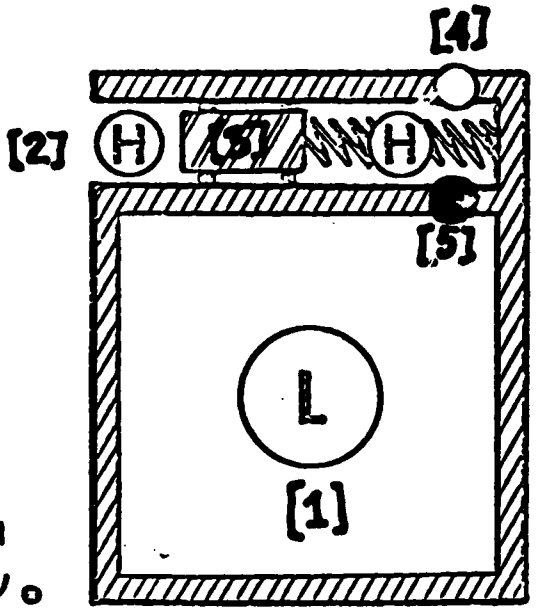

C.

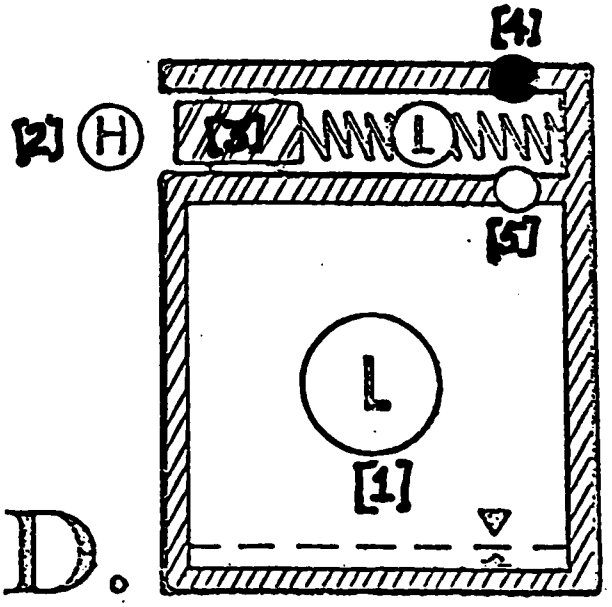

D.

● CLOSED VALVE

○ OPEN VALVE

(H) HIGH PRESSURE (WATER)

(L) LOW PRESSURE (AIR)

V. DEEP-TOWED RECEIVERS

A. WOODS HOLE EXPERIMENT

(G. M. Purdy and J. I. Ewing)

B. PERFORMANCE PREDICTION OF THE HUNTEC DEEP TOW SYSTEM

(R. W. Hutchins, Huntec)

C. TOWED-LINE ARRAY ELEMENT AND HYDROPHONE CALIBRATION

(J. E. Blue, NRL)

D. UNIVERSITY OF WASHINGTON DEEP-TOW ARRAY

(B. T. R. Lewis, U/W)

V.A. WOODS HOLE EXPERIMENT

G. M. Purdy and J. I. Ewing

Recent geological/geophysical measurements have emphasized the structural complexities of the upper kilometer of oceanic basement. IPOD drilling results show small scale lateral heterogeneities overlain on the long term (tens of millions of years) regional increases in velocity with age. We know of no effective geophysical method that is capable of resolving the small scale complexities of the upper one kilometer of oceanic Layer 2.

We are tackling this problem in two ways:

i) Seismic reflection profiling with a deep-towed hydrophone.

It is possible that reflectors exist within Layer 2 but are not routinely detected on conventional seismic reflection profiling systems because they are masked by diffractions and side echoes received by the large beam width surface array and/or are not resolvable by low frequency sound sources. In February 1978 we carried out an acoustically navigated seismic reflection survey near IPOD drill sites 417 and 418 (south of Bermuda) using 40 cu. in. Bolt airgun triggered every 12 seconds and a single hydrophone towed at a depth of ∿5400 m (i.e., about 100 m above the seafloor). The attached paper shows that, compared with a surface reflection record, the reduced (though asymmetric) beam pattern provides significantly better resolution of basement morphology. Only preliminary analyses have been completed on these recently collected data and doubt exists as to the origin of the apparent sub-basement reflections seen on the deep hydrophone record. It is questionable that we can ever be confident that they are 'real'; perhaps an array (2-D?) should replace the single hydrophone to help solve this problem. We have shown this to be operationally a straightforward technique which even in its simplest form, provides significant and useful data.

ii) Deep-towed implosive source for detailed refraction studies of Layer 2

Conventional seismic refraction experiments using surface sources and surface or seafloor receivers provide poor restraints on the velocity structure of oceanic Layer 2. Wave path geometries are such that any velocity determinations are necessarily averaged over several kilometers. If a deep-towed repetitive source could be built that would produce sufficient energy at frequencies less than 30-50 Hz, then, using either fixed seafloor receivers or a deep-towed array, velocity determinations could be made over a few hundred meters. The details and patterns of structural heterogeneities in the upper crust could then be defined.

As an initial step towards the design and construction of such a source we plan to monitor the signal output of a number of different size cylinders with weakened end caps designed to shatter at predetermined depths. The implosion will be throttled by orifices of various diameters. If we find that cylinders of reasonable sizes produce suitable signal levels and spectra, then we hope to begin design studies for the construction of a repetitive device.

May 1978

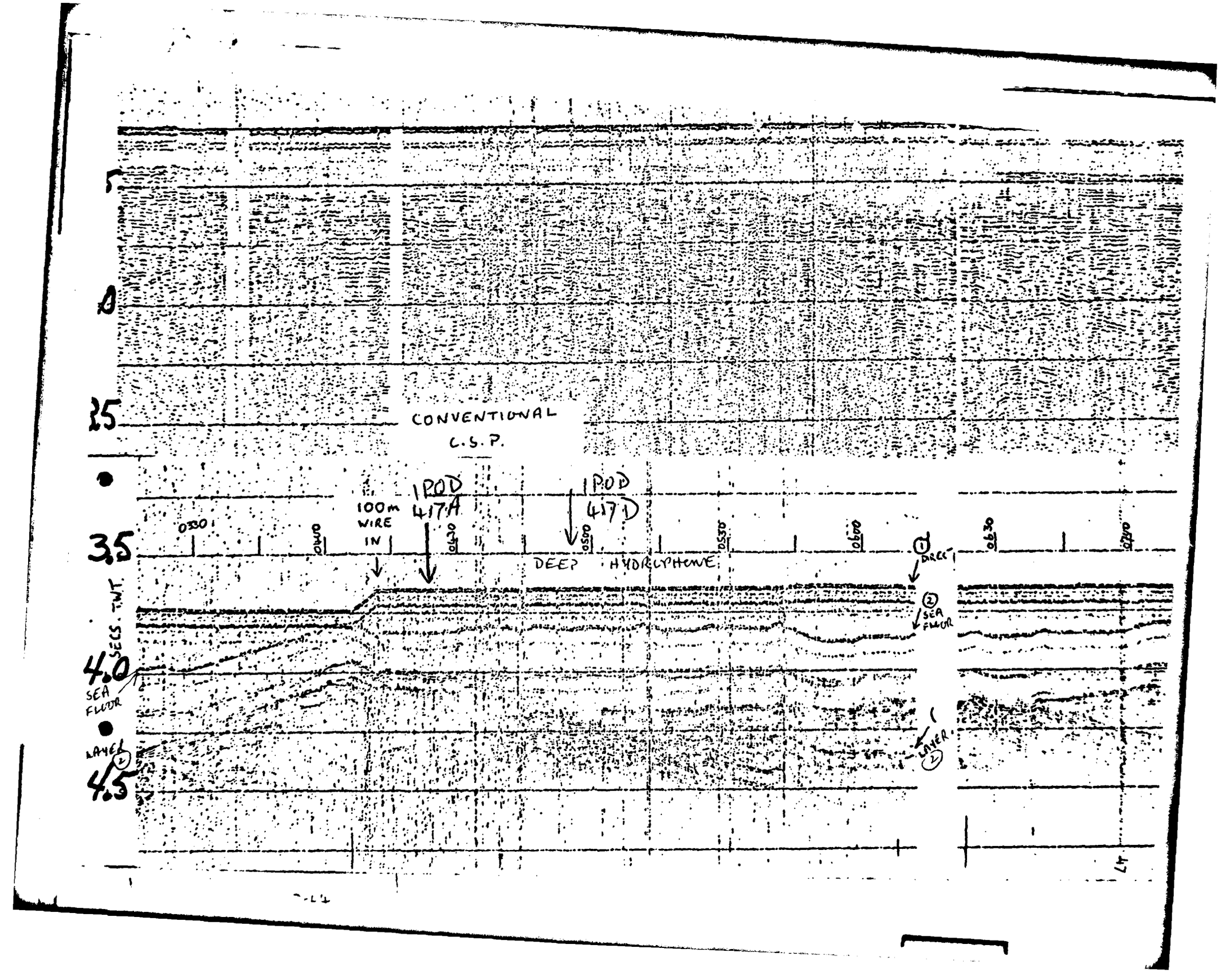
CONVENTIONAL
C.S.P.
100m WIRE IN
POD 417A
POD 417D
0330
0430
0500
0530
0600
0630
0700
DEEP HYDROPHONE
DIRECT
SEA FLOOR
LAYER
SECS. TWT
4.0
SEA FLOOR
LAYER
4.5

A DEEP TOWED HYDROPHONE SEISMIC REFLECTION SURVEY AROUND IPOD SITES 417 AND 418

G. M. Purdy and J. I. Ewing

Woods Hole Oceanographic Institution

Woods Hole, MA 02543

G. M. Bryan

Lamont-Doherty Geological Observatory of Columbia University

Palisades, New York

WHOI Contribution No. 4277

LDGO Contribution No.

Abstract

Seismic reflection data collected using 0.66 litre (40 cu in) airgun and a single hydrophone towed within a few hundred metres of the seafloor defines the basement morphology close to IPOD drill sites 417A and 417D in the Western Central Atlantic Ocean. The high resolution provided by this technique, together with accurate navigation from acoustic transponder beacons, allows the basement hill into which these holes were drilled to be defined. Excellent agreement exists between the drilling results and these deep hydrophone reflection data.

INTRODUCTION

The GLOMAR CHALLENGER recently completed a five month long (20 November 1976 - 21 April 1977; Legs 51-53) drilling program at drill sites 417 and 418 in the western North Atlantic Ocean (Donnelly, Francheteau et al., 1977; Bryan, Robinson et al., 1977; Flower, Salisbury et al., 1977). The objective of this program was to obtain deep samples of oceanic crust generated at anomaly M0 time (approximately 110 m.y.b.p. (Larson and Hilde, 1975) during the Cretaceous) for comparison with younger samples along the same flow line from the Mid-Atlantic Ridge.

Sites 417 and 418 are at the southern end of the Bermuda Rise, just north of the Vema Gap, connecting the Nares and Hatteras abyssal plains (Fig. 1). These sites are in the IPOD survey site AT 2.3 (Hoskins and Groman, 1976). The drilling resulted in four holes of 330-868 m penetration with from 10-544 m of basement penetration (Table 1).

Hole 417A was a single-bit hole that penetrated 211 m of sediments and 206 m of basement. The hole is apparently drilled into the top of a small hill that remained exposed to seawater for some tens of millions of years. The basalt is pervasively altered throughout the hole with only low temperature alteration products present.

Hole 417D was a multiple reentry deep penetration hole which penetrated 343 m of sediments and 365 m of basement. It is located some 450 m west of hole 417A. Sedimentary deposition began shortly after the crust was formed at this site, with no hiatus as at 417A. The basalts recovered from this hole were very similar in composition to those of 417A but they were quite fresh. The upper 190 m of the basalts have a stable steep magnetic inclination which, together with various lithologic indicators, shows that this portion has been tectonically rotated approximately 35° about a nearly horizontal axis.

An oblique seismic experiment was carried out in hole 417D (Stephen, 1977) using a downhole geophone clamped at two different levels in the basement above the bottom hole assembly.

Hole 418A is located about 9 kms south of hole 417D and is near the eastern edge of anomaly M0. Total penetration was 868 m. Sedimentary thickness was 324 m and the sequence was similar to that recovered from 417D. Basalts were sampled to 455 m subbasement and were akin to those samples in hole 417D. Hole 418B was drilled 100 m north of 418A for the purpose of obtaining a complete sedimentary section at the site. Total penetration was 330 m of which 320 m were sediment and 10 m were basalt.

Not unexpectedly, the conventional geophysical survey data collected prior to drilling did not predict the significant variability in the results from these drill holes located so close together. Seismic reflection profiles available prior to drilling did not show the 132 m difference in sediment thickness between holes 417A and 417D. Throughout this region, it is difficult to resolve, with any degree of accuracy, the depth to volcanic basement from conventional airgun seismic reflection profiles (Hoskins and Groman, 1976, Stephen, 1977). Single channel seismic reflection systems, with the source and receiver towed near the sea surface, are essentially omnidirectional, thus reflections from a large area of the seafloor (and sub-bottom) are recorded for each shot. If the reflecting surface is rough, as is the case for Layer 2, the long trains of side echoes make precise mapping of basement topography impossible and any weaker echoes from reflecting surfaces within Layer 2 cannot be identified.

This paper presents the preliminary results of a detailed survey carried out near Sites 417 and 418 in the 20 x 10 km. area shown in Figure 2. Seismic reflection data were collected using a 0.66 litre (40 cu in) airgun and a single hydrophone towed within a few hundred metres of the seafloor. By using a deep towed receiver the area of the seafloor, and more importantly, the area of the basement from which reflections can be received is significantly reduced. Thus basement morphology can be resolved in greater detail and the possibility arises of reliably identifying coherent reflections from within the basement. This technique has been previously used with some success by G.M. Bryan and B. Tucholke (pers. comm.). Conventional 3.5 kHz echo sounding data were collected along the tracks shown in Fig. 3, the majority of which were navigated using acoustic transponders. The bathymetry contour map (Fig. 2) shows there to be about 150 m of seafloor relief within the survey area with a gentle slope downwards to the west.

Twenty-eight heat flow stations were also carried out in this area to determine if there is evidence for hydrothermal circulation in this 110 m.y. old crust. These results will be reported elsewhere (Von Herzen et al, in preparation).

EQUIPMENT AND OPERATIONS

Precise navigation was vital to all our operations within this small area and to this end a net of acoustic transponders was laid as shown in Fig. 3. The Woods Hole Oceanographic Institution acoustic navigation system (known as ACNAV (Hunt et al. 1974) was then used to navigate the research vessel. A relay transponder was fitted to the cable above the hydrophone (and above the heat flow probe) allowing the location of these instruments to be determined independently (see Fig. 4). The position of the research vessel and relay transponder is displayed in real time on board ship on a computer controlled graphics display terminal thus allowing the ship and instrument package to be maneuvered accurately along predetermined tracks. The relative accuracy in position of both the ship and the deep towed hydrophone is estimated at ± 25 m. The acoustic navigation data was merged with the satellite fixes collected during the survey operations to yield an estimated absolute accuracy for ship and hydrophone locations of ± 100 m.

The hydrophone was a Type 8004 manufactured by the International Transducer Corporation with a battery powered FET preamplifier. This was enclosed in a canvas covered steel cage (to reduce flow noise) below which was suspended a 25 kg. spherical lead weight. The top of the hydrophone cage was attached, both mechanically and electrically, to the ships conventional 0.64 cm diameter two conductor wire. The Bolt 600 B 0.66 litre (40 cu. in) airgun was towed from a 4 m long outrigger on the port quarter at depths of 10-16 m. The firing interval was 12 seconds. A conventional single channel surface hydrophone streamer was also towed to provide data for comparison with that recorded by the deep towed hydrophone. The reflection data were displayed on three variable intensity recorders at various frequency passbands and recorded broad-band FM on a Sangamo 14 channel analog tape recorder.

This simple low cost configuration (only the cage for the deep towed hydrophone had to be constructed specifically for this project) resulted in two major problems which significantly marred the quality of the data discussed later in this paper. The elastic limit of the ships conducting cable was 2500 lbs. In the water depths of 5400 m in which we were operating (Fig. 2) approximately 1800 lbs of this limit was taken up by the weight of the cable itself. Thus, to allow a reasonable safety factor (for ships roll, etc.) our instrument packages could not weigh more than 200 lbs. This had two important consequences: in order to keep the hydrophone at a 'reasonable' horizontal distance behind the ship ($\sim$ 1 km) we could not steam faster than 0.5 - 0.75 knots. In a ship with conventional propulsion systems like the R/V Atlantis II, it is difficult to maintain a steady course at such low speeds and the directions in which it is possible to steam at all are dependent upon wind directions, sea state and currents (see Fig. 5). Thus it was not possible to carry out a systematic grid survey of the area of interest. With such little mass attached to the end of the cable the hydrophone was unstable in the vertical plane. Any signficant change in course or engine revolutions caused the hydrophone to 'kite' - to rise away from the seafloor and fall further astern of the ship. Many examples of this effect can be seen in the data shown in Fig. 6. The lack of fairing on the conducting cable resulted in cable strum noise which predominated at frequencies less than 80-100 Hz. The attenuation of higher frequencies in the basaltic basement means that if subbasement reflectors are to be detected then it is in these lower frequency (<50 Hz) bands that we should look. As will be seen later, this is made difficult by the presence of the high amplitude low frequency noise due to the strumming of the tow cable.

DEEP HYDROPHONE DATA

The quality of the deep hydrophone reflection data was variable, being dependent upon weather and current conditions and the proficiency with which the ship was controlled. These factors controlled the noise level, the source-receiver horizontal separation and the stability of the hydrophone in the vertical plane. The track chart in Fig. 5, computed using the acoustic navigation data, shows the erratic path of the research vessel and the large variations in the horizontal separation of the source and receiver. Four deep hydrophone reflection lines pass close to Holes 417A and 417D and one north-south line passes close to 418A (Fig. 2). Most of the data from lines 2 and 6 was of poor quality and difficult to interpret due to large source-receiver separations of 2-5 km or to high noise levels. However, on lines 3, 4 and 5 source-receiver separations of 1-2 km were maintained and noise levels were significantly lower. Much of the following discussion will be directed towards the data collected along line 4, not only because this line passed within a few hundred metres of the drill sites 417A and 417D (Fig. 5), but also, as will be described later in this paper, a ~300 m high basement hill was detected. Sediment thicknesses along lines 3 and 5, and along lines 2 and 6 (where determinations could be made) varied by less than approximately 0.06 secs two-way reflection time.

The data was replayed from the analog recordings at several frequency passbands but the ranges most helpful to our interpretation proved to be 15-40 Hz and 120-300 Hz. The high passband produced the 'cleanest' records by rejecting the low frequency noise generated by the strumming of the tow cable. Before our interpretation of these data is discussed, we must address the geometrical consequences of using a receiver towed just above the seafloor, and with significant horizontal separation between it and the airgun source.

Fig. 6 shows an example of the original data, uncorrected for the motion of the hydrophone. Referring to Figs. 4 & 6, it can be seen that the first and highest amplitude event on the record is the direct wave from source to receiver. The travel time for this ray path is dependent only on the slant range from source to hydrophone which, in practice, is determined by the length and 'shape' of the conducting cable. Discontinuities can be seen in this arrival where cable was paid out or hauled in; elsewhere arrival time variations are due to sudden changes in ships motion which cause the cable to either 'straighten out' or 'sag'. The next arrival is the seafloor reflection, which is obviously sensitive to the hydrophone height above the seafloor and in consequence is seen to undulate although the seafloor is in fact relatively flat. The later reflections from within the sediments and the basement are affected in a similar manner. If the water depth is known, then there is sufficient information to compute the hydrophone height above the seafloor (D_H) from:

$$D_H = (T^2 + 2TL) / 4H$$

where $T = Vo(T_2 - T_1)$ and $L = VoT_1$

H is the water depth, Vo is the velocity of sound in water, and T_1 and T_2 are the arrival times of the direct wave and seafloor reflection respectively. The horizontal separation of the source and hydrophone (R) can then be determined from:

$$R = (L^2 - (H - D_H)^2)^{\frac{1}{2}}$$

The separation in time of the seafloor, sediment and basement reflections is dependent not only on the layer thicknesses and velocities but also upon the position of the hydrophone relative to the source. This can be corrected for, the magnitude of the correction being dependent upon source-receiver horizontal separation as shown in Fig. 7. At separations less than 1km this correction is seen to be insignificant ($\lesssim$ 0.01 sec). If the horizontal separation becomes too large then critically refracted arrivals can be received. The conditions for this are shown in Fig. 8. If these conditions are satisfied then the data must be

interpreted with care as it is impossible to reliably identify such arrivals on the basis of travel time alone given a single receiver. It can be seen from Fig. 8 that this becomes a concern when source-receiver separations exceed ~2km.

The model calculations shown in Fig. 9 illustrate the asymmetry of the deep hydrophone data due to the horizontal separation of source and receiver, and provide a comparison with conventional single channel surface reflection data. The simple model used is a 300 m high basement hill, with steep (40^{o}) sides and overlain by sediments of velocity 2km/sec. The seafloor is flat: 200 m of sediment overlie the top of the hill and 500 m overlie the horizontal basement on either side. For clarity no sediment reflectors are included and diffractions from only the 'corners' of the hill are allowed. In the surface reflection case the reflections from the sides of the basement high are seen to be offset by ~3.5 km from the feature itself. In the deep hydrophone case these same reflections are offset asymmetrically by 0.5-1.0 km. Although this shows clearly the benefit of using a deep towed hydrophone, it also shows that, in water depths of ~5.5 km, the technique is unable to 'resolve' a reflector dipping at 40^{o} beneath ~0.5 km of sediment. That such steep slopes exist in the basement as it is formed today is well documented (e.g. MacDonald & Luyendyk, 1977). If the accretion process occurring ~110 m.y.b.p. at the Mid-Atlantic Ridge was similar to that occurring today, we should expect the deep hydrophone data collected around sites 417A and 417D to be contaminated by side reflections and diffractions from such steep slopes, though to a much lesser degree than the surface data. This is seen to be the case in Fig. 6.

Reflectors within the sediment column cannot be reliably identified on the surface data and there exists considerable uncertainty in the location of the true basement reflector. These data were collected using a conventional surface array at the same time as the deep hydrophone data. These two contrasting records are shown aligned in time (but not in location due to the ~1 km horizontal movement of the deep hydrophone relative to the ship) in Fig. 6. The extremely

diffuse character of the basement reflections in this region (as recorded by conventional reflection profiling systems) has been previously noted by Hoskins and Groman (1976) and Stephen (1977).

Although the position of the basement reflection is significantly more clear on the deep hydrophone record, ambiguities still exist. A specific example in Fig. 6 of where this uncertainty is important is at 0445 hrs. Here the basement reflection cannot be reliably recognised within a complex 0.3 sec long wavetrain. To assist in resolving this problem we replayed the data with a low frequency passband of 15-40 Hz (Fig. 10). The noise levels can be seen to be significantly higher in this case and reflections from the seafloor or from within the sediments cannot be identified. Volcanic basement can be considered to approximate a first order discontinuity and thus reflects all wavelengths with comparable efficiency. Reflection amplitudes from within the sediment column are wavelength dependent being controlled by interference effects, the nature of which is determined by the vertical P and S wave velocity and density structure within the sediments (Stoll 1977, Smith, 1977). The presence of basement diffractions is also wavelength dependent, as they can only be caused by a diffractor of significant vertical extent compared with the wavelength of the incident wave.

Thus we interpret the low frequency ($\sim$30 Hz) reflection seen in Fig. 10 to be the basement reflection, and have used this, together with the high passband record, to produce the interpretation of line 4 shown in the lower part of this figure. The effect of the vertical motion of the hydrophone has been removed from this interpretation by normalising the two way travel time to the sediment and basement reflectors to the seafloor. Correction for variations in horizontal separation of source and hydrophones have not been made, but Fig. 7 and the separation profile in Fig. 6 shows that this effect is small.

Two prominent sediment reflectors can be identified. The first lies generally ~0.2 sec below the seafloor and is clearly seen everywhere along the line. The second can only be clearly seen to the west of the basement high between 0500 and 0600 hrs and lies at a depth of 0.25-0.35 secs beneath the seafloor sloping upwards to the west. This reflector may exist to the east of the basement hill between 0100 and 0300 hrs but it cannot be clearly identified in this region. The most interesting feature of this profile is, of course, the basement high centred at ~0400 hrs. It is helpful to compare the character of the high passband profile shown in Fig. 10 with the model calculations illustrated in Fig. 11. This grossly simplified model shows the reflections and diffractions from a simple 0.3 sec high basement hill with sides sloping at 20^{o} and 40^{o}. This again illustrates the lateral offset of the reflections as recorded by the deep hydrophone and also has some features in common with the high passband profile over the basement hill in line 4 (Fig. 10). The deep hydrophone geometry is capable of resolving the 20^{o} slope on the eastern side of our model hill. The model predicts the presence of pure reflected and diffracted energy along this slope, and this is seen in the original data between 0300 and 0400 hrs (Fig. 10). The model shows we are incapable of 'resolving' the 40^{o} slope on the western side of the hill and predicts the presence over the steep slope of only energy diffracted from the top of the hill, but a concentration of diffracted and reflected energy exists further to the west beneath the true reflection from the horizontal basement. This distribution of energy also has much in common with that seen between 0430 and 0530 hrs on the high passband record in Fig. 10.

Thus our interpretation of the basement morphology along line 4 is as follows. At the eastern end of the line, between 0100 and 0300 hrs, the basement is relatively flat and lies 0.45 ± 0.05 secs beneath the seafloor. Between 0300 and

0445 hrs (a distance of 1.7 km) there exists a basement hill which rises to within 0.15 secs of the seafloor. The eastern side of this hill has a slope of 15-20° and the western side a slope of ~40°. Between 0445 and 0545 hrs the basement reflector lies about 0.5 secs beneath the seafloor. At 0545 hrs the basement appears to shallow abruptly by 0.1 secs. This is a difficult section of the profile to interpret with confidence. Between 0600 and 0700 hrs we can find no reasonable alternative to the basement location as shown in our interpretation in Fig. 10. However, there is no supporting evidence (e.g. diffractions) for existence of the basement step at 0545 hrs and the presence of low frequency energy at 0645-0700 hrs, beneath that which we have interpreted to be basement, causes us some concern.

DISCUSSION

The location of the drill sites 417A and 417D relative to the deep hydrophone line 4 is shown in Fig. 5 and Fig. 10. It can be seen that 417A was drilled into the top of the basement hill and 417D into its steep western slope. This is in complete agreement with the interpretation of the drill samples (Donnelly, Francheteau et al 1977). Indeed our estimate of 40^{o} for the slope of the western wall of the hill into which Hole 417D was drilled, is identical to the angular difference in vertical-reference features, such as cooling cracks or joints, between the recovered cores from Holes 417D and 417A (Donnelly, Francheteau et al. 1977). Fig. 10 shows the sediment thickness at Hole 417A to be 0.2 secs. Drilling determined a sediment thickness of 211 m (Table 1). Combining these two determinations yields an average velocity of 2.1 km/s for the sediments. Our data do not provide a determination of sediment thickness at Hole 417D, but the thickness of 343 m determined from drilling is in agreement with our interpretation.

Our data were insufficient to define the trend or lateral extent of the basement hill: it was not observed on line 6 (Fig. 2) though the data quality especially towards the western end of this line was poor. Indications of a basement disturbance are present at the southern end of line 3, which would suggest a NNE-SSW trend but this is not conclusive.

We have shown that this seismic reflection method is capable of resolving basement topography in significantly greater detail than conventional surface techniques. However, our original goal of detecting subbasement reflectors and being able to identify them as such with some confidence, was not achieved. The scale of roughness of Layer 2 in this region was such that side reflections and

diffractions remained a problem, limiting our ability to 'see' beneath the basement. The possibility remains, of course, that reflectors do not exist within this old (110+ m.y.) well annealed basement. More data of this type should be collected, preferably over younger crust not covered by sediment. Improvements to the data collection technique should be made, the two most obvious steps being to use a faired cable (to reduce cable strum noise) and to use a conducting cable of elastic limit great enough to allow a mass of several hundred kilograms to be attached to the hydrophone package. This would add stability to the system, reduce the source-hydrophone separations to more acceptable levels and permit greater maneuverability of the research vessel.

We plan to carry out more detailed interpretations of the data presented here: specifically we hope to use the airguns direct outgoing waveform, as recorded by the deep hydrophone, to deconvolve selected profiles in an attempt to further improve our temporal resolution.

TABLE 1

Drilling Data from IPOD Sites 417 and 418

Holes	Latitude	Longitude	Z	Penetration Sed.	BSMT	Σ
417 A	25°06.63'N	68°02.48'W	5468m	211m	206m	417m
417 D	25°06.69'N	68°02.82'W	5482m	343m	363m	708m
418 A	25°02.08'N	68°03.44'W	5511m	324m	544m	868m
418 B	25°02.08'N	68°03.45'W	5514m	320m	10m	330m

ACKNOWLEDGEMENTS

We thank the officers, crew and scientific party on board RV ATLANTIS II Cruise 97 leg 2 for their expert assistance in collecting these data. A. Sundberg, H. Hayes and C. Wooding helped considerably with the reduction of this data and the preparation of the figures. This work was supported by a subcontract to Site Survey Management Office of the International Phase of Ocean Drilling.

REFERENCES

Bryan, W.B., P.T. Robinson, et al. 1977. Studying Oceanic Layers, Geotimes, 22, July/August, 22-26.

Donnelly, T.W., J. Francheteau et al. 1977. Mid-ocean Ridge in the Cretaceous, Geotimes, 22, June, 21-23.

Flower, M.F.J., M.H. Salisbury et al. 1977. DSDP Cretaceous Crust sought, Geotimes, 22, September, 20-22.

Hoskins, H. and R.C. Groman, 1976. Informal report to IPOD Site Survey Management on surveys at IPOD Sites AT2.2 and 2.3. Unpublished manuscript, 21 pages, October 1976.

Hunt, M.M., W.M. Marquet, D.A. Moller, K.R. Peal, W.K. Smith and R.C. Spindel, 1974. An Acoustic Navigation System, Woods Hole Oceanographic Institution Technical Report, WHOI-74-6.

MacDonald K.C. and B.P. Luyendyk, 1977. Deep Tow Studies of the Structure of the Mid-Atlantic Ridge Crest near latitude 37°N., Geol. Soc. Am. Bull., 88, 621-636.

Larson, R.L. and T.W.C. Hilde, 1975. A revised time scale of magnetic reversals for the Early Cretaceous and Late Jurassic, Jour. Geophys. Res., 80, 2586-2594.

Stephen, R.A., 1977. An Oblique Seismic Experiment in Oceanic Crust, Unpublished Ph.D. Thesis, Cambridge Univ.

Smith, S.G., 1977. A reflection profile modelling system, J. Roy. astr. Soc., 49, 723-737.

Stoll, R.D., 1977. Acoustic Waves in ocean sediments, Geophysics, 42, 715-725.

Figure Captions

Fig. 1. Location IPOD Drill Sites in the Western Central Atlantic Ocean (from Donnelly, Francheteau et al. 1977).

Fig. 2. Bathymetry contour map in corrected metres of detailed survey area. Tracks are shown in Fig.. 3. Solid contours are based on acoustically navigated data only, dashed contours use satellite navigated tracks. Locations of IPOD drill sites 417A, 417D and 418A are shown as black squares. The five deep hydrophone profiles are annotated with their line number. A more detailed track chart of the deep hydrophone lines around Site 417 is shown in Fig. 5.

Fig. 3. Tracks used to produce bathymetry contours shown in Fig. 2. Black dots mark locations of the six acoustic transponder beacons.

Fig. 4. Schematic depiction of deep hydrophone reflection profiling geometry.

Fig. 5. Ship and hydrophone tracks for deep hydrophone lines (DHL) 3,4, 5 and 6 navigated using the acoustic transponder network. Contours from Fig. 2 are included.

One hour tick marks are shown on the tracks. The location of drill sites 417A and 417D just north of DHL 4 are shown by the capital letters A and D enclosed in squares. The data along DHL 4 is shown in Figs. 6 & 10.

Fig. 6. Data from deep hydrophone line 4. Location shown in Figs. 2 and 5. Figure shows conventional surface reflection data, deep hydrophone reflection data, bathymetry profile from 3.5kHz echo sounder, and horizontal separation of source and deep hydrophone computed from acoustic navigation data. See text for discussion of deep hydrophone data. Location of drill sites 417A and 417D are shown by arrows on the deep

hydrophone profile; horizontal bar is qualitative estimate of the position error. Reflection data in both cases was band pass filtered 120-300Hz. West is to the right.

Fig. 7. Corrections to be applied to sediment thicknesses determined from deep hydrophone data plotted against source receiver separation, for true sediment thicknesses of 0.25 sec. and 0.5 sec i.e. corrections required to convert the non vertical incidence case of the deep hydrophone data to vertical incidence. These curves were computed for a water depth of 5.5 km, a hydrophone height above the seafloor of 0.2 km and a sediment velocity of 2 km/s. Seafloor and basement are assumed to be horizontal.

Fig. 8. Ray theory refracted wave critical distances plotted against basement velocity for the deep hydrophone geometry for sediment velocities of 1.8 km/s and 2.2 km/s. Computed assuming a water depth of 5.5 km and a hydrophone height above the seafloor of 0.2 km.

Fig. 9. Reflections (solid lines) and diffractions (dashed lines) computed from ray theory over a simple model of a symmetrical 300 m high basement hill with sides sloping at 40° for the deep hydrophone case and for the conventional surface reflection case. The x axis in each case represents the true seafloor. Water depth is 5.5 km, hydrophone height above the seafloor is 0.2 km and sediment velocity is 2 km/s. Note the asymmetry of the computed deep hydrophone data due to the assumed 1 km horizontal separation of the source and the receiver: in the deep hydrophone case the receiver was to the right of the source. For simplicity, no sediment reflectors have been included and diffractions from only the corners of the hill have been allowed.

Fig. 10. Deep hydrophone data from line 4 filtered at 15-40 Hz and 120-300 Hz together with our preferred line drawing interpretation which has been normalised to the seafloor i.e. the effect of the vertical motion of the hydrophone has been removed. For discussion, see text, but note vertical offset of low frequency reflection on 15-40 Hz record at 0445 hrs. West is to the right.

Fig. 11. Computed reflections and diffractions over an asymmetric 300 m high basement hill with sides sloping at 20^{o} and 40^{o} for the deep hydrophone geometry. Assumptions as for Fig. 9. x axis is location of the model seafloor.

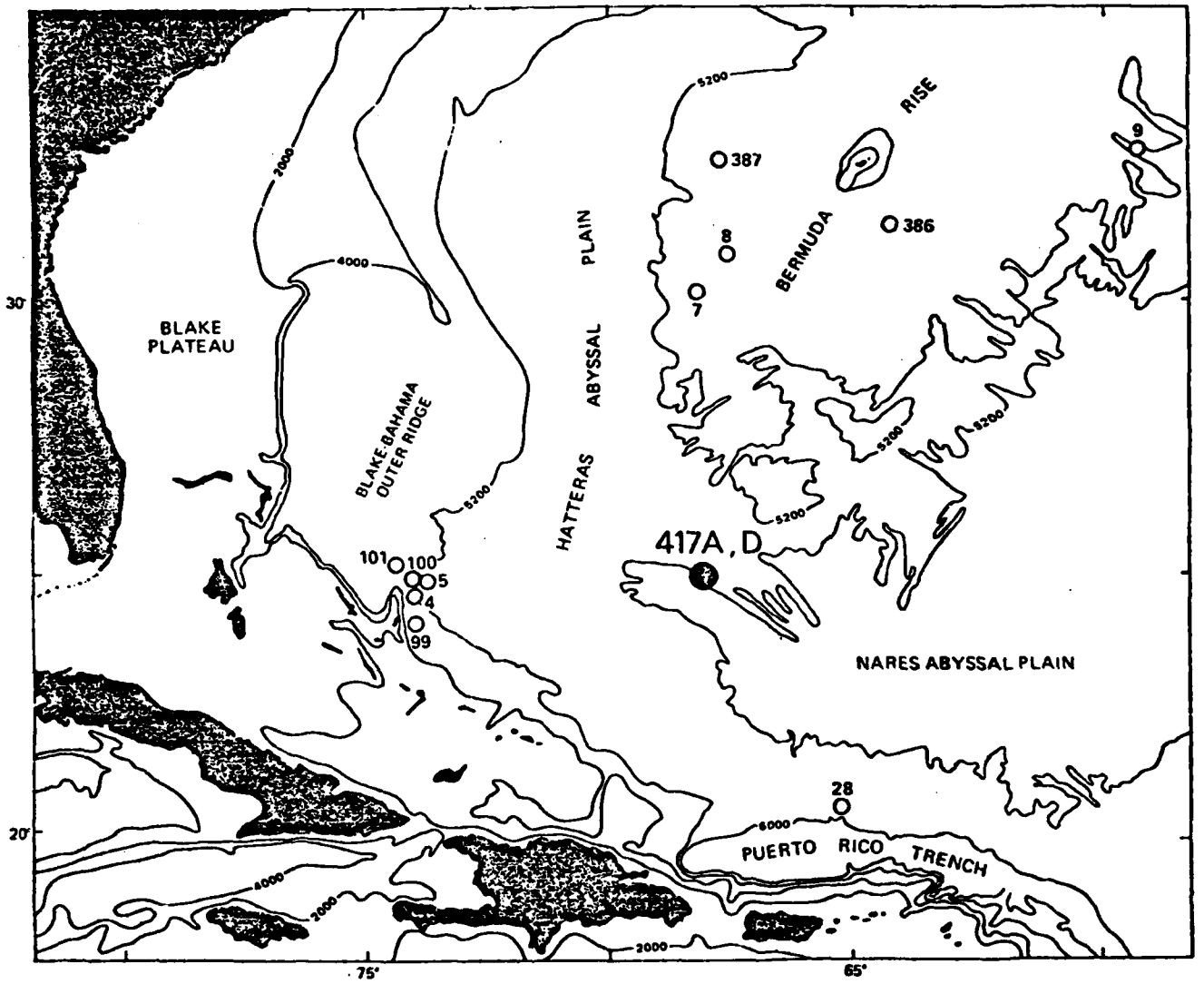
BLAKE PLATEAU
BLAKE BAHAMA OUTER RIDGE
HATTERAS ABYSSAL PLAIN
BERMUDA RISE
NARES ABYSSAL PLAIN
PUERTO RICO TRENCH
417A, D
387
386
101
100
5
4
99
28
9
8
7
2000
4000
5200
6000
30°
20°
75°
65°

fig. 1

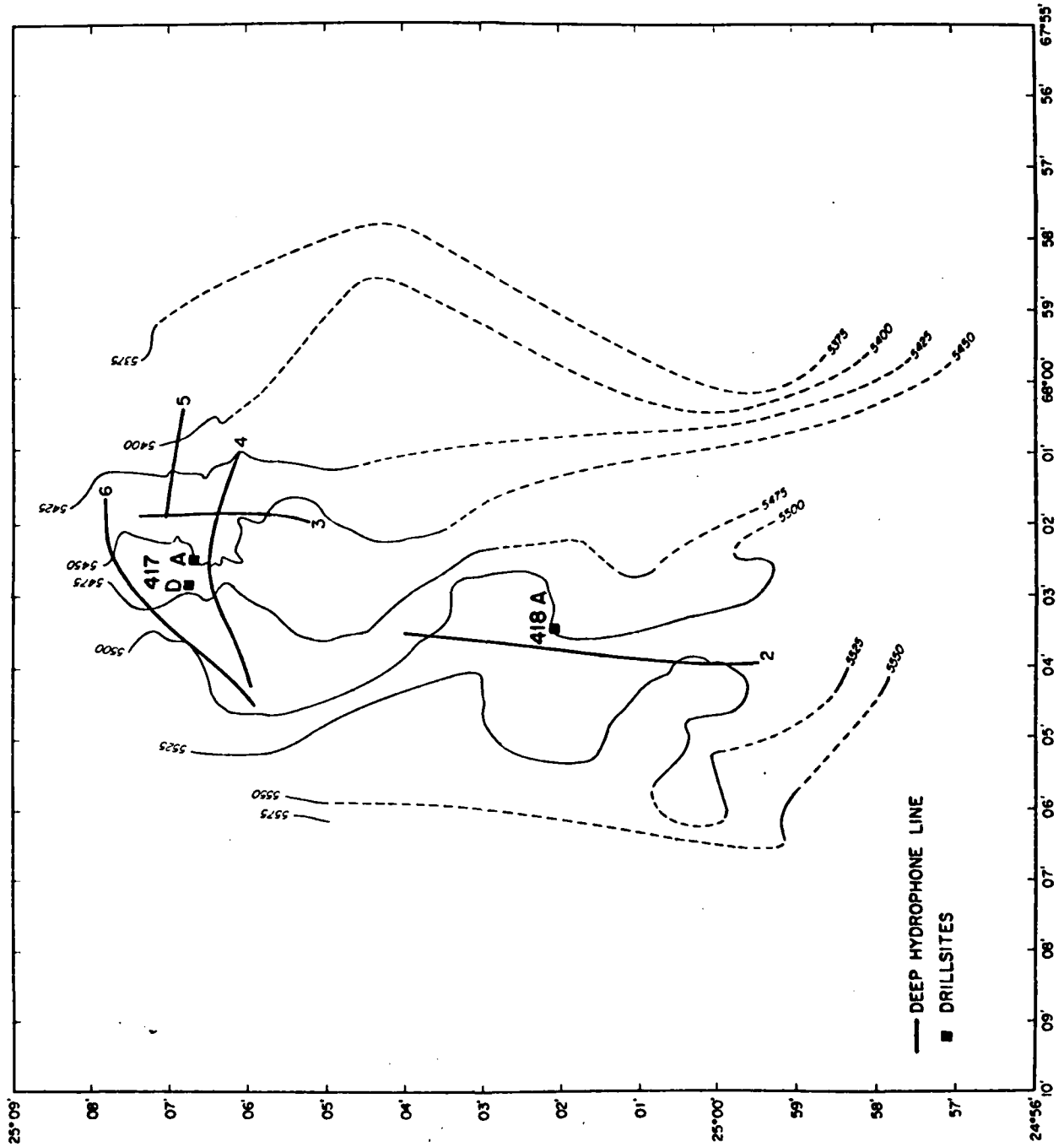
417 D A
418 A
1
2
3
4
5
6
5375
5400
5425
5450
5475
5500
5525
5550
5575
DEEP HYDROPHONE LINE
DRILLSITES
25°09'
08'
07'
06'
05'
04'
03'
02'
01'
25°00'
59'
58'
57'
24°56'
10'
09'
08'
07'
06'
05'
04'
03'
02'
01'
68°00'
59'
58'
57'
56'
67°55'

Fig. 7.4

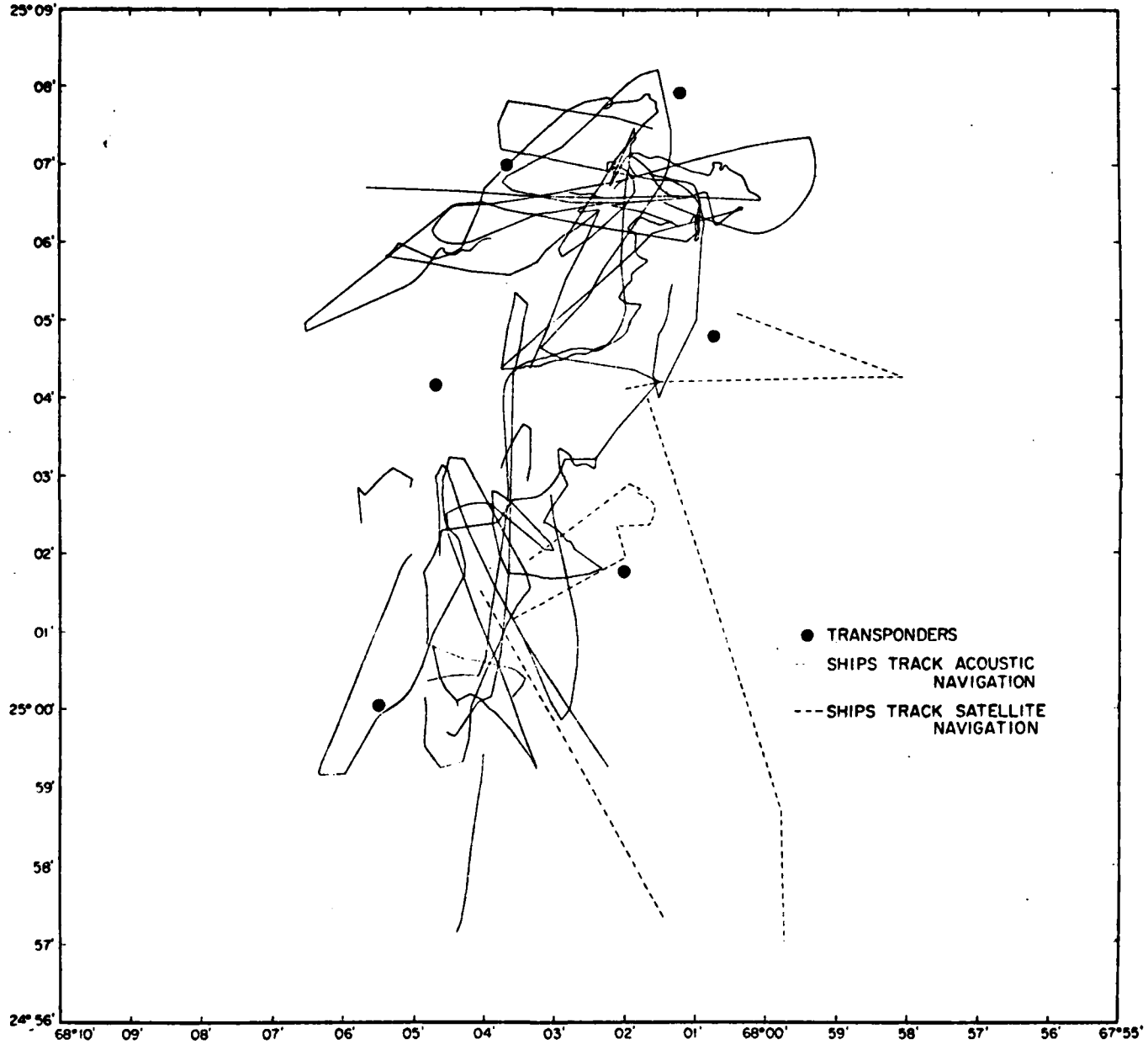
25°09'
08'
07'
06'
05'
04'
03'
02'
01'
25°00'
59'
58'
57'
24°56'
68°10'
09'
08'
07'
06'
05'
04'
03'
02'
01'
68°00'
59'
58'
57'
56'
67°55'
TRANSPONDERS
SHIPS TRACK ACOUSTIC NAVIGATION
SHIPS TRACK SATELLITE NAVIGATION

fig. 3

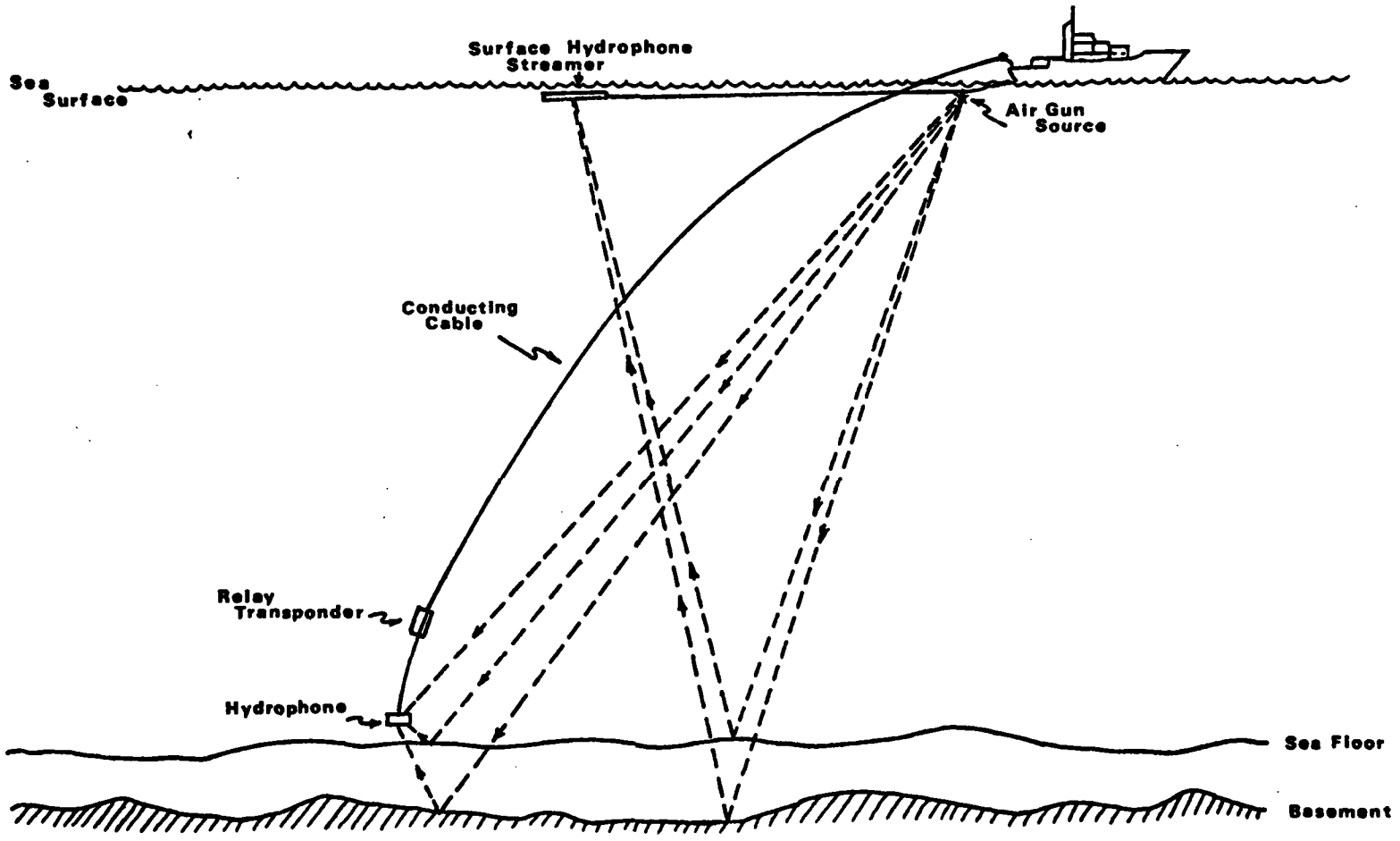
Surface Hydrophone Streamer
Sea Surface
Air Gun Source
Conducting Cable
Relay Transponder
Hydrophone
Sea Floor
Basement

Fig. 4

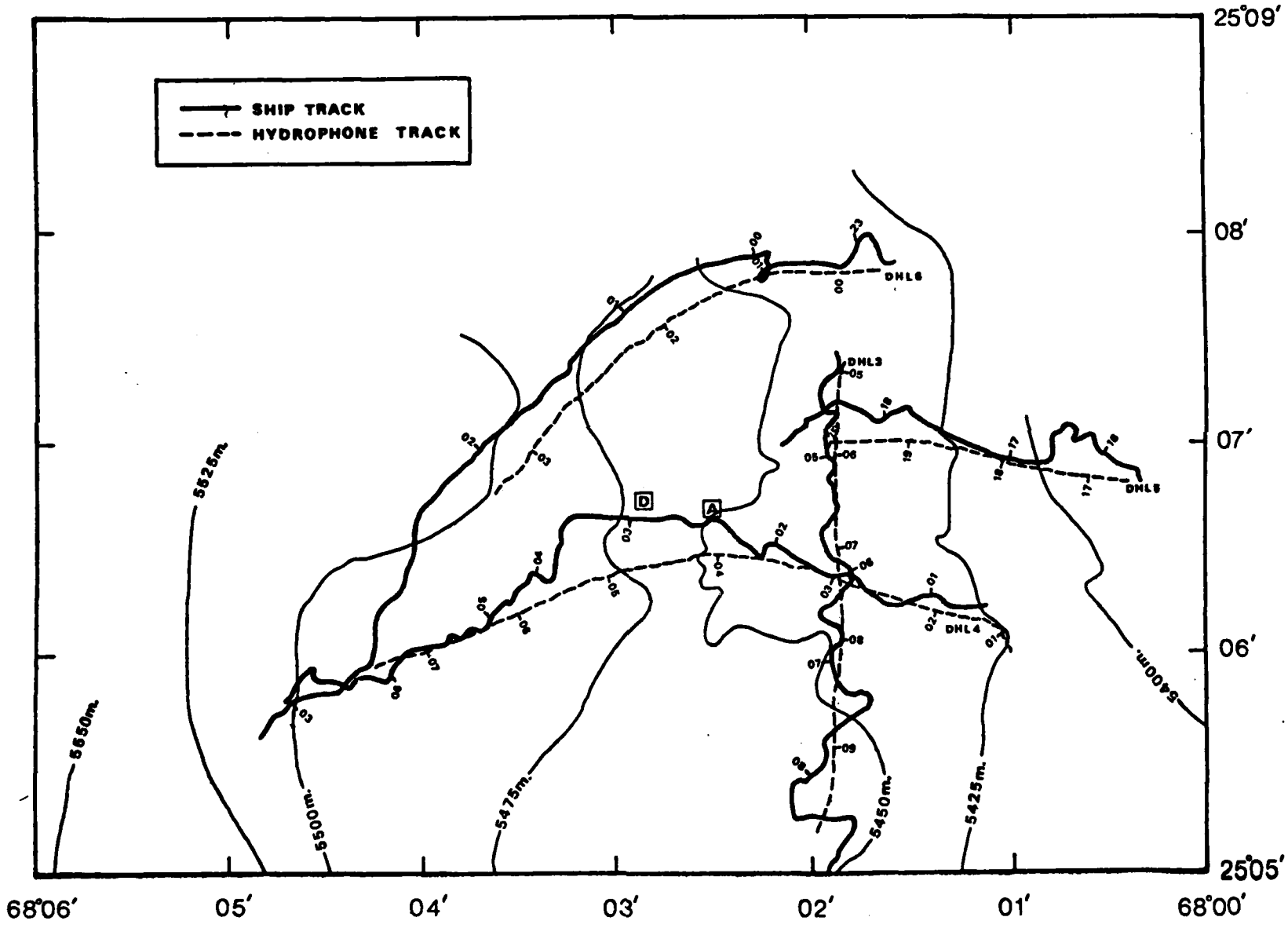
SHIP TRACK
HYDROPHONE TRACK
DHL6
DHL3
DHL5
DHL4
D
A
5625m.
5650m.
5500m.
5475m.
5450m.
5425m.
6400m.
25°09′
08′
07′
06′
25°05′
68°06′
05′
04′
03′
02′
01′
68°00′

73

fig 5

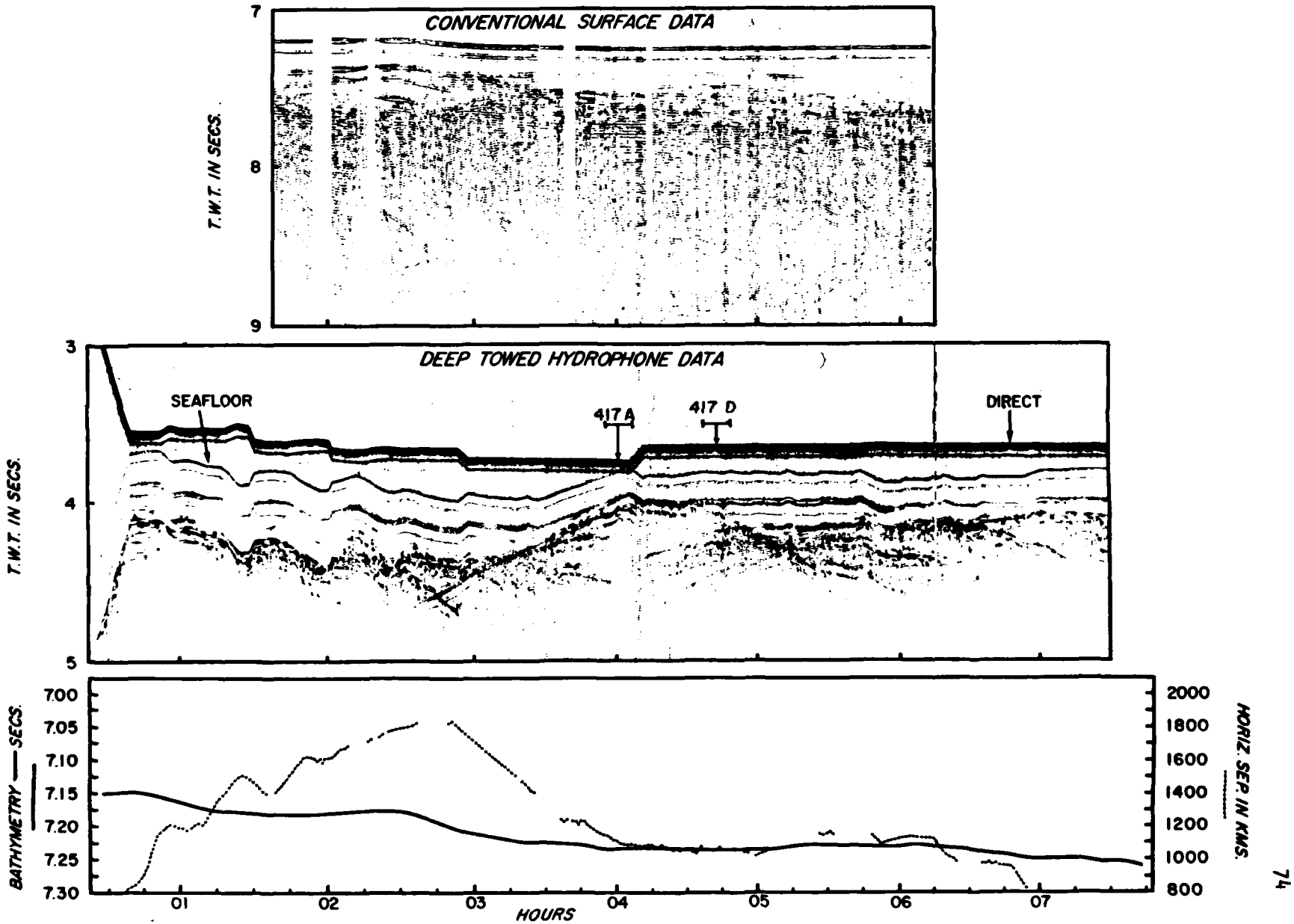
CONVENTIONAL SURFACE DATA
T.W.T. IN SECS.
7
8
9
DEEP TOWED HYDROPHONE DATA
SEAFLOOR
417 A
417 D
DIRECT
T.W.T. IN SECS.
3
4
5
BATHYMETRY — SECS.
7.00
7.05
7.10
7.15
7.20
7.25
7.30
HORIZ. SEP. IN KMS.
2000
1800
1600
1400
1200
1000
800
01
02
03
04
05
06
07
HOURS

Fig. 6

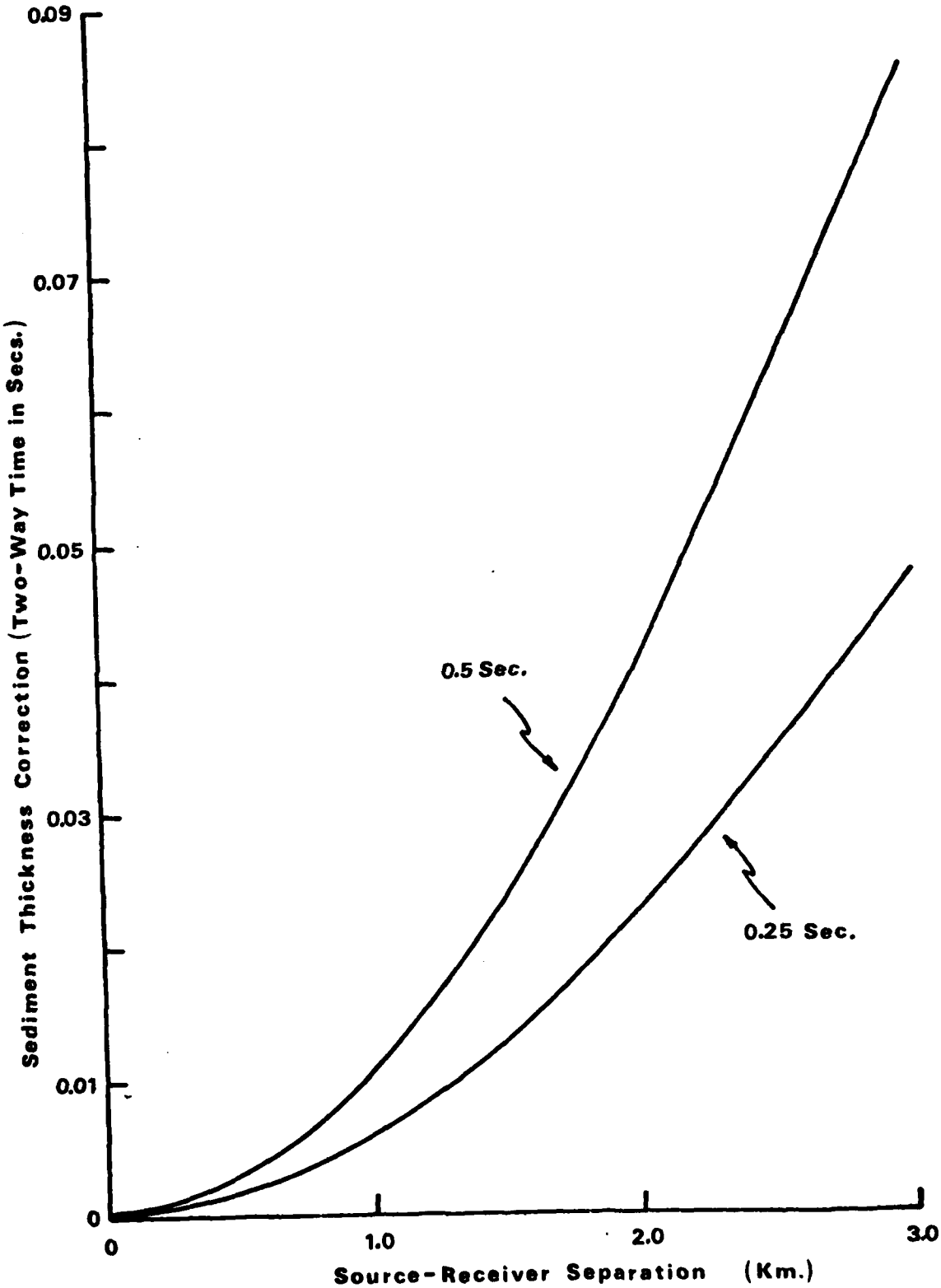
0.09
0.07
0.05
0.03
0.01
0
Sediment Thickness Correction (Two-Way Time in Secs.)
0.5 Sec.
0.25 Sec.
0
1.0
2.0
3.0
Source-Receiver Separation (Km.)

fig 7

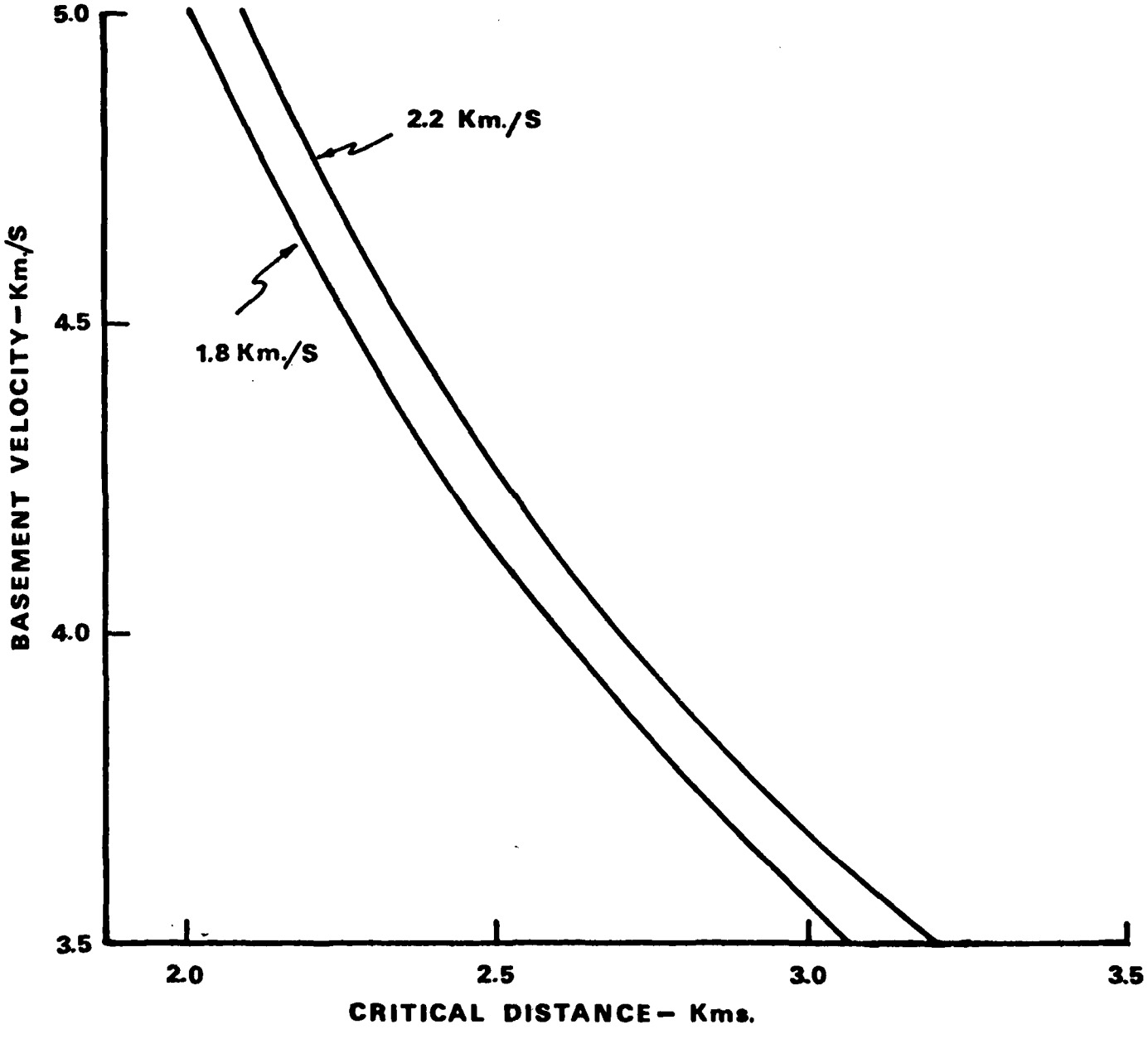
5.0
4.5
4.0
3.5
2.2 Km./S
1.8 Km./S
BASEMENT VELOCITY – Km./S
2.0
2.5
3.0
3.5
CRITICAL DISTANCE – Kms.

fig 8

fig 9

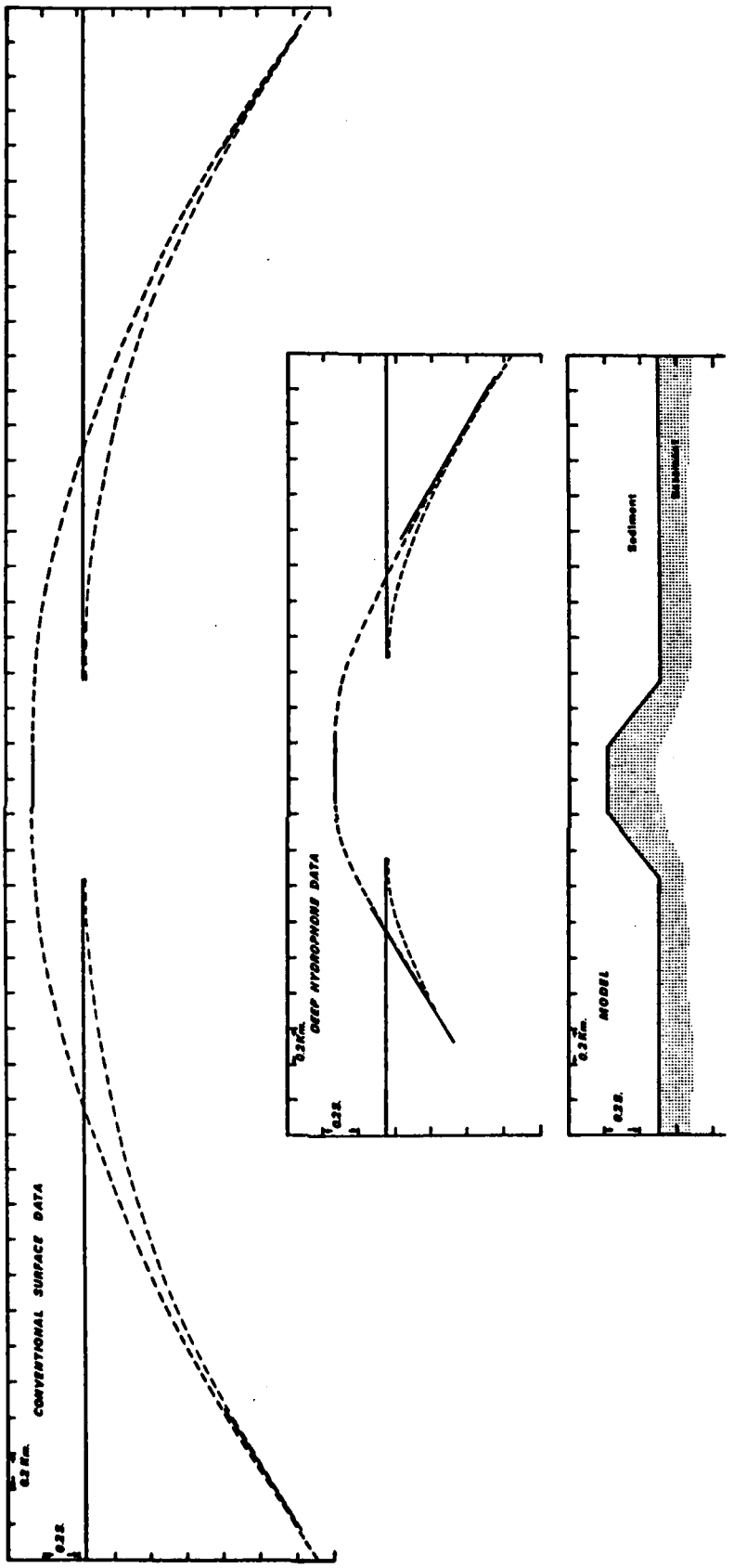
CONVENTIONAL SURFACE DATA
DEEP HYDROPHONE DATA
MODEL
Sediment

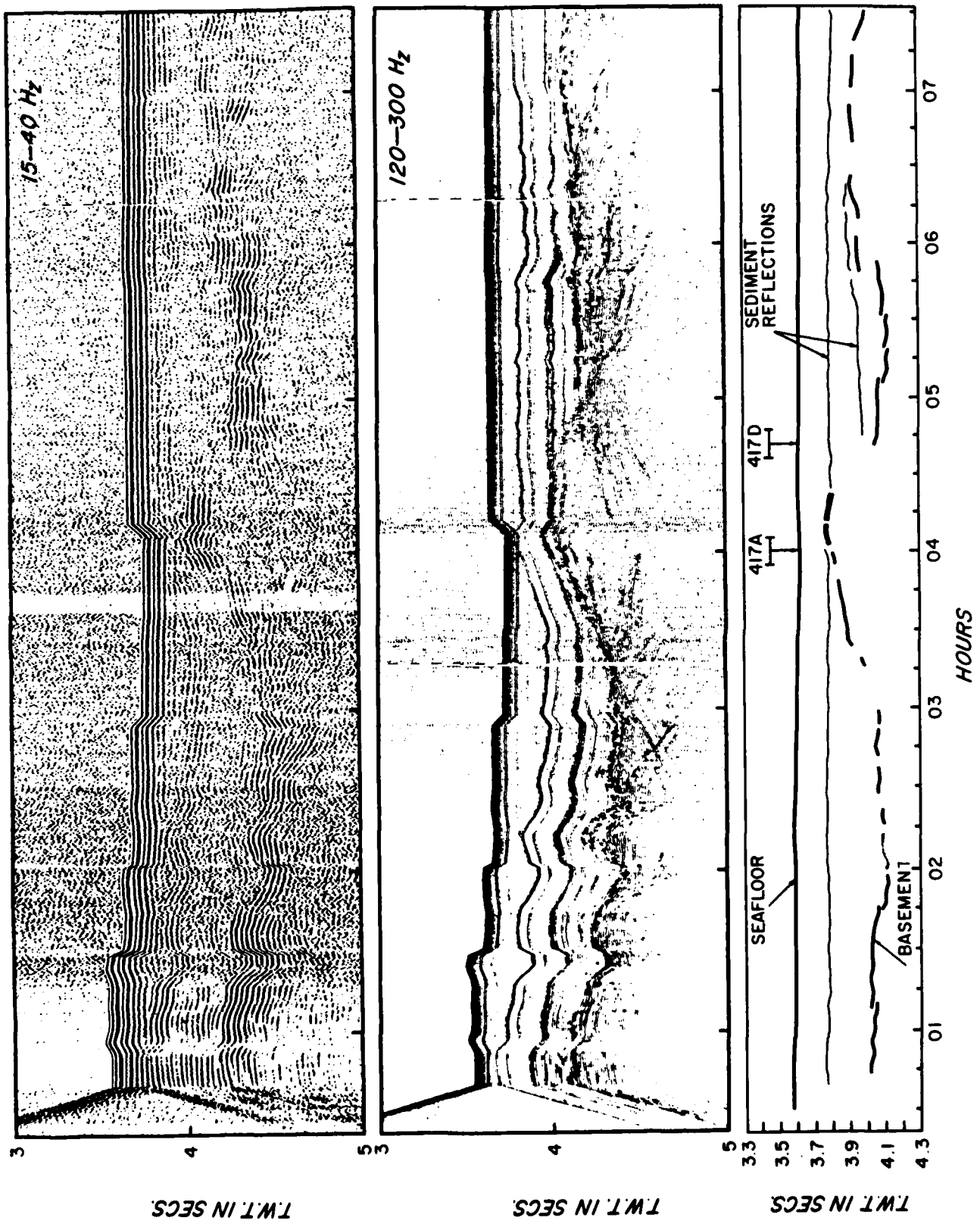
15–40 Hz
120–300 Hz
SEDIMENT REFLECTIONS
417D
417A
SEAFLOOR
BASEMENT
TWT IN SECS
HOURS

Fig. 10

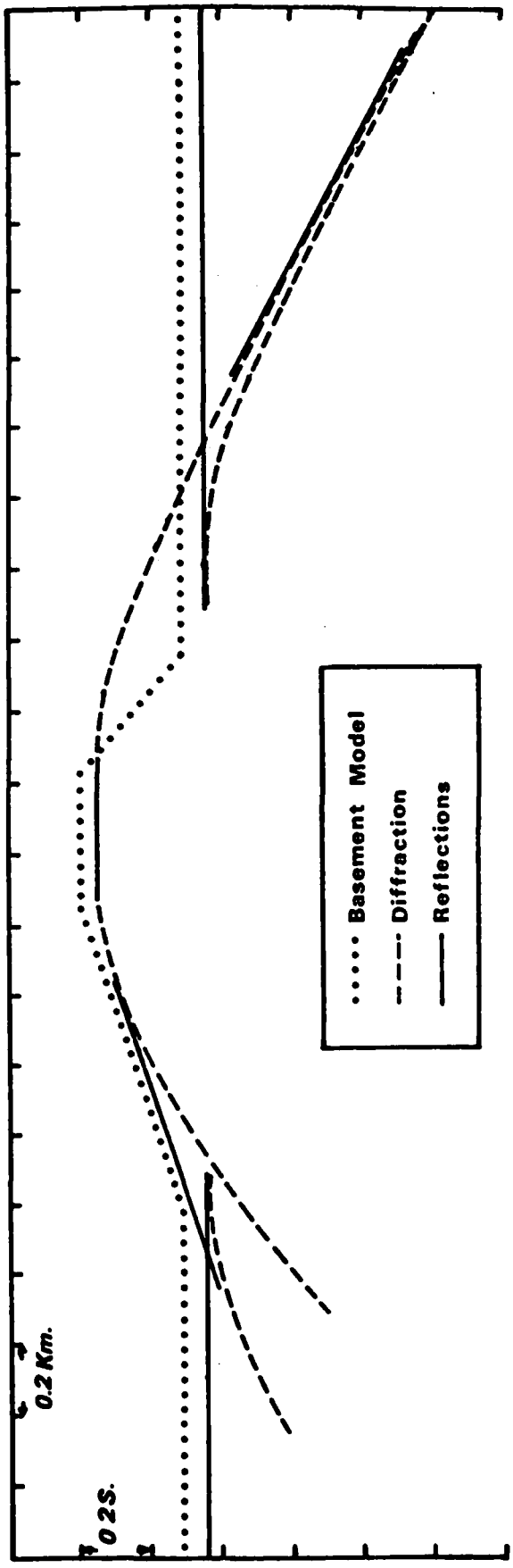

Fig. 11

V.B. PERFORMANCE PREDICTION OF THE HUNTEC DEEP TOW SYSTEM

R. W. Hutchins

Introduction

It is the purpose of these notes to identify those system parameters influencing resolution and penetration and using data from calibration tests on the deep tow system, to determine the resolution and penetration capability of the DTS system for water depths of 1500 to 2000 meters. A familiarity with the general principles of operation of such systems is assumed. An overview of the DTS is given in (1) included herewith as Appendix 1.

This type of calculation can be made for other systems, providing manufacturer's data is made available. Before proceeding with detailed calculations, a few general comments concerning acoustic based systems in general may be helpful.

The science of underwater acoustics owes much of its development to anti-submarine warfare. Sonar, an acoustic equivalent to radar, is concerned with the initial detection, and then with classifying and the simultaneous estimations of both the position (range and bearing) and of the velocity (speed and direction) of a target in the water column (or in some cases near to or on the sea floor)

A set of parameters have been defined for sonar systems, which enable the system engineer to predict the best possible performance under iso-velocity water conditions. Typical performance criteria might

be range of ultimate detection for a specified target, and the position and velocity resolution of that target. Calculations of this type provide meaningful criteria for the comparison of different systems.

The performance of a high resolution sub-bottom profiler from the geologists point of view may be stated in terms of its ability to resolve closely spaced reflections or thin geological units and small objects such as boulders, pipelines, debris, etc on and below the sea floor, and also its ability to penetrate both hard and soft layers to the bedrock surface below the sea floor.

Results achieved in practice from any acoustic based system are influenced by external factors in addition to the system parameters themselves. These factors include sea state, type of ship, water depth, bottom type and roughness and the way in which the system is rigged (hull mounted, surface towed, underwater towed body, etc). It is therefore misleading to talk about resolution and penetration unless the above conditions are all specified.

It is however possible to identify those system parameters which impose an upper bound on penetration and resolution for any particular sub-bottom profiling system, much in the way that sonar systems are compared.

We shall consider here the performance limitations imposed by the source hydrophone system itself, and not by other system components such as graphic recorder, type of signal processing, etc.

Units and Dimensions

In the following discussion the MKS system of units are used throughout. For convenience these units and the corresponding CGS system of units utilized in the development of underwater acoustics and the physics of sound are given in Table 1 along with their dimensional equivalents.

Source Characteristics and Performance

A rough sea floor will scatter incident sound arriving at oblique angles back to the source receiver. (The receiver is assumed to be located at the source.) Since oblique ray paths are longer than the reflected ray path at normal incidence, bottom scattering results in a stretching or smearing of the first bottom returns (see Fig 3 of Appendix 1) thus degrading vertical resolution for wide beam angles.

The area of the sea floor illuminated by the source is the product of beam angle and elevation above the bottom. Energy scattered by small objects such as boulders, etc will be but a small proportion of the total energy arriving at the receiver, and thus, wide beam angles also degrade horizontal resolution.

Horizontal resolution is also affected by sampling rate. A high sampling rate improves the signal to noise ratio at a given speed and also permits a larger scale to be used in the graphic display, reducing the vertical exaggeration.

The DTS source has well defined directional properties which are a function of frequency. These properties can be exploited by appropriately filtering of the received signal to reduce the effective beam angle. The price that is paid is a reduction in signal energy.

In addition to beam angle, resolution in time of closely spaced individual reflectors is simply the reciprocal of the frequency bandwidth of the entire system. The higher the bandwidth the higher the resolution. The system frequency bandwidth can be narrower, (due to filtering or due to graphic recorder limitation) but never broader, than the frequency bandwidth of the source itself. It should be noted, that the frequency bandwidth is always less than twice the centre frequency for a finite energy pulse.

Penetration is a function of the magnitude and of the spectral distribution of the energy density along the main beam axis of the source. Attentuation in most geologic materials is proportional to the first power of frequency.

The pressure signature of the on-axis (main beam) and at 30° off axis of the ED10C PC transducer utilized in most DTS systems* is shown in Fig 1 (a).

The corresponding energy spectra are shown in Fig 5 for four different direction angles.

The following equations apply:

$$E(t) = \frac{1}{dc}\int_{-\infty}^{\infty} p(t)^2\,dt \qquad 5.1$$

$$a(\omega) = \frac{1}{2\pi dc}\int_{-\infty}^{\infty} p(t)\,e^{-j\omega t}\,dt \qquad 5.2$$

$$E(\omega) = \frac{2\pi}{dc}\int_{-\infty}^{\infty} |a(\omega)|^2\,d\omega \qquad 5.3$$

In Fig 5, the function $E(\omega)$ is plotted as $E\left(\frac{\omega}{2\pi}\right) = E(f)$

Where $E(t) \longleftrightarrow E(\omega)$ is the energy flux density in joules per square meter per cycle of bandwidth for the pressure signature $p(t)$ along the specified direction angle referred to a distance of 1 meter.

The data plotted in Fig 5, enables us to determine the effective acoustic beam angle, and the signal energy, given the centre frequency and the frequency bandwidth of the band pass filter employed in the signal processor.

---

*Huntec manufactures a variety of transducers which are interchangeable with the ED10C PC, having different spectra.

From Fig 5, the peak energy flux density occurs at about 1.3kHz, and is 20db//1 pascal^2/Hz at 1 meter.

The half energy density points are at 1kHz and 5kHz yielding a 4kHz frequency bandwidth and an effective acoustic beam width of about 29° x 2 = 58°.

We calculate the main beam energy flux density as follows:

$$SE = \log\{[E(\omega)]_1^5\} = 20 + 10\log(5000 - 1000) - 10\log dc$$

$$= 20 + 36 - 61.9$$

$$SE = -5.9 \text{ db // 1 joule/Sq. meter at 1 meter.} \qquad 6.1$$

(This is at 5.6kv excitation voltage, 470 joules)

Where SE is referred to as source energy level.

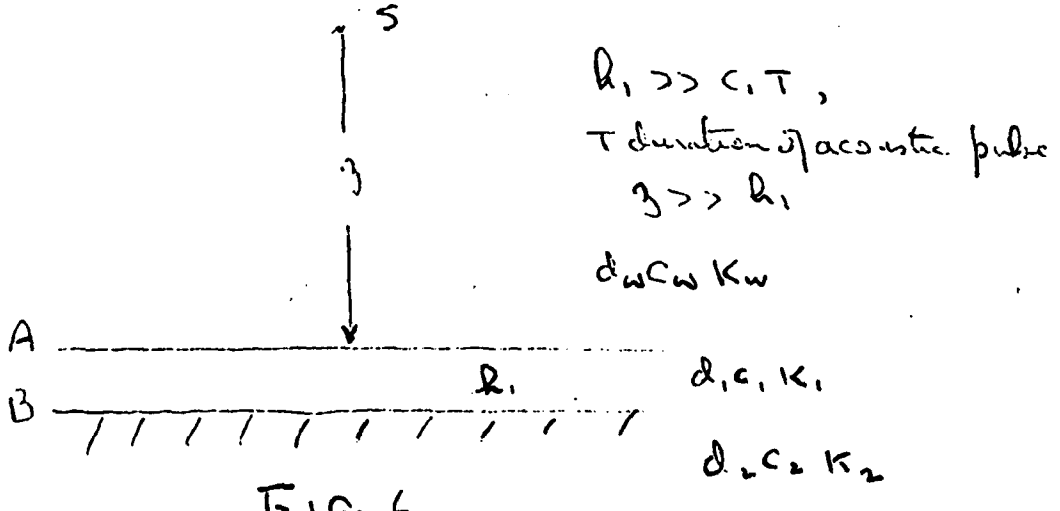

FIG 6

In Fig 6, S is a source/hydrophone at elevation z above a smooth, specularly reflecting sea floor A, of layer thickness h_1, overlying a smooth hard bedrock surface B of infinite extent.

The density d, sound velocity c and attenuation coefficient k for each of the three layers (water, sea bed and bedrock) are designated by corresponding subscripts W, 1, 2.

Physical properties of various geologic materials is given by Hamilton (2) For fine sand these are

(d_1) Density 1.96 x 10^3 kgs/cu meter

Porosity 44.8%

(c_1) Sound volocity 1753 meters/sec

(k_1) Attenuation coefficient at 2kHz = 1db/meter

(R_1) Acoustic Impedance $R_1 = d_1 c_1 = 3.44 \times 10^6$ Rayls

We define the following

$E_i \downarrow_A$ is the energy density of the downward travelling wave incident on A.

$E_r \downarrow_A$ is the energy density of the upward travelling wave reflected from A

$E_T \downarrow_A$ is the energy density of the downward travelling wave transmitted through the boundary A

(2) Hamilton, Edwin L (1974) Prediction of Deep Sea Sediment Properties: State of the Art. Deep Sea Sediments Vol 2 Plenum Press

$$a_r f_A = \frac{E_r f_A}{E_i f_A} = \left(\frac{R_1 - R_w}{R_1 + R_w}\right)^2 \qquad 8.1.$$

$$a_r f_A = \frac{E_T f_A}{E_i f_A} = \frac{4 R_1 R_w}{(R_1 + R_w)^2} \qquad 8.2.$$

Under the approximation that

$$3 + R_1 \cong 3 \quad \text{when} \quad R_1 \ll 3$$

and that the thickness h_1 is much longer than the pulse duration times the velocity of sound, then we can compute the signal returned from the sea floor surface A, and from a perfectly reflecting bedrock surface B (Since $R_2 \gg R_1 > R_w$).

We locate an image source S^1 at a depth z below the sea floor.

Signal Losses

Two way divergence loss	=	$20 \log 2z$	8.3
Two way attenuation loss in water column	=	$2 z K_w$	8.4
Bottom loss	=	$10 \log a_r f_A$	8.5
Two way attenuation loss in layer	=	$2 R_1 K_1$	8.6
Two way transmission loss through boundry A	=	$20 \log a_r f_A$	8.7

Thus, the echo levels EL_A for the bottom and EL_B for the bedrock are given by

$$EL_A = SE - 20 \log 2z - 2z K_w - 10 \log a_r f_A \qquad 8.8$$

$$EL_B = SE - 20 \log 2z - 2z K_w - 2R_1 K_1 - 20 \log a_r f_A \qquad 8.9$$

Using Hamilton's values we obtain for our example

$$a_V \uparrow_A = \left(\frac{3.44 \times 10^6 - 1.54 \times 10^6}{4.98 \times 10^6} \right)^2$$

$$= .14 \qquad 9.1.$$

$$a_T \downarrow_A = \frac{4 \times 3.44 \times 1.54 \times 10^{12}}{24.8 \times 10^{12}}$$

$$= .85 \qquad 9.2$$

and thus at 1700 meters bottom clearance, Kω = .001db/meters

h_1 = 10 meters

EL_A = -5.9 - 71 - 3.4 - 8.5

= -89db//1 joule/sq meter 9.3.

EL_B = -5.9 - 71 - 3.4 - 20 - 1.4

= - 102db 9.4

Noise

From Fig 7 the spectrum level for sea state 5 at 1.3kHz is -57db//1 pascal per cycle of bandwidth. In a 4kHz band this is -57 + 36 = - 21db//1 pascal

Dividing by Rw (-62db) we obtain an ambient sea noise intensity of -83db//1 watt per sq meter. This power must now be integrated over the rise time through the filter (-36db) to obtain noise energy.

Thus noise energy arriving at hydrophone during arrival of signal is -119db. Using this, and equation 8.9 we obtain the recognition differential for the bedrock of

$$-101.3 - (-119) = 17.6\text{db} \qquad (10.1)$$

as the signal to noise energy.

The signal energy of -101db//1 joule/sq meter represents an average signal power over the time duration of the signal of

$$10 \log 4000 - 101 = -65\text{db//1 watt/sq meter.} \qquad (10.2)$$

Corresponding to a sound pressure level of

$$-65 + 10 \log d\omega c\omega = -3\text{db//1 pascal.} \qquad (10.3)$$

The hydrophone sensitivity is -84db//1 volt/pascal and thus the hydrophone output is

$$-87\text{db//1 volt} \equiv .05 \text{ millivolts} \qquad (10.4)$$

During a recent cruise in a calm sea, at a speed of 2.6 knots, a wide band noise of 3 millivolts RMS was measured at the preamplifier output corresponding to a preamplifier input of .06 millivolts.

There appeared to be a dominant 150Hz component in this noise.

Conclusion

The limit of penetration through fine sand in 2000 meters water depth at a fish depth of 300 meters and a ship speed of 2.6 knots is of the order of 10 meters.

At a bottom clearance of 1200 meters (water depth 1500 meters) the gain in echo level is 4db.

AD-A081 246 WASHINGTON UNIV SEATTLE DEPT OF OCEANOGRAPHY F/G 17/1
WORKSHOP ON DEEP-TOWED, LOW FREQUENCY ACOUSTIC SOURCES AND RECE--ETC(U)
MAY 79 N00014-75-C-0502
UNCLASSIFIED NL

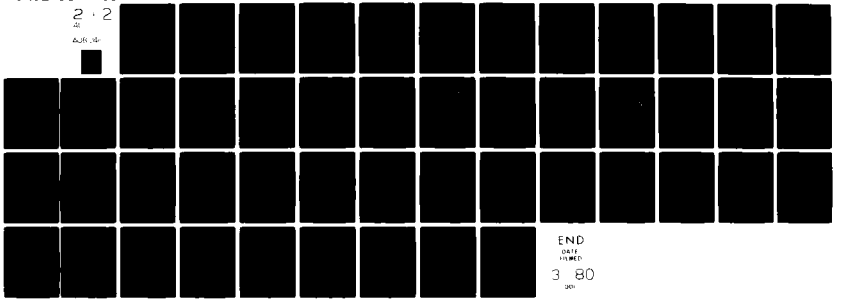

END
DATE FILMED
3 80
DTIC

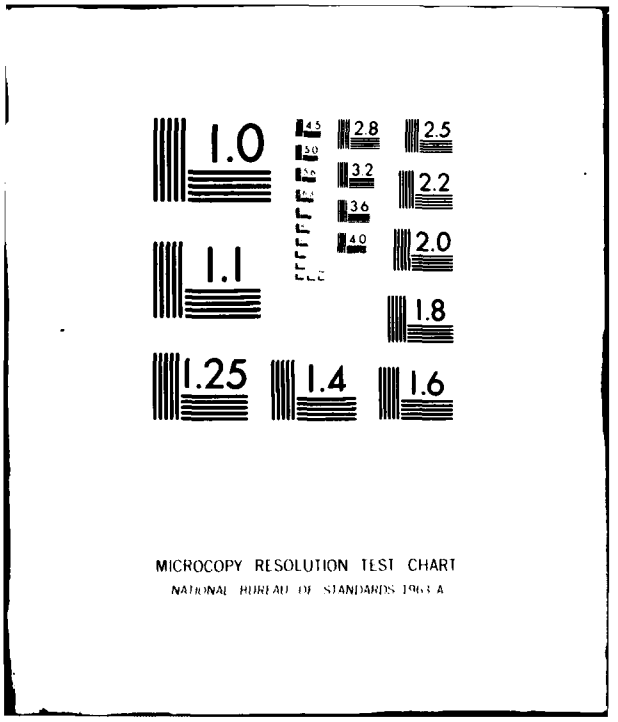
1.0
1.1
1.25
1.4
1.6
1.8
2.0
2.2
2.5
2.8
3.2
3.6
4.0
4.5
5.0
5.6
MICROCOPY RESOLUTION TEST CHART
NATIONAL BUREAU OF STANDARDS 1963 A

TABLE 1

ACOUSTIC AND RELATED UNITS

Quantity	Symbol	Dimensional Equivalent	MKS Unit	Multiply MKS Unit by	To Obtain Value in CGS Units
Bulk Density	d	ML^{-3}	Kilograms per cubic metre	10^{-3}	Grams per cubic centimeter
Sound Speed	c	LT^{-1}	Metres per second	10^{2}	Centimeters per second
Pressure	p	$ML^{-1}T^{-2}$	Newtons per square metre (Pascals)	10^{-1}	Dynes per square centimeter or microbars
Acoustic Intensity	I	MT^{-3}	Watts per square metre. Joules per square centimeter per second	10^{3}	Ergs per square centimeter per second
Characteristic Acoustic Impedance	dc	$ML^{-2}T^{-1}$	Kilograms per square metre per second (Rayleighs) Fresh water $1.L18 \times 10^{6}$ Rayls Sea water 1.54×10^{6} Rayls	10^{-1}	Grams per square centimeter per second
Energy Flux Density	F	MT^{-2}	Joules per square metre	10^{3}	Ergs per square centimeter
Energy Directivity Density	$E = \frac{I}{C}$	$ML^{-1}T^{-2}$	Joules per cubic metre	10	Ergs per cubic metre

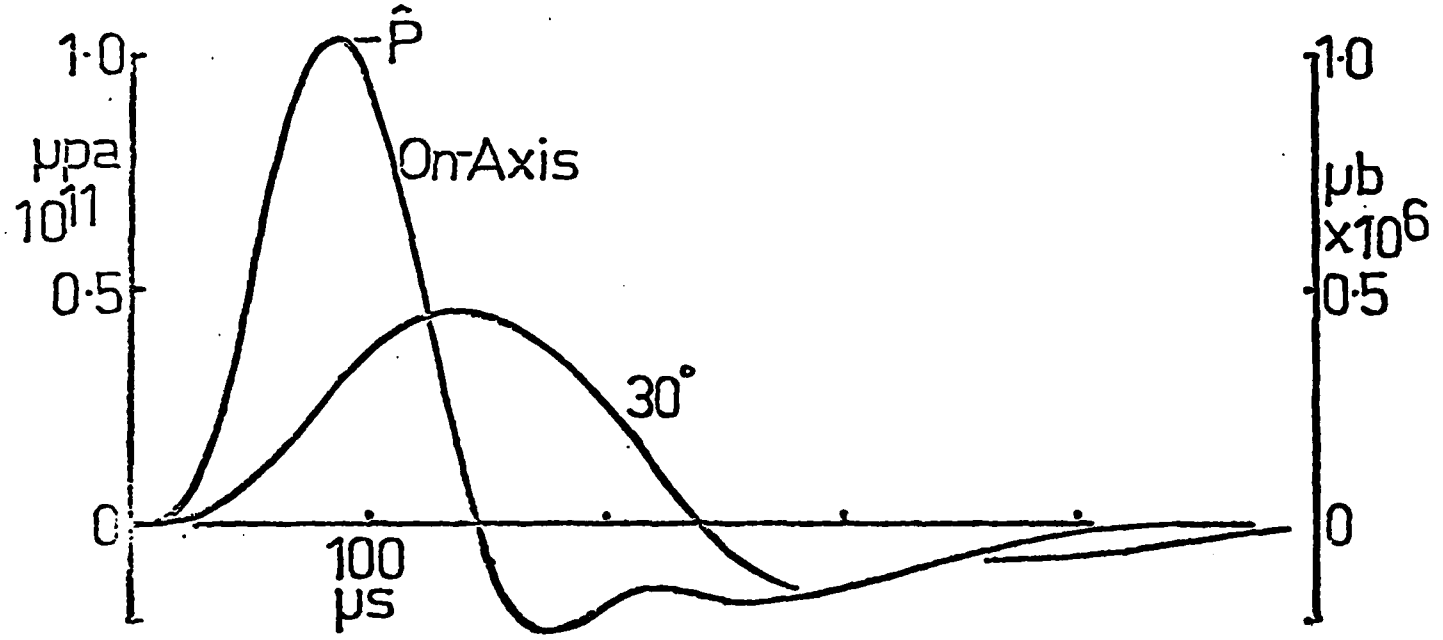

Figure 1 (a)

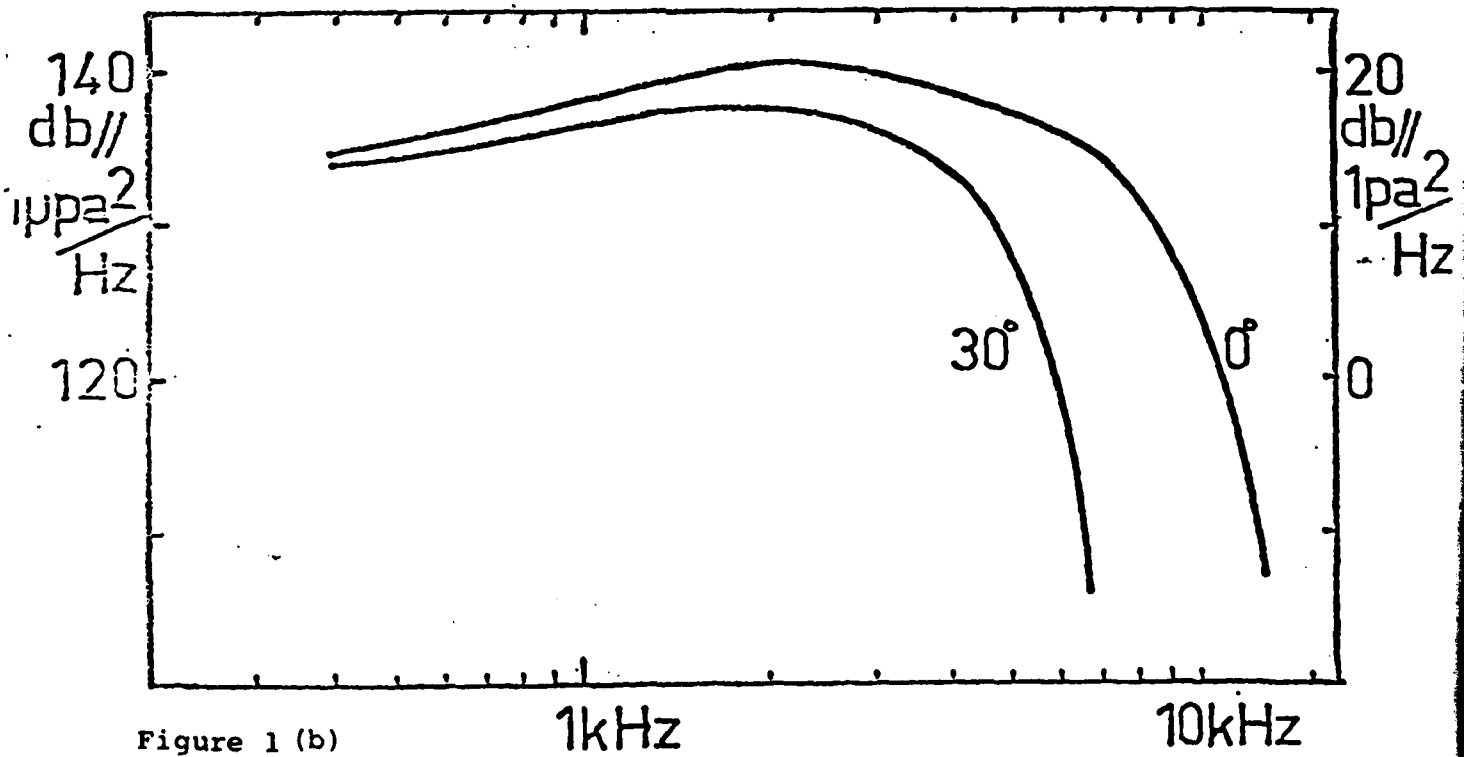

Figure 1 (b)

FIGURE 1: Pressure pulse and power spectrum for Huntec ED10C boomer measured on-axis and at 30° off axis. Measurements referred to 1 metre with input energy 500 Joules.

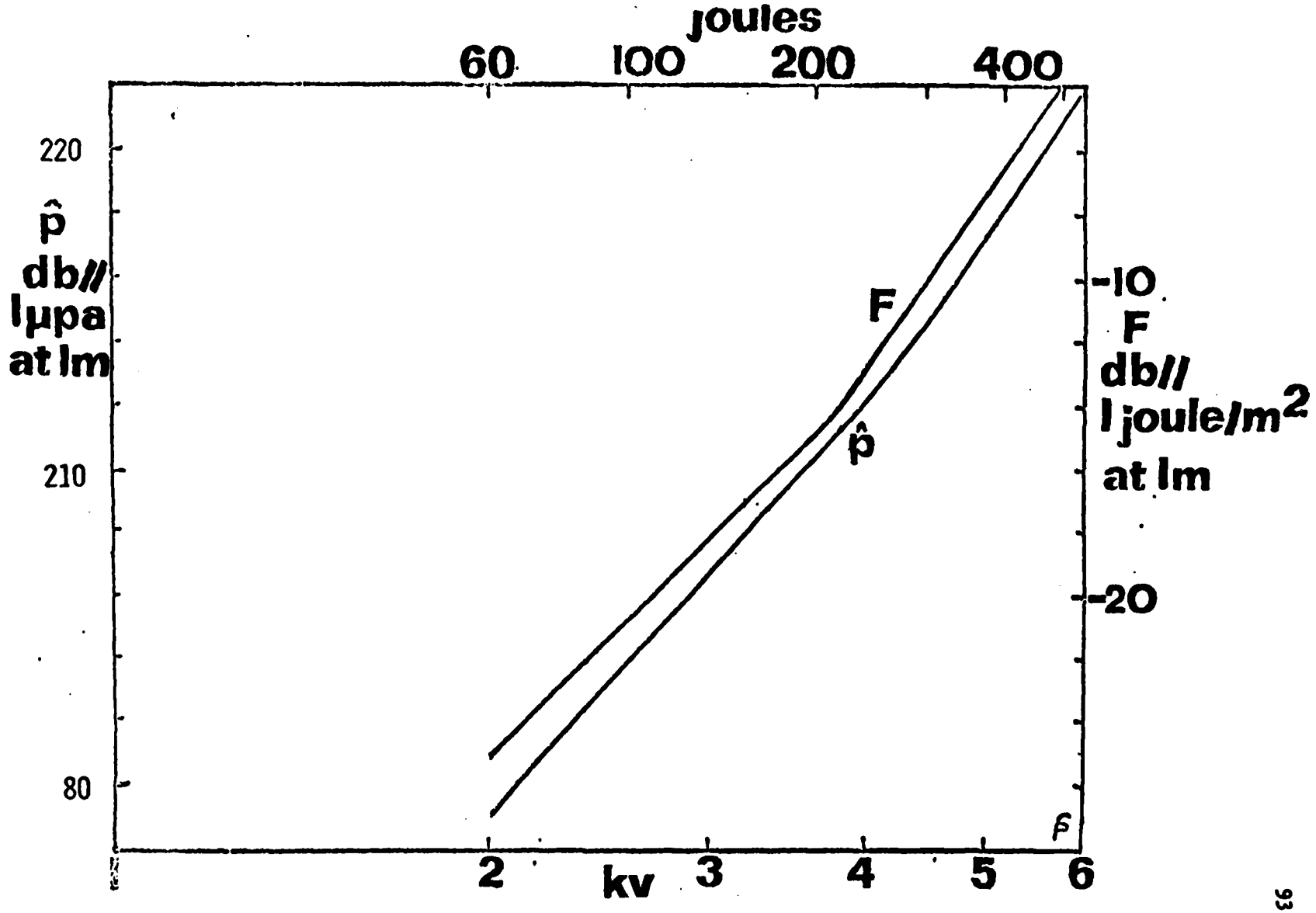

Figure 2. Peak pressure, $\hat{p}$, and energy flux density, F, against excitation voltage.

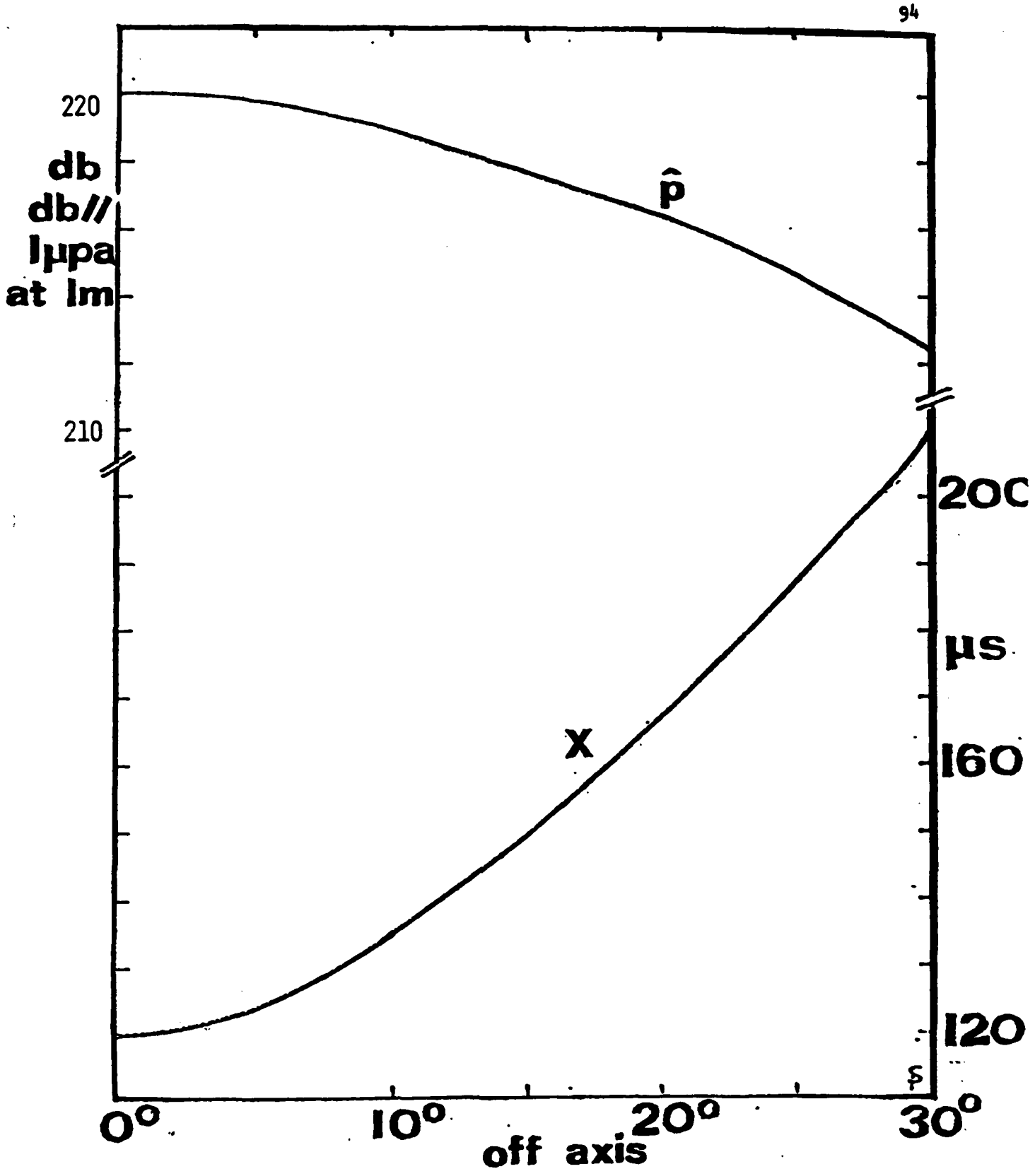

Figure 3. Peak pressure, $\hat{p}$, and pulse length, X, against boomer orientation. Excitation voltage = 5.6 kv.

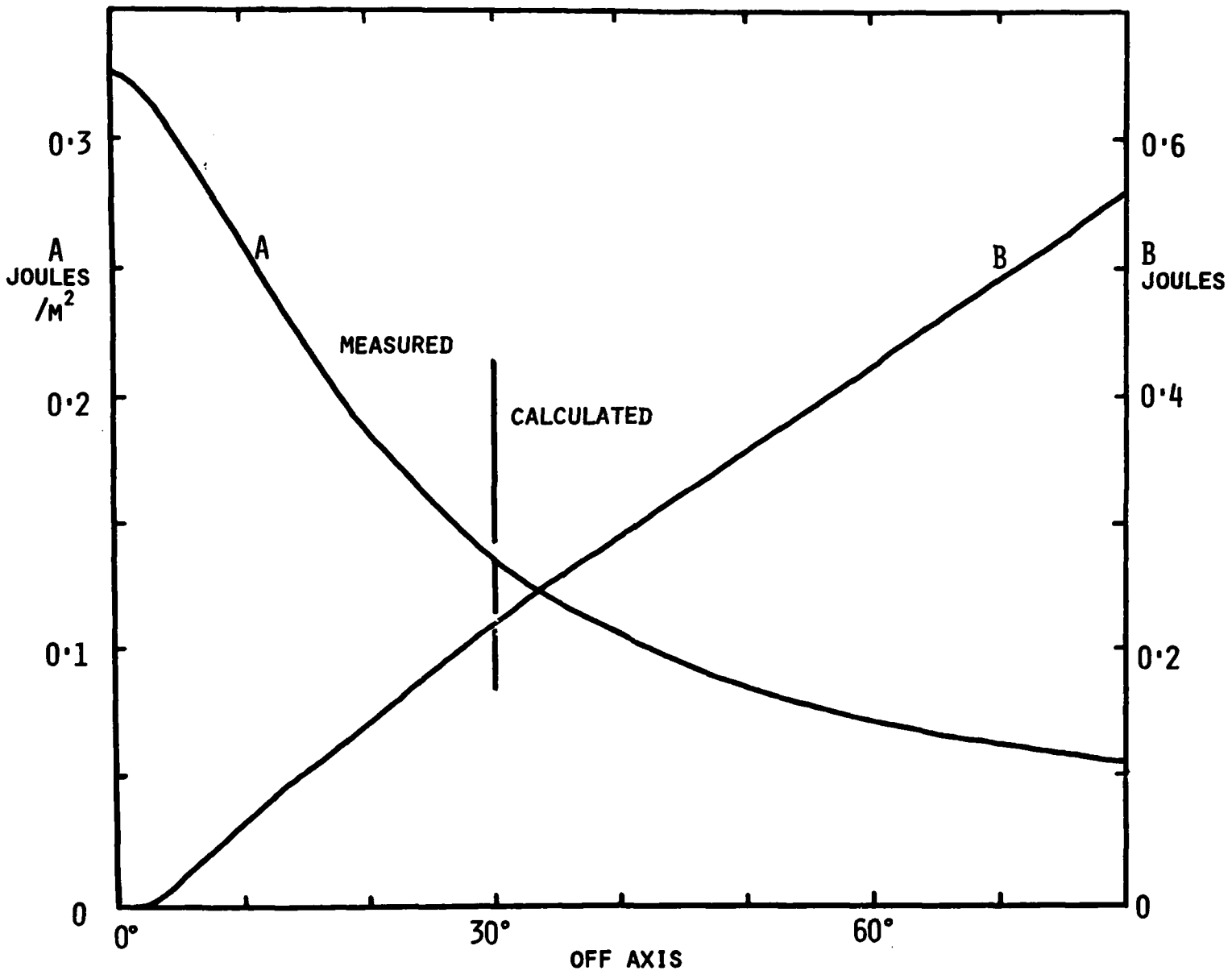

Figure 4. Energy flux density and energy distribution against boomer orientation. Excitation voltage = 5.6kv.

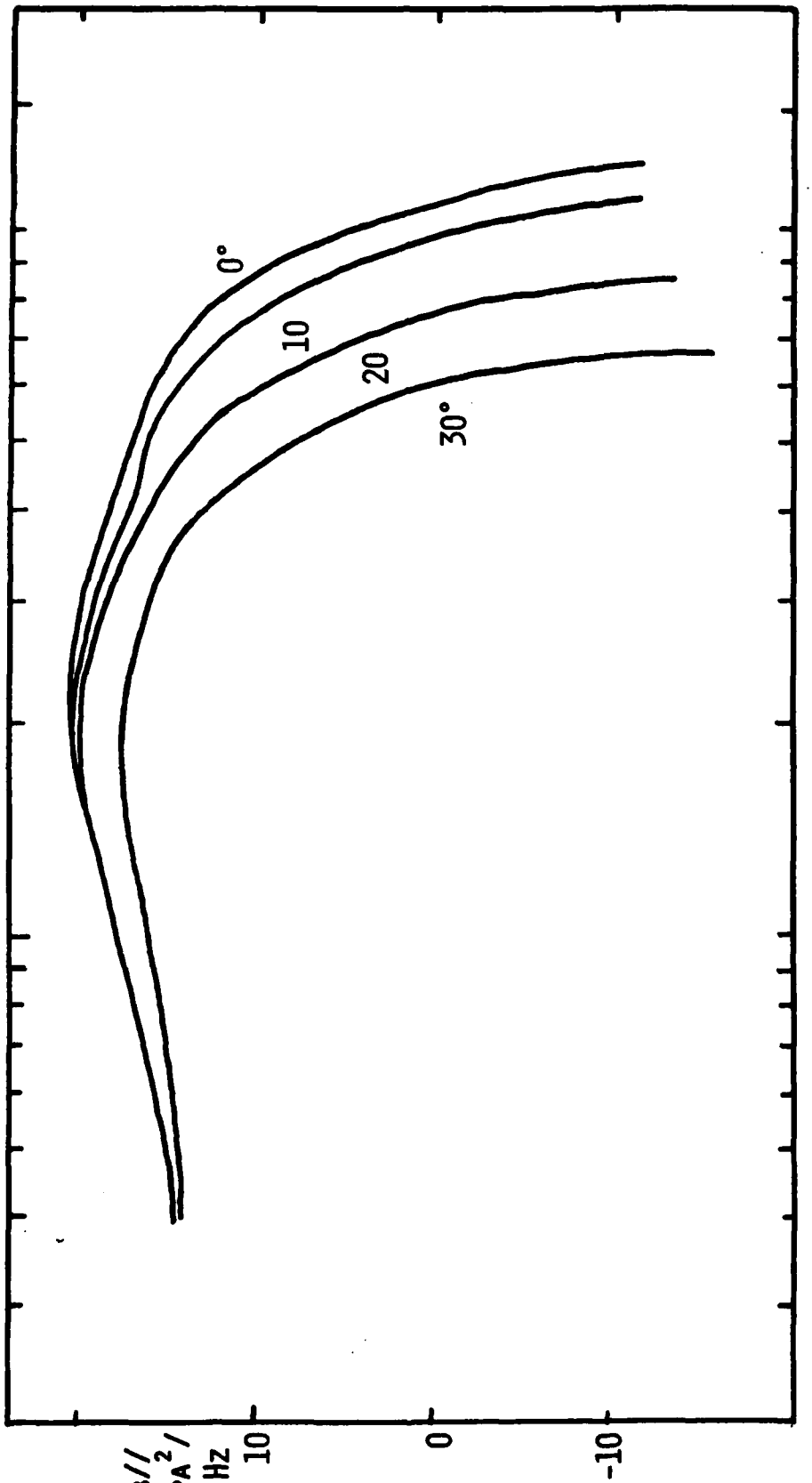

Figure 5. Energy spectrum E(ω) of output waveform for various angles of boomer orientation. Excitation = 5.6 kv.

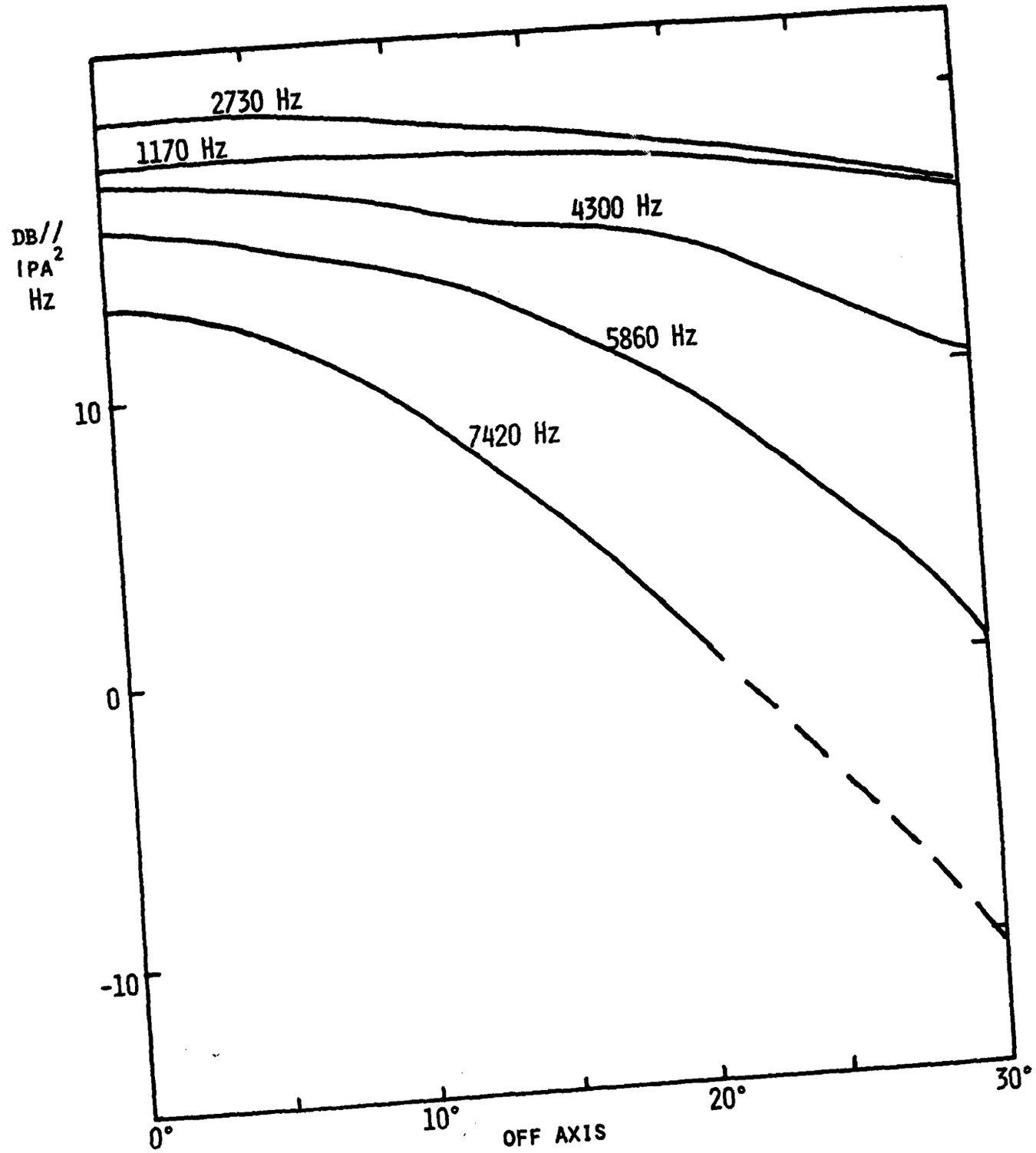

Figure 6. EDIOC PC directivity at various angles of boomer orientation.

a guide to

Ambient Noise IN THE DEEP OCEAN; GREATER THAN 1,000 FATHOMS

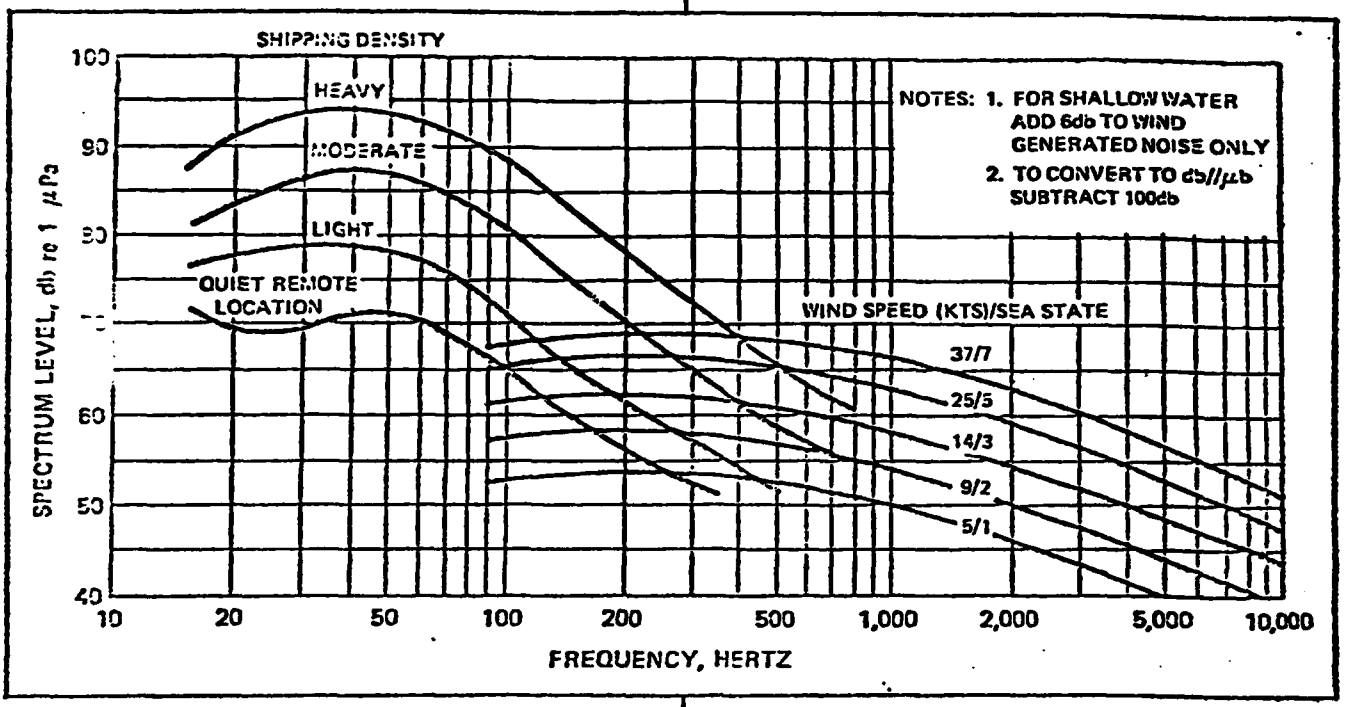

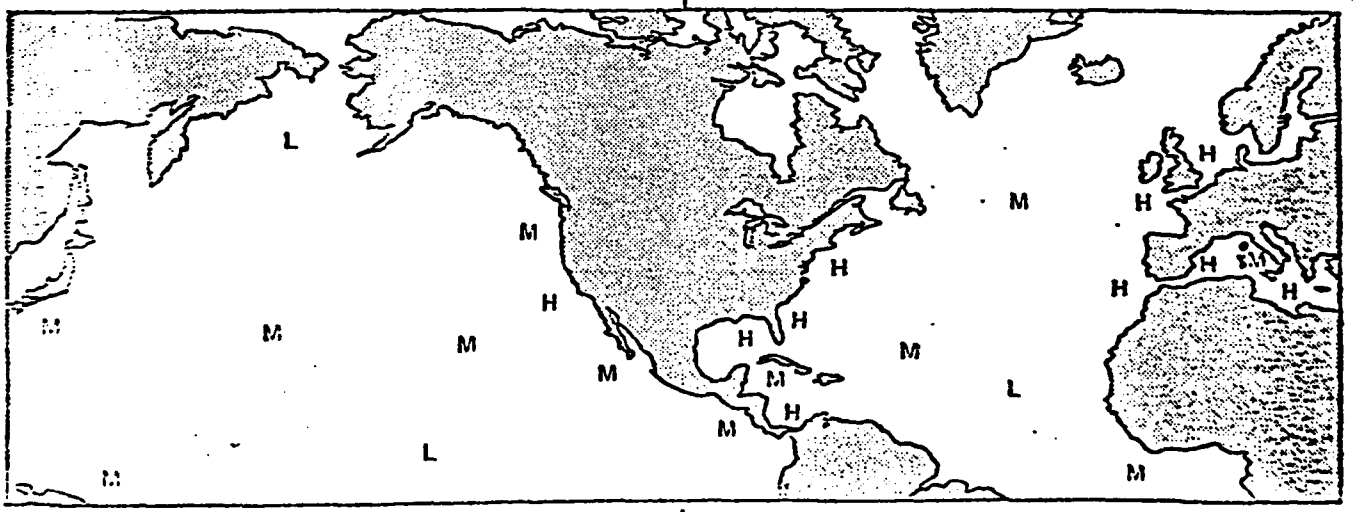

H = HEAVY TRAFFIC
M = MODERATE TRAFFIC
L = LIGHT TRAFFIC

For either a copy of this guide on heavy stock, or a plasticized wallet sized version, please write: Director of Marketing, Ocean Surveillance Systems.

DEEP OCEAN TECHNOLOGY—MEASUREMENT SYSTEMS, OCEAN ENGINEERING AND ASW.

BUNKER RAMO

ELECTRONIC SYSTEMS DIVISION
31717 La Tienda Drive, Box 5009, Westlake Village, California 91359
Telephone: (213) 889-2211

OHIO: Claypool Building - Suite 200-5 / 4130 Linden Ave. / Dayton, Ohio 45432 (513) 254-2659 VIRGINIA: 1500 Wilson Blvd. / Suite 400 Arlington, Virginia 22209 (703) 524-8700 NEW JERSEY: P. O. Box 834 / Red Bank, New Jersey 07701 (201) 747-5353 NEW YORK: 1333 E. Dominick / Rome, New York 13440 (315) 337-6100.

V.C. TOWED-LINE ARRAY ELEMENT AND HYDROPHONE CALIBRATION

J. E. Blue
Naval Research Laboratory
Underwater Sound Reference Detachment
Orlando, Florida 32806

The Underwater Sound Reference Detachment (USRD) of the Naval Research Laboratory has performed extensive measurements of towed-line arrays and their hydrophone elements. About six years ago, a consistent measurement program was initiated at the USRD to aid in the development and evaluation of towed-line arrays. This paper deals with our experience with this program and points out weaknesses in our calibration program in achieving good complex sensitivity calibrations down to 1 Hz. A program will be described to correct some of these weaknesses.

When the Navy's advanced towed-array development program began, there was no consistent program in calibration. Figure 1 shows the effect of hydrostatic pressure on the sensitivity of one of the hydrophone elements that had been selected for use in one of the Navy's towed-array sonar system. It changes sensitivity by more than 10 dB over the operational depth of the array. The USRD notified the NAVSEA program manager that the manufacturer had selected an unsuitable element, and a program was developed to assure that elements chosen for towed-line arrays were stable over operating depths and temperatures.

The program developed utilizes 2 of USRD's calibration facilities, the Low Frequency Facility and the Leesburg Facility. Measurements are made in the Low Frequency Facility to assess the effects of temperature and pressure on hydrophone sensitivity and to determine whether the hose material and filling fluid affect the sensitivity. We have found that the sensitivities of a number of towed-line array elements change sensitivity drastically as a function of both temperature and pressure. An example of pressure effect was shown in Figure 1. Figure 2 shows an example of the effect of temperature on sensitivity of a hydrophone element. After a stable element has been selected, the hydrophone groups in the towed array are tested. One such test showed that the sensitivity in the array differed by 2 dB from that measured in the Low Frequency Facility. The manufacturer suspected the measurements, but the difference was finally traced to different element grounding conditions used by the manufacturer in the test sections.

The Leesburg Facility is used to test towed-line arrays because of its stability and depth. It is 52 meters deep and small in size to maximize barge stability. Remember that a vertical displacement of 1 cm is equivalent to a 160 dB re 1 μPa noise pressure on a hydrophone. People walking on deck make it impossible to make calibration measurements on some arrays that don't roll-off drastically in sensitivity at low frequencies. At the Leesburg Facility, two test geometries for line arrays are used depending on the length of the hydrophone grouping in the arrays. Hydrophone group lengths up to 5 feet are calibrated by hanging the line vertically as depicted in Figure 3. The hydrophone group is in an approximate plane wave field but the line has a pressure-gradient along it. Figure 4 shows the effect of distance from the source to the line on the hydrophone sensitivity. Lines that have the hose wall as their strength member usually show this

effect. Since the pressure-gradient along the line decreases at 12 to 18 dB per distance doubled while the pressure decreases only 6 dB, the apparent sensitivity becomes smoother with increasing distance. Lines that have an internal strength member show less effect from pressure-gradients. Multipath interference and lack of low frequency calibration sources limit calibration of hydrophone group lengths to about 5 feet when hanging vertically. Good signal-to-noise ratios can't be obtained for the distances necessary for longer grouping. Therefore, for the longer hydrophone groupings, the test geometry shown in Figure 5 is used where the spherical wave hitting the array wrapped on the reel simulates a plane wave hitting a linear array.

At present, we can obtain the amplitude sensitivity down to about 1 Hz with an accuracy of ± 0.3 dB and phase sensitivity down to about 5 Hz with an accuracy of ± 4° in our 10,000 psi low frequency tube facility. In our open-water Leesburg Facility, we can obtain amplitude sensitivity down to about 7 Hz with an accuracy of ± 1 dB and phase sensitivity down to about 20 Hz with an accuracy of ± 5°. These limitations are imposed by our instrumentation, and signal-to-noise ratio capabilities. We have an exploratory development effort ongoing aimed at overcoming these limitations. Subproblems in this program include:

1. A computer-controlled Low Frequency Facility measurement system with software to improve signal-to-noise ratio. The objective is to provide complex sensitivity down to 0.1 Hz with an amplitude accuracy of ± 0.2 dB and a phase accuracy of ± 2°.

2. A low frequency calibration source or method to allow complex sensitivity measurements down to 1 Hz in the Leesburg Facility with an amplitude accuracy of ± 0.5 dB and a phase accuracy of ± 4°.

3. A low frequency coupler for towed-line arrays in Figure 6 with capabilities down to 0.5 Hz.

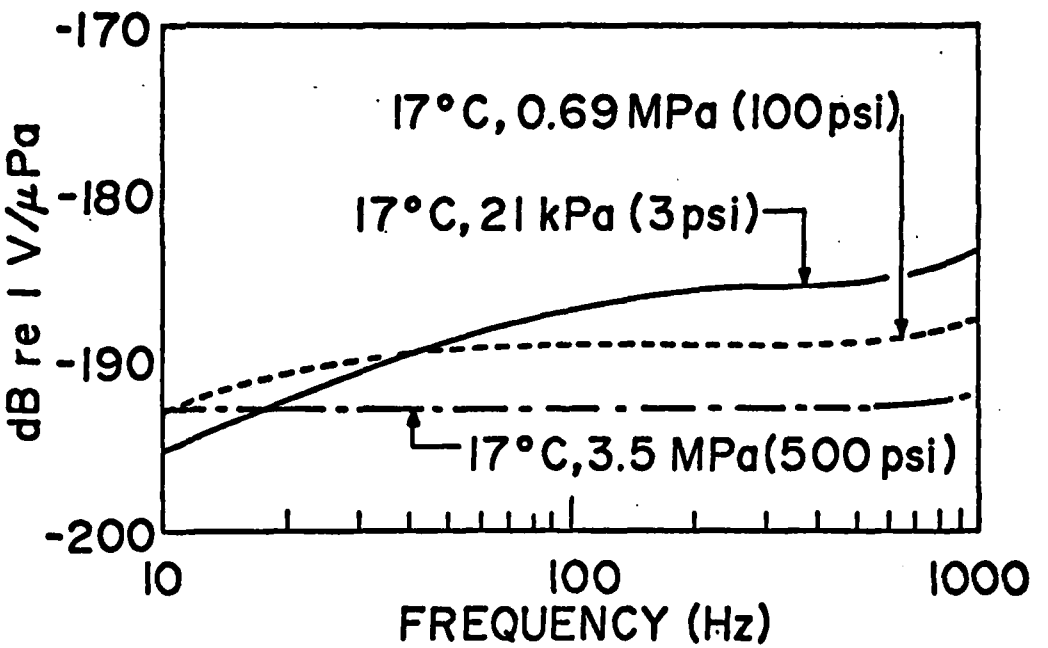

Figure 1. Effect of pressure on the sensitivity of a hydrophone element that had been selected for use in a towed-line array.

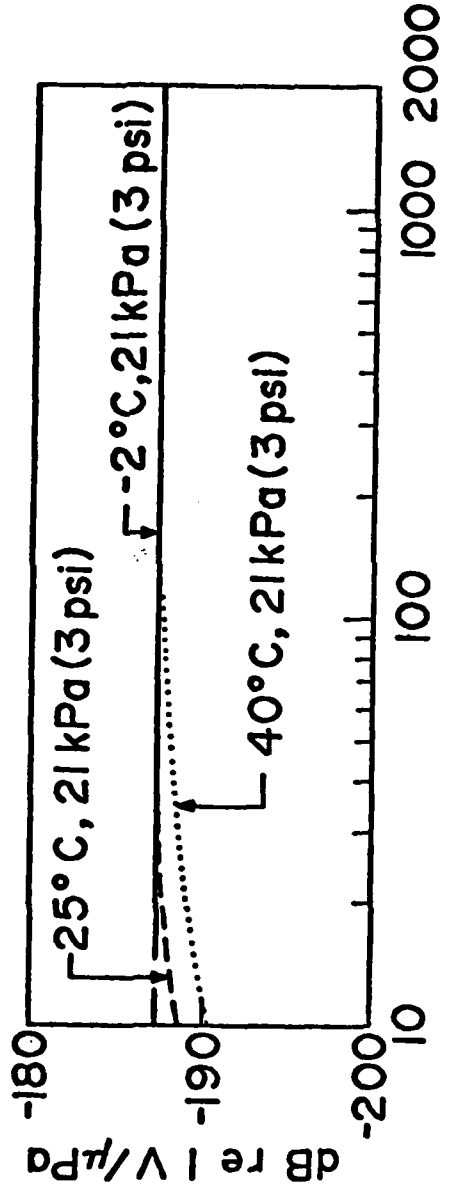

Figure 2. The effect of temperature on hydrophone sensitivity with constant pressure.

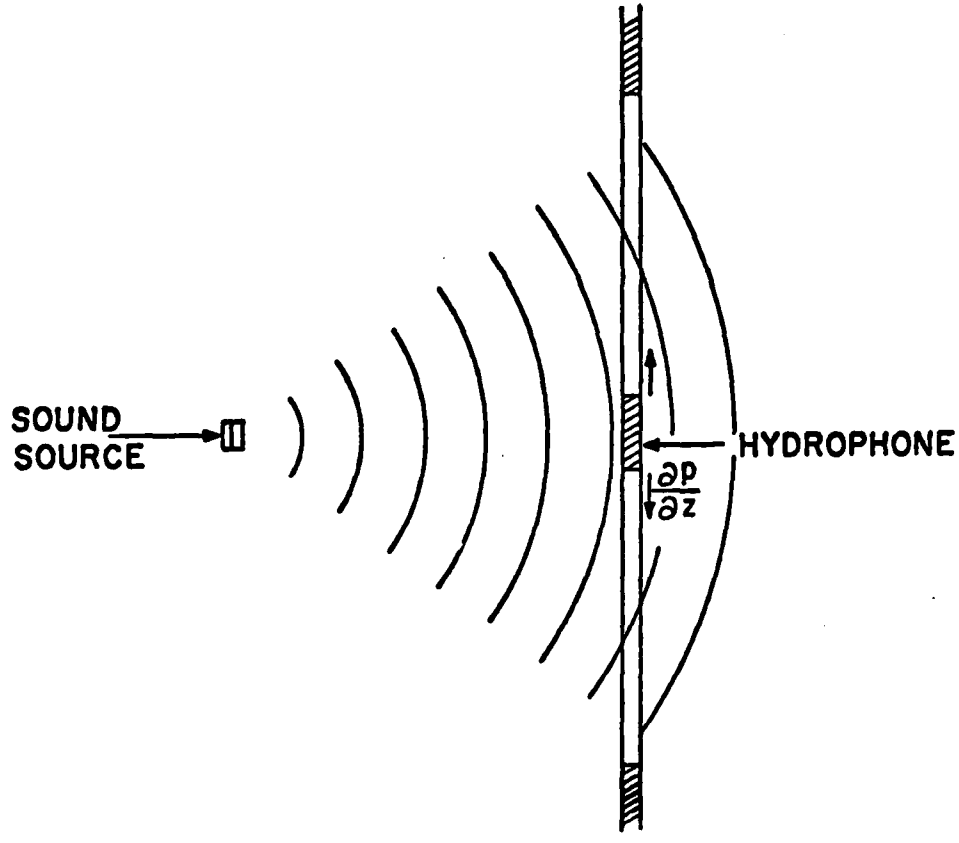

Figure 3. Hydrophone in the far field with a pressure gradient along the line.

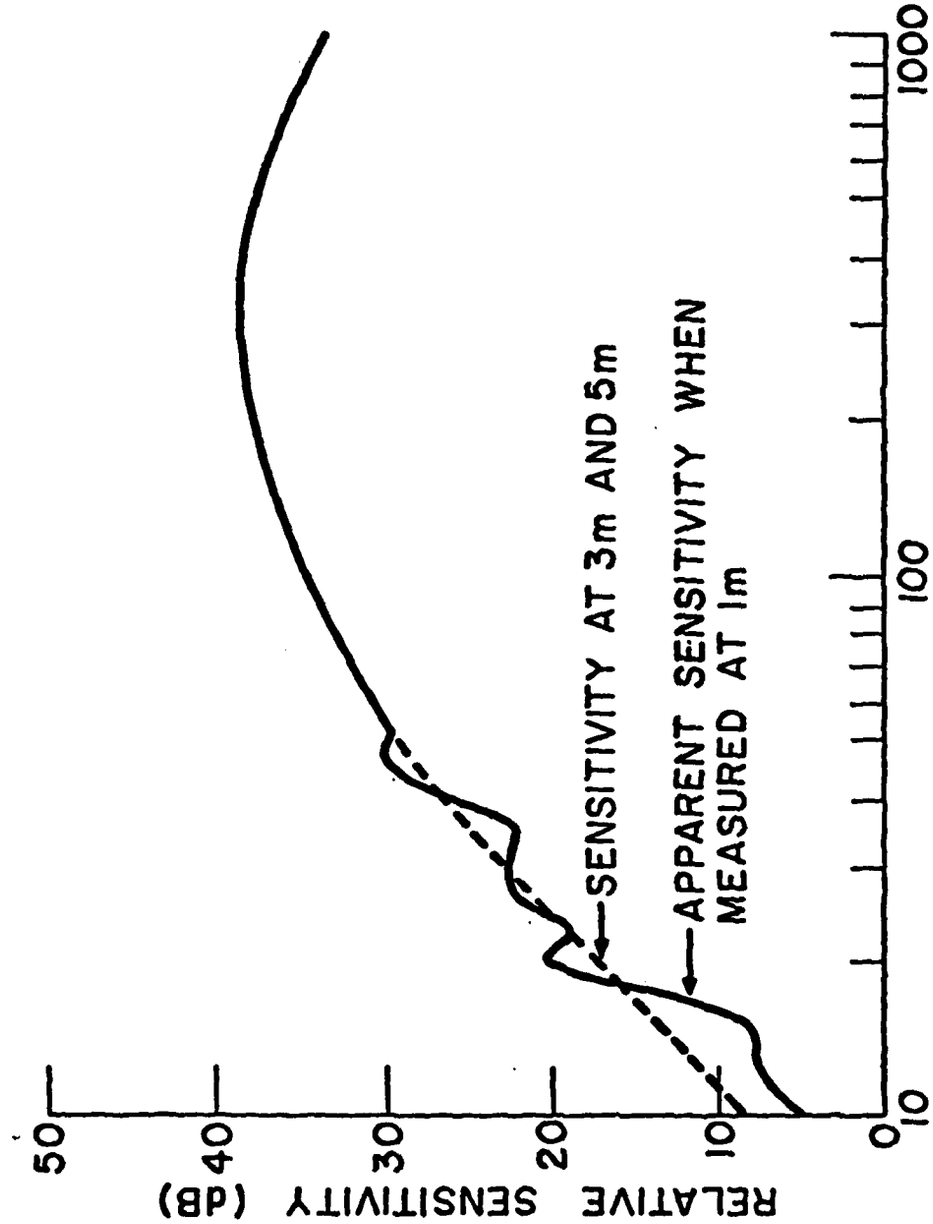

Figure 4. Apparent relative sensitivity of a towed-line array hydrophone when the line responds to the pressure gradient.

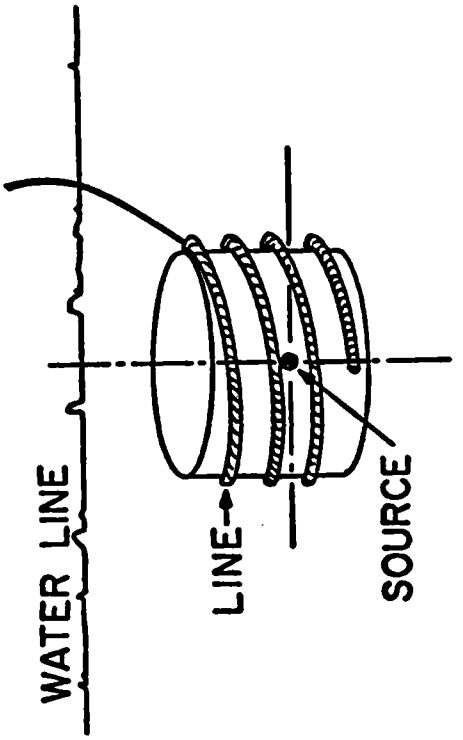

Figure 5. Calibration geometry for a reel-rigged towed-line array.

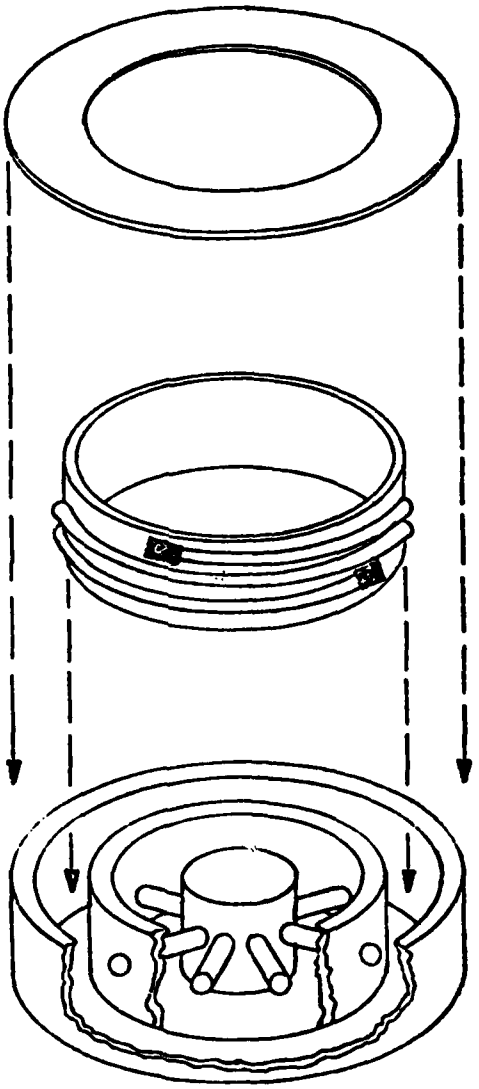

Figure 6. Water coupler for towed-line array calibration.

V.D. UNIVERSITY OF WASHINGTON DEEP-TOWED ARRAY

B. T. R. Lewis

The motivation for developing deep-towed seismic systems is primarily resolution. Reflection profiling systems operated from the surface (including multichannel systems) record both vertical incidence reflections and back scattering from irregular topography around the array. In deep water both single and multichannel arrays do not have the frequency wavenumber resolution to discriminate against energy arriving from unwanted azimuths. The result is a record containing energy at the same time as the events of interest and therefore a blurred picture of the subbottom. By placing at least the receiving array, and even better both the source and receiver near the seafloor, back-scattering energy from topographic irregularities will arrive later and with less energy than the data of interest. This results in a record giving a more clear view of the subbottom structure.

Another motivation for developing deep-towed arrays and sources is to map refraction velocity of the upper few hundred meters of the crust. In surface-to-surface refraction experiments these data are masked by water arrivals. In OBS experiments the situation is better but it is difficult to obtain more than one or two estimates of this velocity. There are good reasons to believe that the upper crustal velocity may be laterally variable and anisotropic, related to cracks and their orientation, hydrothermal systems, and the sealing of cracks with age. These results can be obtained with a deep-towed low frequency array.

Our deep-towed array consists of an array 2 km long using a Kevlar strength member with 20 hydrophone sensors spaced 100 in apart. At the head of the array is a pressure housing with a 4 kHz pinger and digitizing electronics which digitize 32 channels each 200 times per sec at 12 bits per channel.

The multiplexed digital data is transmitted up a 5 km long Amergraph co-axial tow cable in biphase L form at a frequency of about 200 kHz. On the ship the serial data stream is demultiplexed and logged on a minicomputer (LSI-11) as well as being displayed on a 24-channel optical recorder.

The system was built in 1978 with ONR support and first field tested in September 1978 off the Washington coast. The source for the array has been 2 lb explosive shots which were slid down a wire towed from the ship. The end of this wire is attached to a float via a sinker and spacer wire. This ensures that shots are at a constant distance and depth. The first tests were successful in that data was obtained but we found that:

(1) There was a great deal of noise produced by motion of the ship being transmitted down the tow cable;

(2) The array was not neutrally buoyant, but heavier than water.

In the next field test during the ROSE experiment in February 1979, the array was decoupled from the tow cable by 100 feet of elastic cord and syntactic foam floats were added at regular intervals along the array. This produced a great improvement in the noise and the buoyancy. Figure 1 shows a comparison of data before and after decoupling.

Figure 2 shows a comparison of array data taken in mid water and near the ocean bottom in the ROSE area. In the ROSE area the array unfortunately touched bottom and wiped out several hydrophones, but did not damage the cable. However, we can still clearly see refracted arrivals near the bottom. Of course these are not seen in the mid water shot. One of the great advantages of this system is that one can directly measure the source function free of interference of surface or bottom boundaries. We are presently experimenting with deconvolution methods using the observed source function. To use the refracted wave velocities or to stack the array for reflections one must correct for the array geometry. At present we have been using the direct water wave and either the bottom bounce or surface reflection to determine the geometry. Figure 3 shows a determination of the geometry while lowering the array. Presently this is the weak point in the system. The 4 kHz pinger receiver has never worked satisfactorily and we encountered problems using the precision pressure transducers that are situated at three positions along the array. These features need to be fixed before adequately precise geometries can be obtained.

Figure 4 demonstrates that the array can be useful for determining the frequency dependence of the amplitude of the refracted arrivals. It is a comparison of shots at two different depths, one at about 25 m; the other at about 50 m. The dominant frequency on the deeper shot is higher than the other shot and one can clearly see that the amplitude ratio between the direct water wave and the refracted arrival is substantially less at the higher frequencies. We will be using synthetic seismograms to model these data to establish how well the theory predicts the observations.

Another feature that we expected to see was that near the bottom side echoes and diffracted waves off inhomogeneities would appear at later times than the events of interest and at anomalous velocities. This was verified in the ROSE area. Figure 5 shows a negative velocity event that must be a reflection off an object behind or behind and to the side of the array. Stacking would greatly reduce the effects of such events.

Thus far we have verified the original concept that an array towed near the bottom behind a surface ship using surface shots can be used to measure near bottom refraction velocities. Additional improvements need to be made before the device can be used routinely, such as making the pinger system and the pressure transducers work.

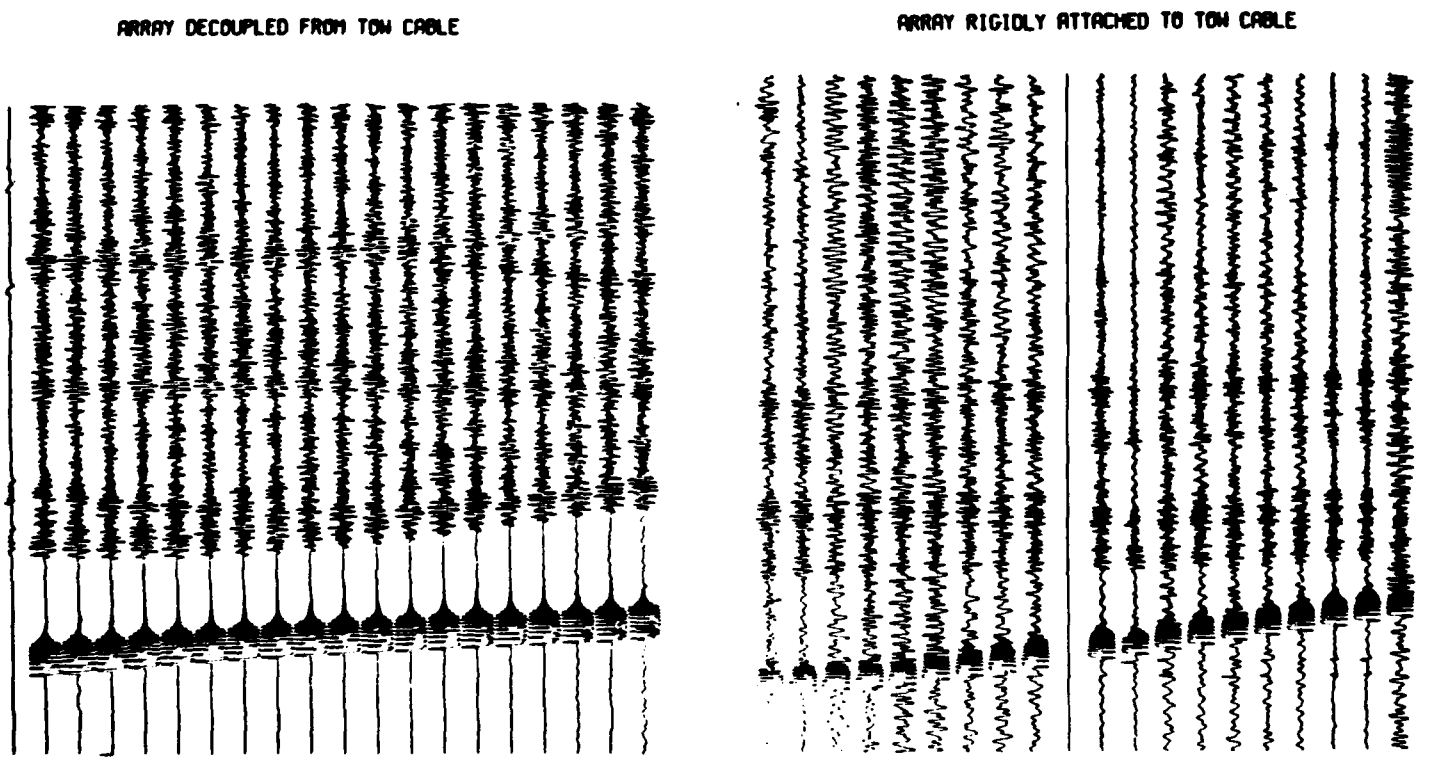

FIGURE 1: A comparison of signal-to-noise levels before and after decoupling the hydrophone array from the tow cable. The source in both cases is 2 lb. of explosives.

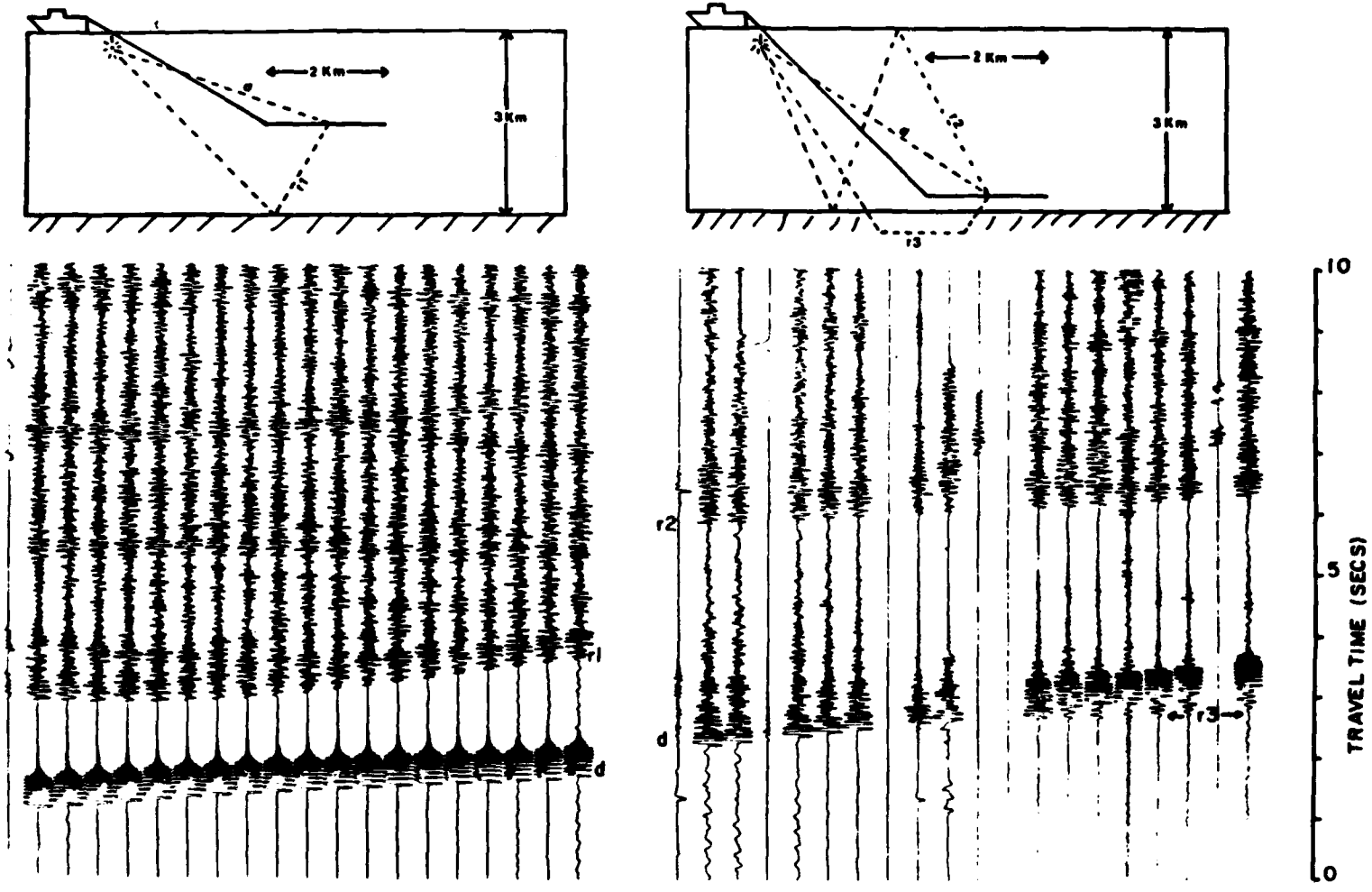

FIGURE 2: A comparison of records from a 2 lb. shot with the array in midwater and near the bottom. Near the bottom refracted energy traveling through the bottom can be clearly seen arriving before the direct water path.

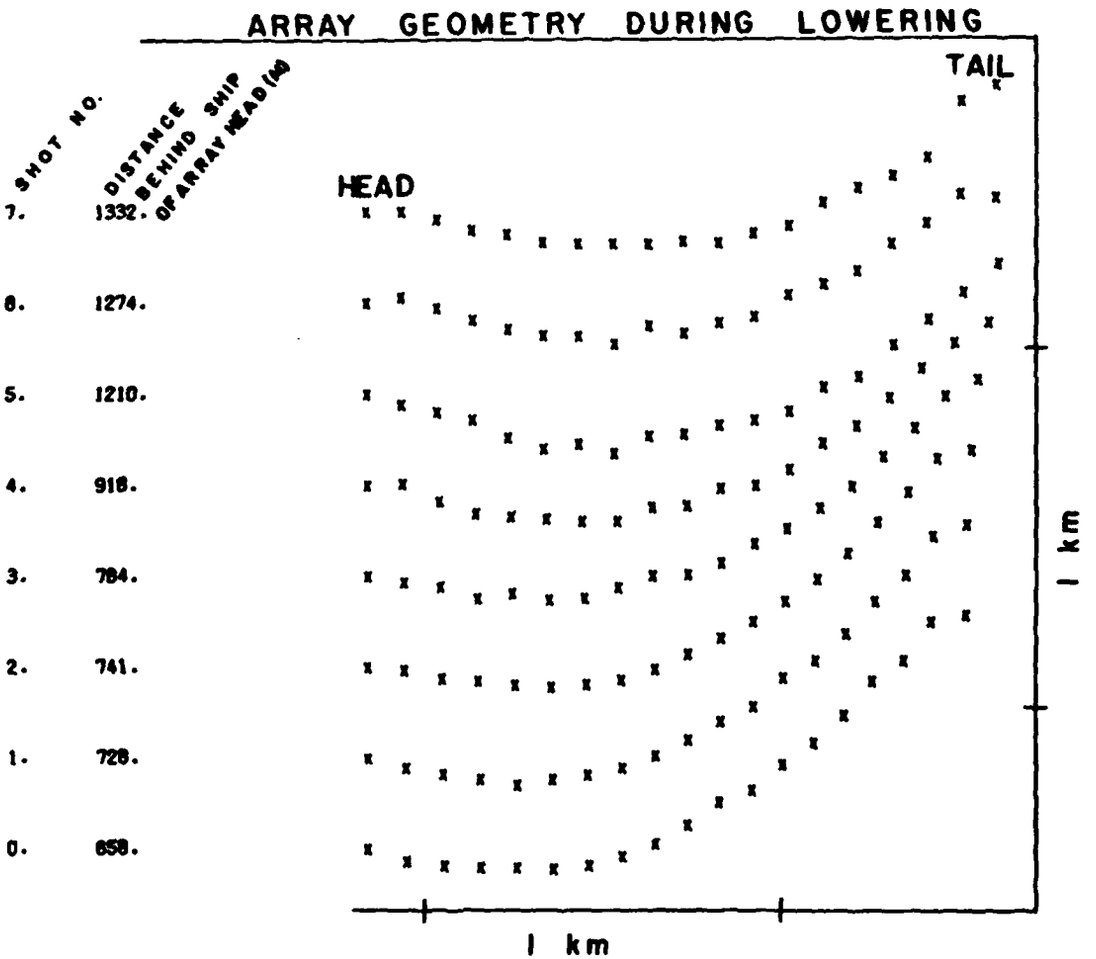

FIGURE 3: A determination of the array geometry during lowering of the array. The travel times of the direct and bottom reflected energy were used to determine the location of each array element. Only the relative shape of the array is shown; the vertical and horizontal scales do not refer to depth and distance behind the ship.

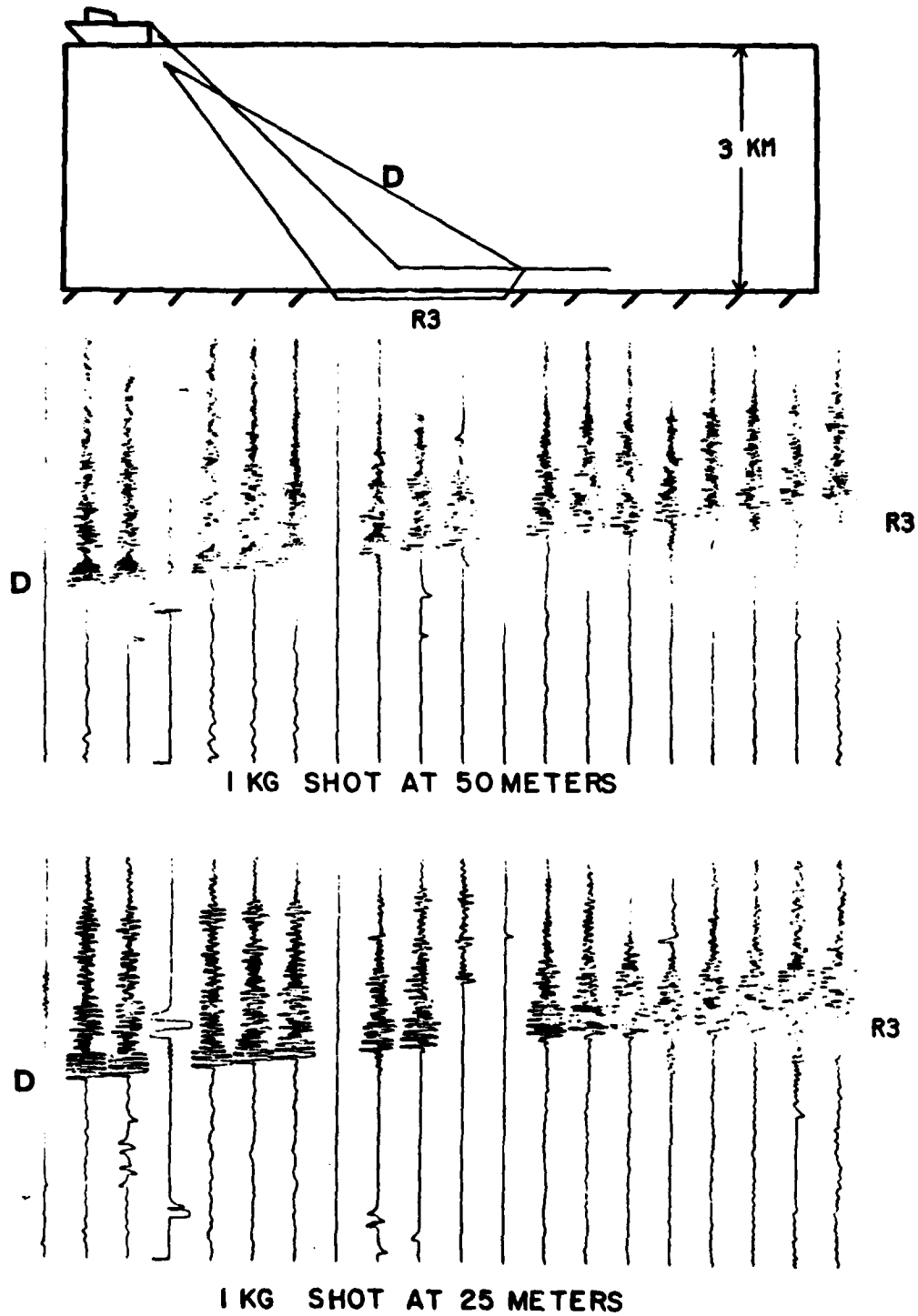

FIGURE 4: A comparison of shots at two depths. The deeper shot has higher frequencies, a shorter energy envelope, and the amplitude of the refracted arrivals is smaller than for the shallower shot.

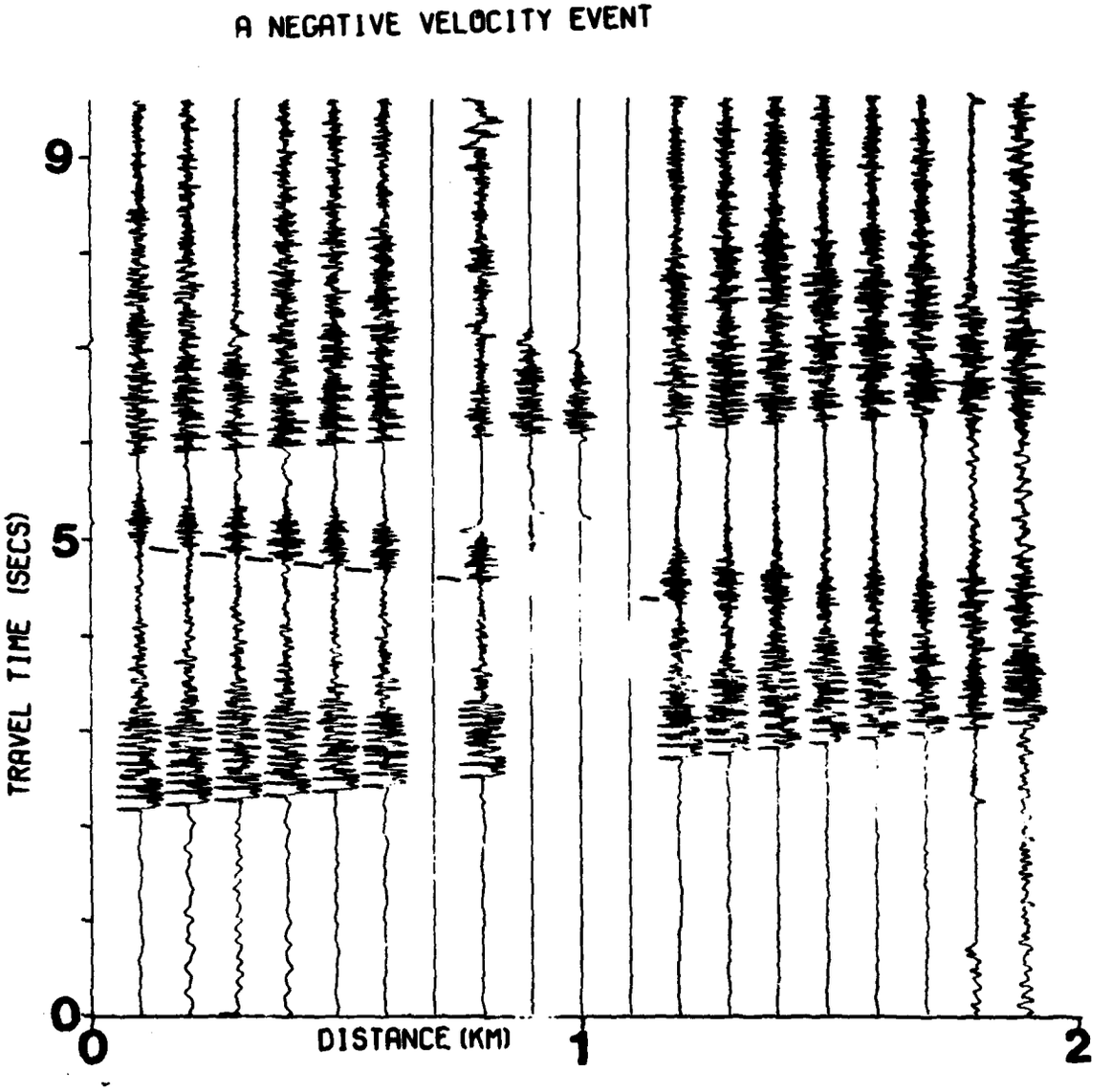

FIGURE 5: An example of energy traveling with a negative velocity, probably caused by reflection off an object behind the array.

VI. APPLICATION OF DEEP-TOWED SYSTEMS

A. EVALUATION OF BROADBAND, HIGH RESOLUTION SEISMIC DATA FOR SEAFLOOR SEDIMENT CLASSIFICATION

(P. G. Simpkin, Huntec)

B. COHERENCE OF BOTTOM-INTERACTING SOUND

(J. M. Berkson, NORDA)

VI.A. EVALUATION OF BROADBAND, HIGH RESOLUTION SEISMIC DATA FOR SEA FLOOR SEDIMENT CLASSIFICATION

by

Dr. P.G. Simpkin

SYNOPSIS OF PAPER FOR SUBMISSION TO OCEANOLOGY INTERNATIONAL 1978 AT BRIGHTON, ENGLAND

With the development and use of deeptow high resolution seismic systems, there has appeared an opportunity for a more theoretical investigation of shallow seismic data. Huntec '70 Limited, of Toronto, along with the Government of Canada under the auspices of the Atlantic Geoscience Centre have, over the last three years, been involved in joint field and research programs aimed at evaluating broadband, high resolution seismic data with the ultimate goal of establishing a strategy for remote classification of seafloor sediments.

The addition of a high resolution seismic system to continental shelf surficial geology mapping programs has resulted in a significant increase in both the data quality and in the value of such programs to geologists and sedimentologists.

The research program has involved the application of well established data processing techniques to the shallow seismic data and the introduction of pattern recognition methods. The significant increase in the signal bandwidth of high resolution systems and the resulting high information rate has highlighted inadequacies in conventional data analysis and display techniques. The aim of the research work is to establish a philosophy for on-line measurement, analysis and display of acoustic parameters of the seafloor and beneath. This will allow the full potential of the Huntec high resolution seismic system to be realized for defining sea floor characteristics on offshore site survey projects.

INTRODUCTION

Recognizing that future trends in offshore development lay in both the deeper waters and in the more remote areas of the continental shelves, Huntec '70 Limited of Toronto submitted a proposal in 1974 to the government of Canada for a joint research and development program titled "Remote Sensing of Geotechnical Properties and Geological Classification of Marine from a Ship Underway". The proposal was based on the results of successful trials of a deeptowed high resolution "boomer" undertaken by the Bedford Institute of Oceanography, Dartmouth, Nova Scotia (McKeown, 1975). This specially designed "boomer" is the heart of the deeptowed seismic system developed by Huntec as a natural extension to their range of high resolution surface towed systems.

The project ("Seabed") was planned to run for five years with the following objectives:

1) To provide high resolution, vertical incidence seismic profiles for the continental shelf mapping programs off eastern Canada.

2) To identify characteristics within the seismic echoes which correlate with surficial sediment types, texture and geotechnical properties.

3) To develop an on-line signal processing system for real-time display of parameters described in 2).

The success of the first phase of "Seabed" in 1976 has led to continued support for the program.

In the first two field seasons some 15,000 km of high resolution seismic profiles were collected (Simpkin et.al.,1976); these data form an important addition to the marine reconnaissance data collection programs off the eastern seaboard of Canada and complement other side scan and air gun data.

The research aspect of the project is aimed at obtaining a greater understanding of the physical characteristics of the seafloor sediments that generate seismic echoes following illumination by the broadband acoustic pulse. If the surface and the subsurface sedimentary units can be modeled in terms of their acoustic characteristics using the seismic echoes, then estimates of their physical and mechanical properties can be made. The main advantage of such remote mapping techniques to both engineers and geologists is that semiquantitative and continuous information may be available on-line to supplement the more normal graphical recordings of a seismic section. This is not to say that sampling methods will be eliminated or that ground truthing will not be required, but knowledge of the extent and the continuity of the surficial sediments between sampled points will add significantly to the degree of confidence that can be placed in surficial geology maps of both large and small areas of investigation.

BASIC REQUIREMENTS OF A HIGH RESOLUTION PROFILING SYSTEM

One important consideration in high resolution seismic profiling is the ability to resolve individual reflecting layers within the first 100 metres or so of seafloor sediments. A resolution limit of 100 mm is thought necessary particularly with the finer units (silt, clay). Other basic requirements of a proposed system are:

1) Acoustic Source - This should emit a very repeatable and reliable pressure pulse with broadband characteristics for high resolution in the vertical sense and a narrow beam width for good spatial resolution in the horizontal sense.

2) Hydrophones - These should be located in a quiet environment with fixed geometry with respect to the sound source and positioned so that surface echoes or multiples do not contaminate the profile.

3) Operational - The system should be capable of continuous use in poor weather conditions alongside other survey systems (air guns, sparkers, side scan sonars, etc.)

4) Display - The resolution capability of the field graphic recorder should equal and possibly exceed that of the seismic system. A large dynamic print range is considered essential.

A system with all the above attributes would indeed be complex. Several conflicting requirements mean that certain "trade offs" are necessary. For example, the need to maintain a tight geometrical configuration between the source and receivers means that the hydrophones must be positioned in close proximity to the source. Thus the possibility of noise interference caused by the outgoing acoustic pulse is increased. Another conflict is that of penetration against resolution. Because of the attenuating properties of sediments, lower frequencies are necessary for good penetration. However, lower frequencies imply longer source pulses and pulse length in turn limits the system resolution or ability to distinguish between adjacent reflecting interfaces. Also, if the narrow beam characteristics are to be maintained at the lower frequencies, physically larger sources are necessary. Thus in some way every system is a compromise although if certain parameters can be placed under the jurisdiction of the operator in the field, system performance may be optimized for a greater portion of shallow and deep water environments.

Huntec's answer to the above specification is in the form of a self-contained sound source and receiving equipment that is towed from the stern of a survey vessel.

DESCRIPTION AND PERFORMANCE OF THE HUNTEC SYSTEM

The Huntec DeepTow Seismic (DTS) system is designed to be towed up to 300 metres deep. The heart of the system is an impulsively driven, plane piston transducer (boomer) producing a high intensity, broadband acoustic pulse with exceptional repeatability and long term stability. The system (Figure 1) employs a hydrodynamically efficient towed body (fish) containing the boomer, capacitor discharge system, hydrophones for the acoustic returns and an attitude sensor package. The boomer is pressure compensated so that the acoustic pressure pulse (Figure 2) remains constant with depths to 300 metres. Depending on the particular situation, firing rates can be as high as eight times per second. Although some reduction in energy output level is necessary at high firing rates, pulse shape (and therefore spectral content) of the boomer remains unchanged. Fish roll, pitch, vertical acceleration and depth, along with two channels of seismic information are transmitted via the double armoured faired tow cable to the surface while the fish high and low voltage power supplies, and trigger signal are sent down the cable from the surface. The shipborne equipment consists of a high voltage power control unit to charge the storage capacitor to a maximum of 540 Joules, a signal processing unit and filter for the graphic recorder, a tape interface and calibration unit to allow direct analogue tape recording of the seismic information and an attitude display unit to monitor the towing characteristics of the fish.

During the development phase it was found necessary to electronically compensate for the vertical movement of the fish through the water caused by the heave induced motion of the tow point. Some mechanical decoupling does exist due to the lay back of the tow cable, but this is often insufficient to maintain data quality. Thus an electronic heave compensating system which delays or advances the boomer firing instant in response to changes in fish position was developed. Fish position is obtained either by a double integration of the vertical acceleration signal or by the pressure (depth) signal available from the Attitude Display Unit. Figure 3 shows an immediate advantage of heave compensation when detailed mapping is required. The buried pipelines that are easily distinguishable with heave compensation are not readily detected without compensation. In this case fish vertical motion was of the order of 1.5 metres. Another example (Figure 4) shows the resolution capabilities of the DTS system in an area of layered continental shelf sediments (Josenhans, in press). The geologic interpretation of the various units has been made on the basis of accumulated experience gained over many years by geologists from Bedford Institute in mapping the continental shelf regions off eastern Canada. This example shows a buried pockmark (King and Maclean, 1970) and an acoustic mask within the silt unit. The layer resolution has been maintained beyond 70 metres of penetration indicating low acoustic absorption. The very thin seafloor reflector indicates a very smooth topography with little scattering of the incident sound.

QUANTITIVE ANALYSIS

Traditionally the presentation of continuous seismic profiles has involved the time displacement rather than the amplitude content of the separate events that constitute a seismic echo. Generally the delineation of the various geologic units, and textural variations within those units have been sought and fortunately time, (and hence spatial) information is conveniently represented on graphic recorders. However, in recent years the amplitude and energy information contained in seismic echoes have received more attention because of their use in interpreting geologic structure. The introduction of signal processing schemes such as time varied gain, signal compression and digital analysis has made this possible. Deep seismic reflectivity data are now being processed more thoroughly using modern signal processing techniques to reveal more accurate and detailed information concerning the geologic structure. More relevant in the shallow seismic field are the studies on remote identification of surficial sediments by Smith and Le (1966), King and MacLean (1970), Clay and Leong (1974), Lonsdale, Tyce and Spiess (1974), Bell and Porter (1974) and Tyce (1976). These and other workers have used acoustic reflectivity and bottom loss measurements in several ways to estimate sea floor sediment type and topographical characteristics.

There are several reasons why amplitude and energy analysis together with the display of certain parameters are considered an important part of shallow seismic investigation. The limited dynamic range of graphic display systems is often insufficient to cover the range of echo amplitudes from the various seafloor and subsurface reflectors. Techniques mentioned above help to increase the display range but graphic quality is often very dependant on the skill and judgement of the operator. The natural averaging process that occurs

during the printing of a graphic record is very useful in that it allows the detection of coherent events below the noise threshold, however, this same process serves to reduce the sensitivity of the display system to subtle changes in echo level and therefore produces a reduction in the horizontal resolution capabilities. Thus, quantified estimates of the bottom and sub-bottom reflection coefficients, and perhaps their statistical parameters may lead initially to more reliable estimates of acoustic parameters, and thence to physical parameters of the layers.

Two methods that could be used here are 1) a comparison technique using a library of standard echoes, or parameters derived from the echoes, for common types of sedimentary structure, and 2) an acoustic model where an average echo is considered as the output function of a system that is excited by the source pulse.

Identification using 1) could involve modern techniques in pattern recognition and features extraction probably without involving any acoustic parameters. In method 2) the model variables (e.g., acoustic impedances and a scattering function for each interface) would be continually updated across the section to give a "best fit" between the synthetic and actual echoes.

Both of the above methods are complex. They involve the latest techniques in signal processing and features extraction. It is difficult to perceive how the above systems can be adopted for on-line operation without some simplification. One scheme is to use modern signal processing methods off-line to identify those characteristics of the echoes that are most suitable for identification purposes. The algorithms could then be transposed into hardware for on-line use.

ASPECTS OF "SEABED" RESEARCH

Apart from the basic physical parameters such as sound speed, bulk density, and bulk and shear moduli, many factors affect the reflection and transmission characteristics of an interface between two different media; e.g., system geometry, topography, micro-relief and scattering characteristics. In addition, acoustic absorption characteristics of the material must be included in the analysis of deeper relfectors and system performance is ultimately limited by noise considerations. Any data processing techniques must not ignore the above effects, all of which cannot be considered as time invarient.

The effects of surface roughness on the length of a reflected pulse has been discussed in detail by Clay and Leong (1974). Briefly, the amount of energy reflected back from an illuminated surface at angles other than normal incidence (backscattered energy) is a function of the acoustic impedance of the two media and the surface roughness. A perfectly smooth interface will reflect incident energy only in a specular direction whereas a rough surface will scatter energy at other incident angles back towards the source. This scattered energy will arrive later than that from normal incidence thus the length of a reflected pulse is indicative of the degree of roughness of the interface. A suitable model for estimating the shape and spectral content of reflected echoes from various types of sediment interfaces and geometrical situations has not yet been fully developed for the broadband Huntec boomer pulse. However, a method that may prove suitable for applying pattern recognition techniques to the classification of seafloor sediments has shown promise (Simpkin et.al 1976). Figure 5 shows the average normalized reflectivity coefficient using data windows of 0.2 ms (E1) and 3.2 ms (E3) for various ensembles of signals from different materials. On this type of

display a significant scattering term would reduce the value of the reflection coefficient obtained for a short window, thus the distance a point is removed from the line of equality, is indicative of the amount of scattering. Two groups with low reflectivity coefficients are completely isolated from the majority of the data. These are for areas of soft sediments which by inspection of the graphic record only, appear similar in nature to each other. However, when displayed as above, their reflection coefficients are quite different.

The majority of the data anlyzed, when grouped together in localities exhibit a large range of reflection coefficients but the grouping tends to be paralled to the line of equality. This poses the question, "Are the changes due to factors not considered in the anlaysis (e.g., fish motion) or are they due to natural causes?" A solution may be found by involving other parameters in this type of analysis. A large part of "Seabed" is aimed at identifying such parameters.

A more recent analysis of Huntec data using a cummulative energy concept similar to that of Knott et. al.(1977) has been described by MacIsaac and Dunsiger (1977) Here a Normal Cummulative Energy function (N.C.E.) defined as:

$$E(t) = \frac{1}{E_t} \int_o^t x_i^2(t)\, dt \qquad (=1 \text{ for } t \geqslant T)$$

where $x_i(t)$ is the i'th seismic echo of an ensemble, has been obtained for sets of data over four types of sediment from the Scotian Shelf (King 1970). Each point on the curves (Figure 6) is the average of 10 consecutive echoes.

A typical N.C.E. function for Emerald silt is seen in Figure 6a. The rapid increase in energy near the beginning of the plot is the return from the water-silt interface. There is some stratification in the silt, and a corresponding increase in returned energy as time increases.

The N.C.E. function for Sable Island sand (Figure 6b) shows an initial high intensity echo from the water-sand interface, with little internal reverberation, as is expected from a smooth homogeneous medium.

The N.C.E. function for La Have clay is shown in Figure 6c. The initial echo is similar to that obtained from sand but contains less energy. This is followed by the low level reverberation from a homogeneous sediment. The effect of a second layer is seen in the large contribution to the total energy in the latter half of the N.C.E. function. This is due to a highly stratified silt underlying the clay.

Figure 6d shows the N.C.E. function for glacial till. For this rough sediment, the initial increase in returned energy is immediately followed by a relatively high reverberation level due to both surface and internal scattering.

Shot to shot coherence has also been included in this study. For spatial translation of the sound source it is assumed that the reflected component of the echo changes slowly while the scattered component fluctuates rapidly from shot to shot. Based on this assumption it is expected that the echoes from smooth sediments would be largely coherent while those from rough surfaces would fluctuate rapidly from shot to shot. Figure 7a and b show the coherence coefficient and standard deviation of the mean for the

four sediment types. Coherence within the silt unit is found to be the highest with a corresponding low standard deviation. However, the high frequency variations within this unit suggest small but very local changes in surface reflectivity characteristics.

A first attempt to model the sediment column using the Huntec data has been made by El-Hawary and Vetter (1977). The method applied is not unlike that introduced by Robinson (1967) and Mendal (1976), for deep seismic data. It characterizes the subsurface in terms of multilayered media using space variables such as time intervals and reflection coefficients. Although the time scales and the reflection coefficients tend to be orders greater in deep seismic work than in surficial sediments, it is encouraging to learn that techniques developed for oil exploration are applicable.

DATA DISPLAY

Various techniques of displaying parameters in analogue form computed from seismic echoes have been developed. Breslau (1967) hand plotted acoustic and geological data derived from a ship's echo sounder and Lonsdale et.al.(1974) and Tyce (1975) have automatically plotted the equivalent reflected energy received from the top 5 metre and 50 metre zones of a section of deep water sediment alongside the graphic profile. This data was obtained from a deep tow using a normal incidence, 4 kHz pinger. A different technique of remote sediment classification has been described by Bell and Porter (1974). A computerized system using wide angle reflection techniques produced analogue displays of reflection coefficient. More recently Knott et.al.(1977) have presented energy contours from ocean sediments obtained using normal incidence, low frequency acoustics.

One advantage in displaying relevant analogue data alongside the graphic profile is that if perfect alignment is achieved correlation between the parameters and the graphic record are more easily detected. Figure 8 shows such a display technique applied to Huntec boomer data. The energy parameters E(1) and E(3) described earlier are displayed alongside a digitally expanded profile generated off-line using a PDP-11 computer and an ANAC Type 911 Graphics Printer. This type of printer offers certain advantages in that it interfaces directly with the computer, has high sweep speed (12.5 ms) and has a marking system that covers sixteen discrete grey tones. This last property has been used to advantage in plotting a continuous "histogram" of the energy values, thus adding a third dimension to a normal analogue display. The grey level of the display is an indication of the distribution of the individual measurements and complements the absolute reflectivity data as an identifying parameter. It is hoped that further development of this display technique will result in the selection of further identifying parameters for use in an on-line, real-time sediment classifier scheme.

FUTURE DEVELOPMENTS

During the "Seabed" program significant improvements in data quality and reliability have been made. However, the need to extend system performance in many directions demands that further development take place. The advent of a real-time sea floor mapping system will allow a more thorough investigation and assessment of the resources of the continental shelves. From an operational point of view it is likely that deep tow, high resolution seismic systems will become essential for deep water site surveys for large ocean structures and pipelines. In this context true fish position with respect to the surface ship will become necessary. Huntec have plans to develop such a system

using acoustic links. The present ability to operate the Huntec system in poor weather conditions and still maintain data quality has been an important asset in the field. It is realized that extended operation in deeper water will involve higher performance specifications from all the component parts of the system. For example, the development of a second generation heave compensation system with improved characteristics is underway and plans to increase the boomer output have reached an advanced stage.

The shallow water environment is a different yet no less demanding problem. On-line multiple removal, very high horizontal and vertical resolution and absolute fish positioning are seen as major requirements.

As far as the data analysis program is concerned the establishment of a library of characteristic echoes from many types of sedimentary units will precede the full implementation of a classifying system, although continued work along the lines discussed in this paper will certainly lead to improved understanding of sediment properties and their relationship to modern day sedimentation processes. Also the development of a surface and subsurface theoretical model of the sea floor will be necessary to allow the particular directivity characteristics of the "boomer" to be fully evaluated and utilized.

CONCLUSION

As the exploration into deeper areas of the continental shelves and eventually the abyssal depths proceeds the demand for instruments for remote sensing will increase. Underwater acoustics is probably the most suitable technology not only for the delineation and identification of sedimentary units but also for the estimation of physical properties, for monitoring and controlling purposes, communication and remote position fixing.

We see the high resolution boomer playing an important role in both the deep and shallow water environment and we look forward towards a totally integrated survey system involving on-line evaluation and display of seismic data and sediment characteristics, complete with good positional control.

ACKNOWLEDGEMENTS

Over the last three years many scientists, engineers and support staff at the Bedford Institute of Oceanography, at Huntec '70 Limited and at the Memorial University of Newfoundland have been involved in the "Seabed" Project. The author takes this opportunity to acknowledge their continued support without which many objectives would not have been achieved.

REFERENCES

Bell, D.L., and Porter, W.J., 1974. Remote Sediment Classification Potential of Reflected Acoustic Signals. In Physics of Sound Marine Sediments. Edited by Loyd Hampton, Plenum Press, 1974.

Breslau, L.R., 1967. The Normally Incident Reflectivity of the Sea Floor at 12 kHz and its Correlation with Physical and Geological Properties of Naturally-Occurring Sediments. Woods Hole Oceanographic Institution. Reference 67-16.

Clay, C.S. and Leong, W.K., 1974. Acoustic Estimates of the Topography and the Roughness Spectrum of the Sea Floor Southwest of Iberian Peninsula. In Physics of Sound in Marine Sediments. Edited by Loyd Hampton, Plenum Press.

El-Hawary, F.M. and Vetter, W.J., 1977. Estimation of Subsurface Layer Parameters by use of a Multiple Reflection Model for Layered Media. 4th International Conference on Port and Ocean Engineering Under Arctic Conditions. POAC 1977. Memorial University of Newfoundland.

Josenhans, H.W. In press. A Side Scan Sonar Mosaic of Pockmarks on the Scotian Shelf.

King, L.H., 1970. Surficial Geology of the Halifax-Sable Island Map Area. Paper 1. Marine Sciences Branch, Dept. of Energy, Mines and Resources, Ottawa, Canada 16 p.

King, L.H., and MacLean, B., 1970. Pockmarks on the Scotian Shelf. Geol. Soc. Am Bull 81, pp. 3141-3148.

Knott, S.T., Hoskins, H., and LaCasce, E.O., 1977. The Energetics of Normal-Incidence Marine Seismic Profiles and Estimation of the Acoustic Impedance Structure of the Seabed. Pts. I & II. Proc. of International Symposium on Computer-Aided Seismic Analysis and Discrimination, Falmouth, Mass., U.S.A. IEEE Computer Soc.

Lonsdale, P.F., Tyce, R.C., and Spiess, F.N., 1974. Near Bottom Acoustic Observations of Abyssal Topography and Reflectivity. In Physics of Sound in Marine Sediments. Edited by Loyd Hampton, Plenum Press, 1974.

MacIsaac, R.R. and Dunsiger, A.D., 1977. Ocean Sediment Properties Using Acoustic Sensing. 4th International Conference on Port and Ocean Engineering under Arctic Conditions. POAC 1977. Memorial University of Newfoundland.

McKeown, D.L., 1975. Evaluation of the Huntec '70 Hydrosonde DeepTow Seismic System, B.I.O. Report Series BI-R-75-4/March 1975.

Mendal, J.M., 1976. White Noise Estimators for Seismic Data Processing in Oil Exploration. Proc. Joint Automatic Control Conference. JACE 1976.

Robinson, E.A., 1967. Predictive Decomposition of Time Series with Applications to Seismic Exploration. Geophysics, 32, No. 3, June 1967.

Simpkin, P.G., Parrot, D.R., Hutchins, R., and Ross, D.I., 1976. Seabed '75 - Objectives and Achievements. Bedford Institute of Oceanography, Dartmouth, Nova Scotia. Report Series/BI-R-76-15/Dec. 1976.

Smith, D.T., and Li, W.N., 1966. Echo-Sounding and Seafloor Sediments. Marine Geology, 4, pp. 353-364.

Tyce, R.C., 1975. Real Time Processing and Display of Near-Bottom Acoustic Reflectivity Measurements. Proc. IEEE Ocean '75 Conference.

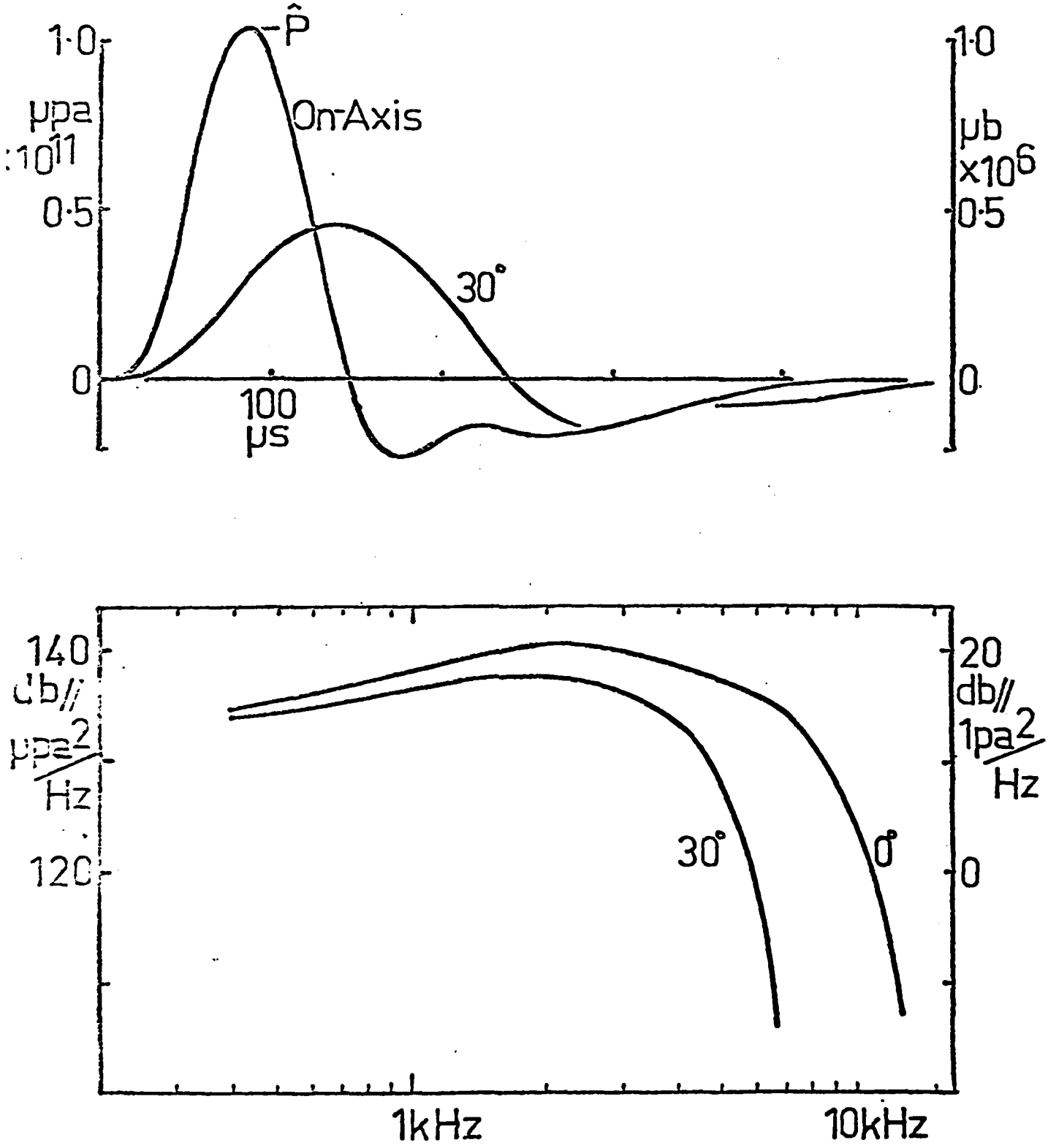

Figure 2 - Pressure pulse and power spectrum for Huntec ED10C boomer measured on-axis and at 30° off axis. Measurements refered to 1 metre with input energy 500 Joules.

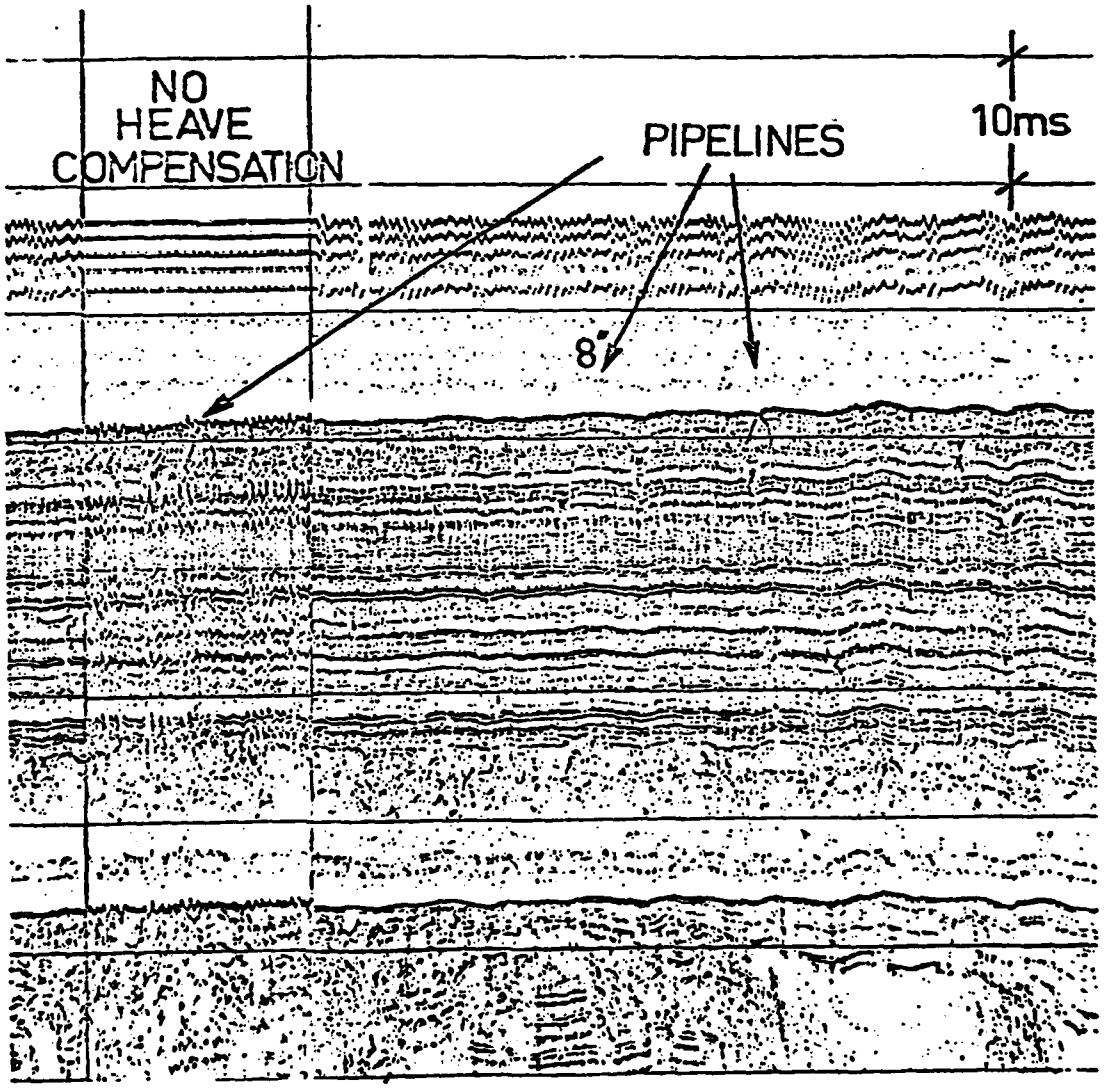

Figure 3 - Huntec graphic record showing advantages in using heave compensation to maintain system resolution. Parabolic reflectors are echoes from buried pipelines off Louisiana. Firing rate 8 per second.

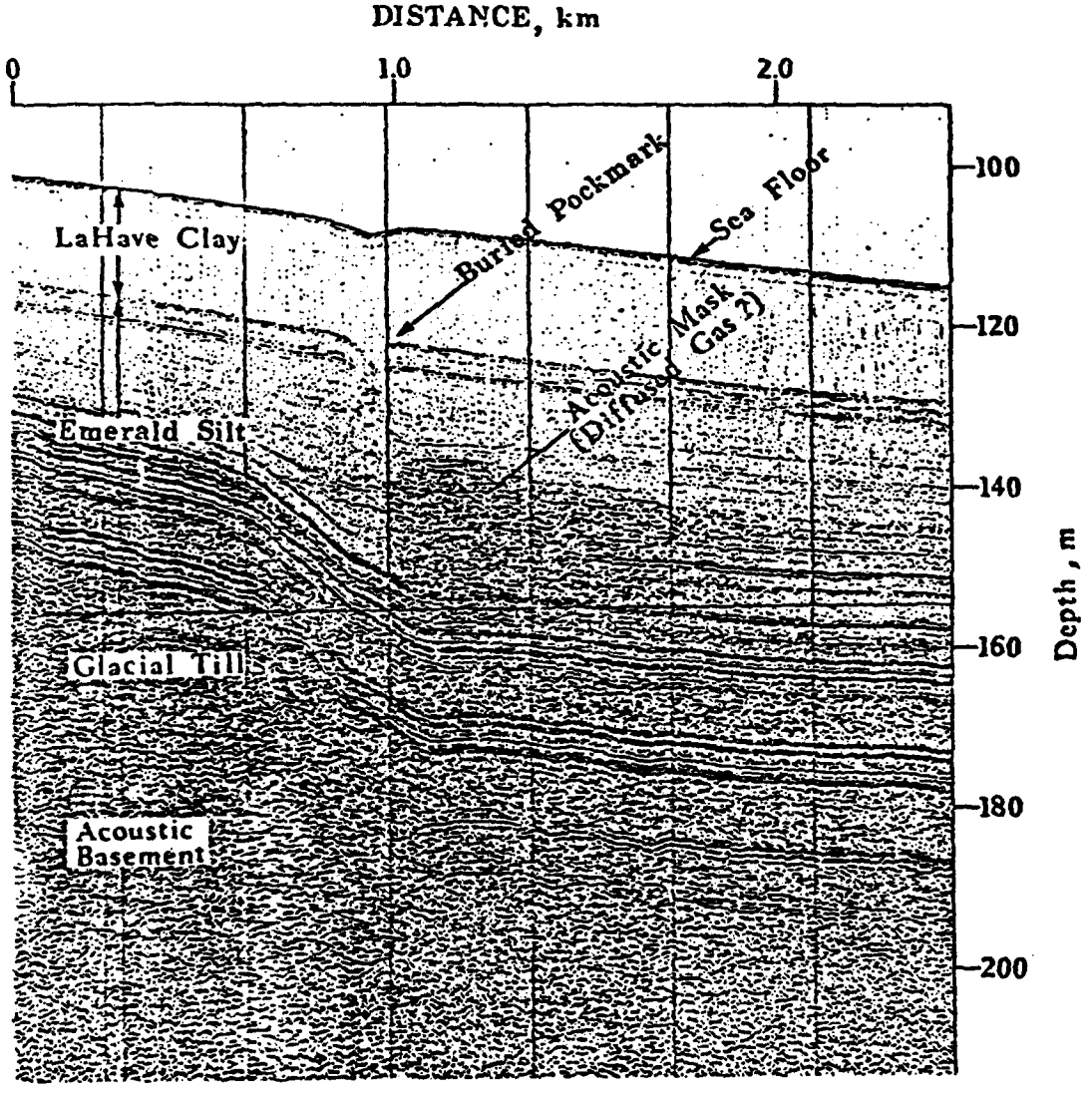

Figure 4 - Section of a Huntec graphic record showing a buried pockmark and a diffused gas region in an area of the Scotian Shelf. Scale calibrated using the sound speed of the water column. Firing rate 0.75 second.

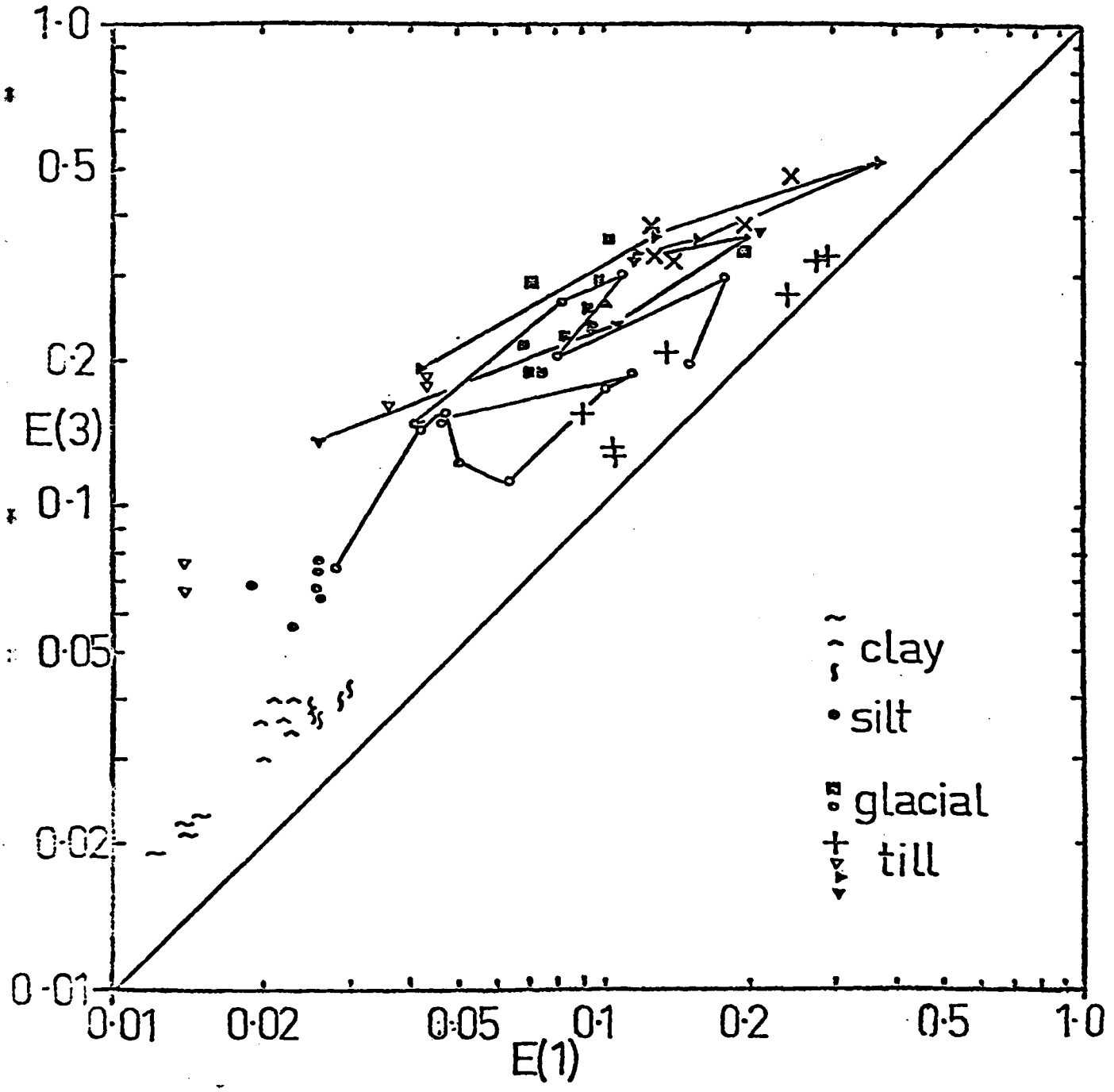

Figure 5 - Averaged, normalized reflectivity coefficient using windows of 0.2 ns E(1) and 3.2 ns E(3) for a variety of sediments. Clusters are of neighbouring ensembles in areas of apparently homogeneous sediment type. Lines connect neighbouring ensembles in areas of apparently variable sediment type.

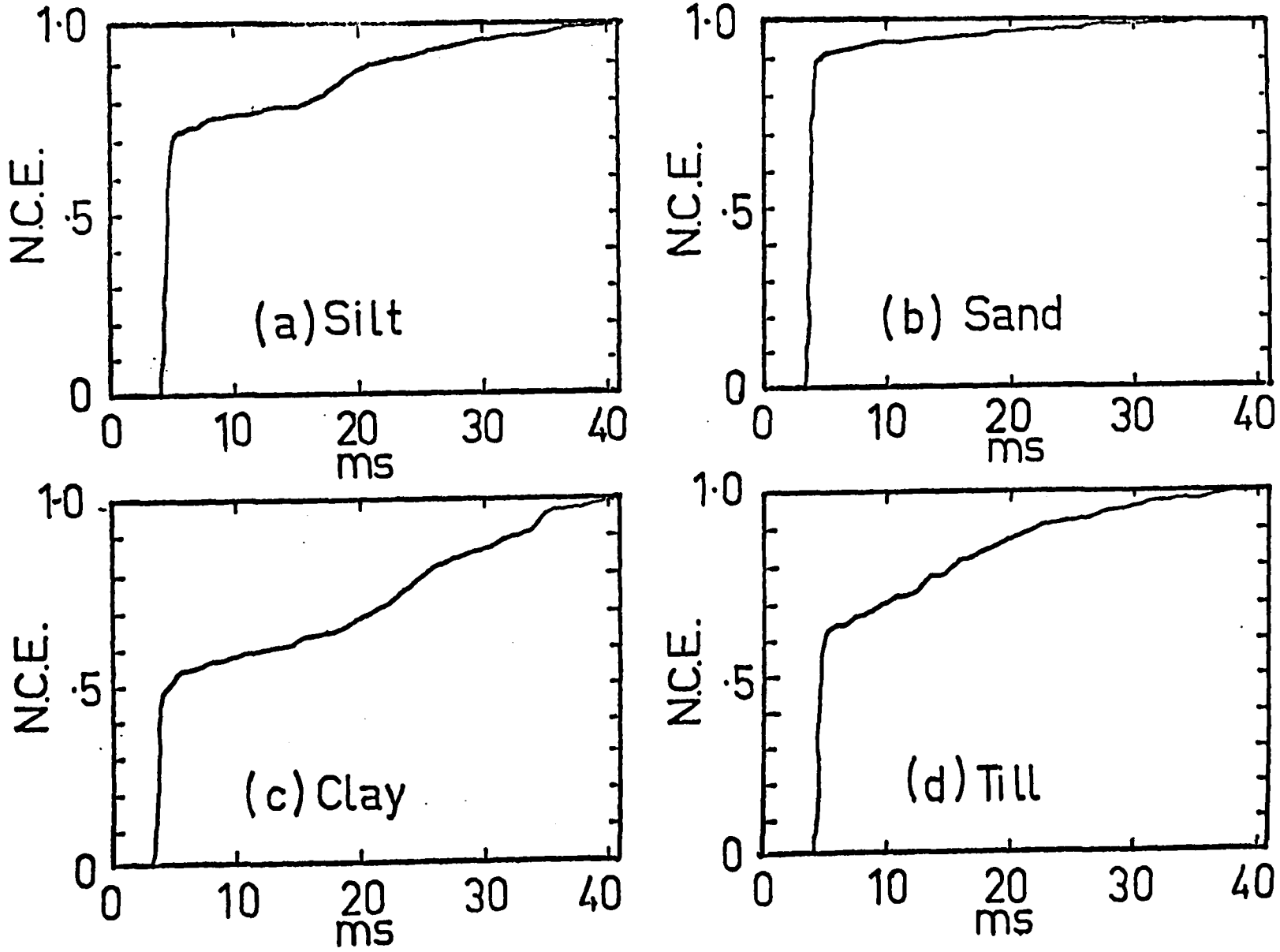

Figure 6 - Averaged Normalized Cummulative Energy function for various sediment types.

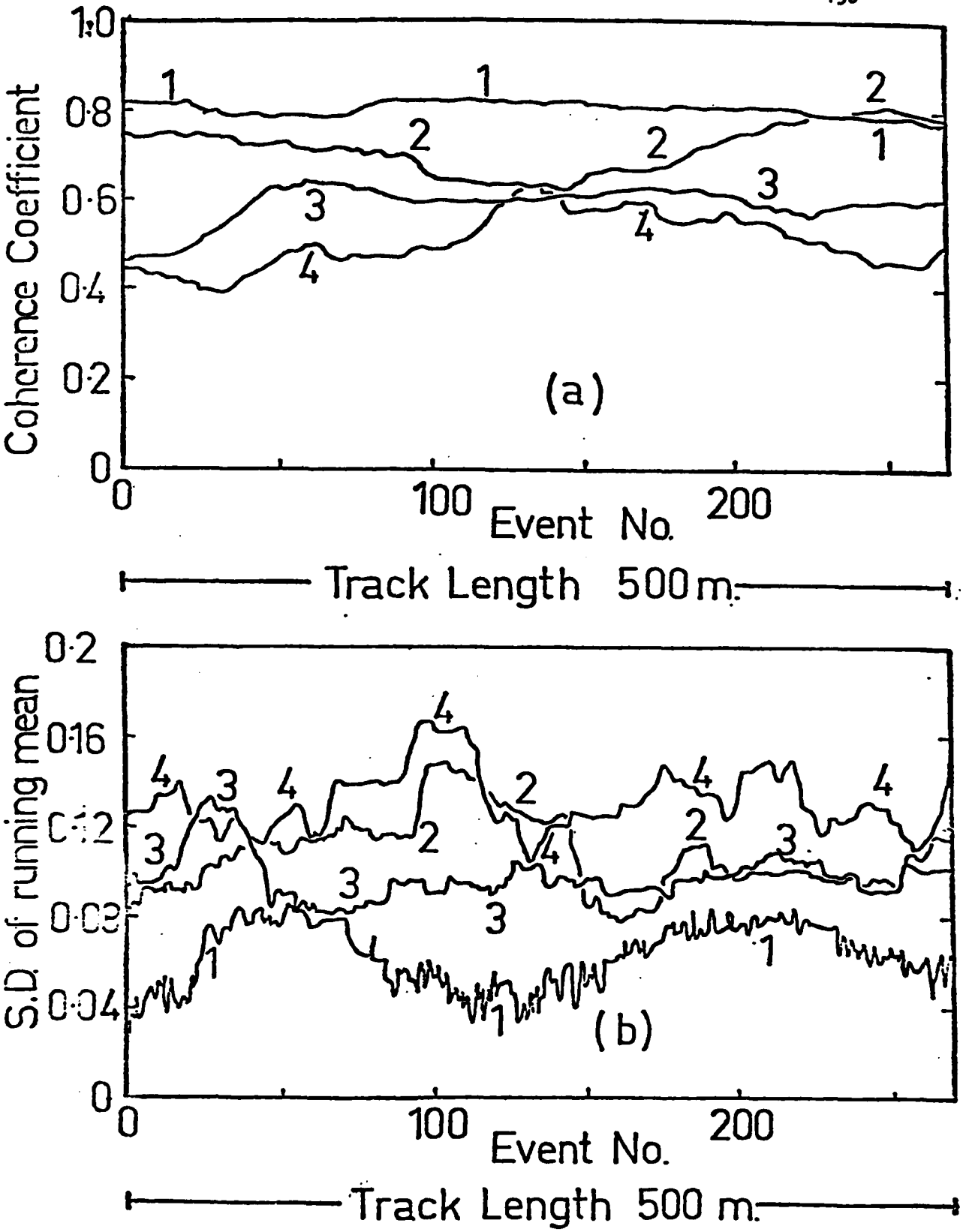

Figure 7 - Coherence coefficient between adjacent echoes against track length.
a) Running average over 50 shot pairs,
b) Running standard deviation for same events as in a).
1) Emerald Silt, 2) Sambro Sand, 3) LaHave Clay, 4) Glacial Till.

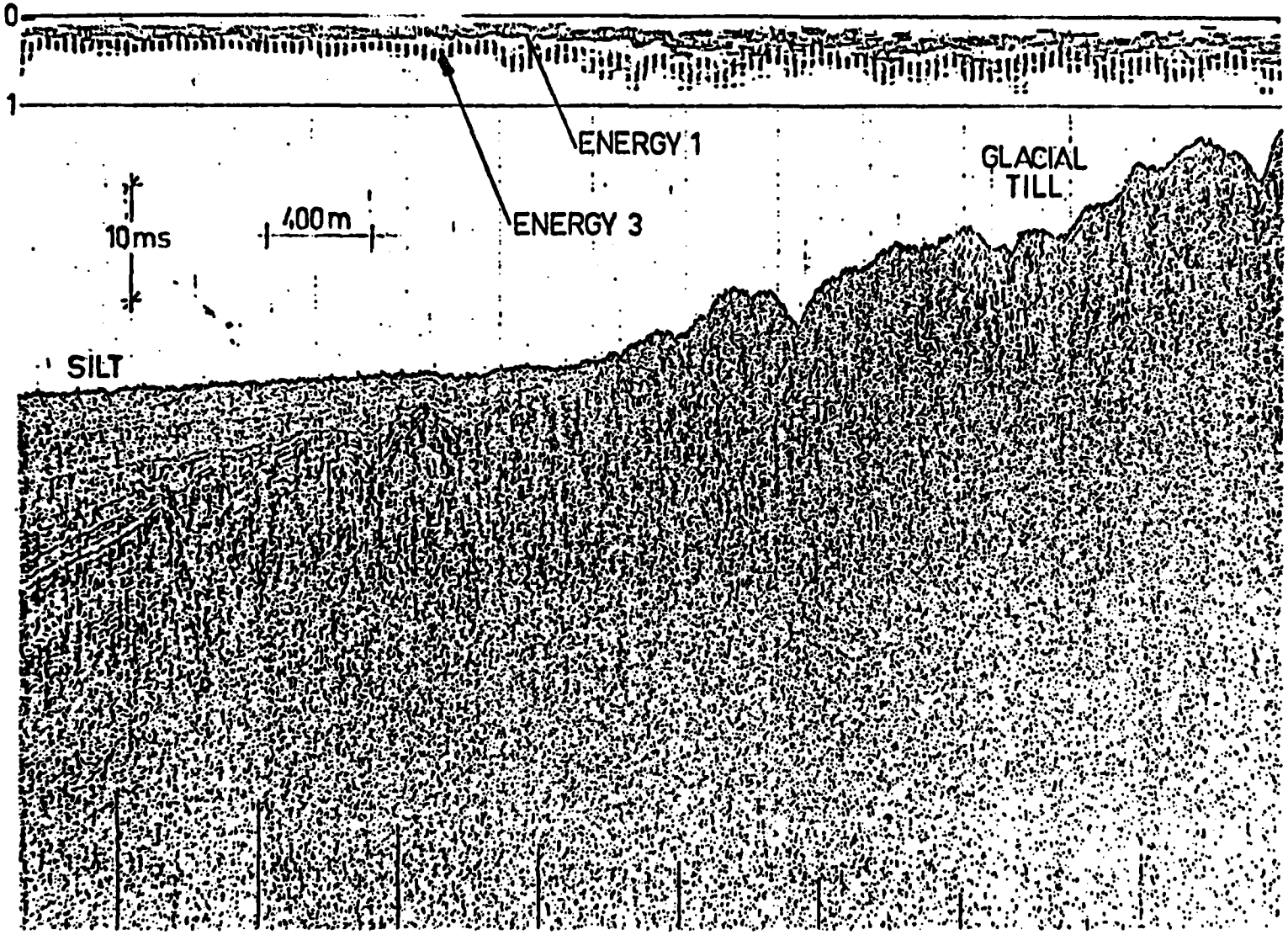

Figure 8 - Energy parameters E(1) and E(3) displayed alongside graphic profile. Display shows bottom reflectivity and the amplitude distribution over an Emerald Silt - Glacial Till transition.

VI.B. COHERENCE OF BOTTOM-INTERACTING SOUND

J. M. Berkson (NORDA)

A deep-towed array provides an excellent opportunity for a coherent reflectivity experiment. Two experimental geometries using impulsive or pulsed sources are of particular interest. 1) The source (surface or deep) moves with the array so that the bottom-interacting geometry is fixed. The coherent reflection coefficient $\frac{\langle P \rangle}{P_m}$ is calculated. $\langle P \rangle$ is the ensemble average for the reflected pressures and P_m is the pressure reflected from a mirror surface for the same geometry. 2) A coherence function γ^2 is calculated from a single bottom interaction. $\gamma^2(\omega,\phi,\theta) = \frac{|S_{xy}(j\omega)|^2}{S_{x(\omega)}S_{y(\omega)}}$ where S is a sample estimate of the power spectral density, j is $\sqrt{-1}$, ω is the radian frequency, and x, y are the indices of adjacent array elements at bearing ϕ and grazing angle θ.

The objective of the experiments is to relate the coherent reflection coefficient to the nature of the bottom. For example, Eckart has shown that the coherent reflection coefficient for a totally reflecting rough surface having a gaussian probability density function is $\frac{\langle P \rangle}{P_m} = e^{-2k_z{}^2\sigma^2}$ where k_z is the vertical component of the acoustic wave number and σ is the rms roughness of the surface. The NORDA bottom coherence program involves two data sets:

(A) Data from the VEKA array,

(B) Data from adjacent shots received by a single hydrophone.

Post workshop note: Using a data set of type (B) where shots were dropped in a circular pattern (grazing angle 15°) in the Tagus Abyssal Plain, the coherence was calculated for frequencies 50 - 500 Hz. We found that for a given frequency the coherence vs bearing exhibits a degree of symmetry in which features occur in pairs 180° apart. This observation suggests a directionality dependent, coherence degrading effect operating at the bottom.